AD_____

Award Number: DAMD17-00-1-0507

TITLE: Involvement of Reactive Oxygen Species in Breast Cancer Cells Development, Maintenance and Death

PRINCIPAL INVESTIGATOR: Nitsa Rosenzweig, Ph.D.
Kim O'Connor, Ph.D.
David Jansen, M.D.

CONTRACTING ORGANIZATION: Xavier University of Louisiana
New Orleans, Louisiana 70125

REPORT DATE: July 2002

TYPE OF REPORT: Final

PREPARED FOR: U.S. Army Medical Research and Materiel Command
Fort Detrick, Maryland 21702-5012

REPORT DOCUMENTATION PAGE

Form Approved
OMB No. 074-0188

1. AGENCY USE ONLY (Leave blank)	2. REPORT DATE	3. REPORT TYPE AND DATES COVERED
	July 2002	Final (1 Jul 00 - 30 Jun 02)

4. TITLE AND SUBTITLE
Involvement of Reactive Oxygen Species in Breast Cancer Cells Development, Maintenance and Death

5. FUNDING NUMBERS
DAMD17-00-1-0507

6. AUTHOR(S)
Nitsa Rosenzweig, Ph.D.
Kim O'Connor, Ph.D.
David Jansen, M.D.

7. PERFORMING ORGANIZATION NAME(S) AND ADDRESS(ES)
Xavier University of Louisiana
New Orleans, Louisiana 70125

nrosenzw@xula.edu

8. PERFORMING ORGANIZATION REPORT NUMBER

9. SPONSORING / MONITORING AGENCY NAME(S) AND ADDRESS(ES)
U.S. Army Medical Research and Materiel Command
Fort Detrick, Maryland 21702-5012

10. SPONSORING / MONITORING AGENCY REPORT NUMBER

11. SUPPLEMENTARY NOTES

12a. DISTRIBUTION / AVAILABILITY STATEMENT
Approved for Public Release; Distribution Unlimited

12b. DISTRIBUTION CODE

13. Abstract ***(Maximum 200 Words)*** *(abstract should contain no proprietary or confidential information)*

Oxygen Free Radicals (OFR) have different effects on cellular processes. They were implicated in cell damage, apoptosis, and carcinogenesis. The hypothesis of this proposal is that the effect of OFR is concentration dependent. At high concentration OFR cause damage, at low concentration they cause apoptosis, and at even lower concentration they fail to activate the apoptosis signal, leading to the development of cancer. To test this hypothesis we proposed to measure the level of OFR in normal and cancer breast cell lines and primary human breast tissue, and to correlate the OFR concentration with apoptosis and carcinogenesis. We have shown, in cell-line, that there is a correlation between the growth curve, number of apoptotic cells, and number of dead cells and the concentration of H_2O_2 added to the culture. We also showed correlation between Cytochrome P-450 activity and the OFR levels, connecting the regulation of OFR to the Cytochrome P-450.

14. SUBJECT TERMS
breast cancer, cell signaling, apoptosis, oxygen free radicals

15. NUMBER OF PAGES
110

16. PRICE CODE

17. SECURITY CLASSIFICATION OF REPORT	18. SECURITY CLASSIFICATION OF THIS PAGE	19. SECURITY CLASSIFICATION OF ABSTRACT	20. LIMITATION OF ABSTRACT
Unclassified	Unclassified	Unclassified	Unlimited

Table of Contents

INTRODUCTION

In the last year, publications have shown that Oxygen Free Radicals (OFR) are involved in the growth of carcinogenic lesions (1), cause DNA fragmentation and, as a result, cell death (2), and occur in high levels in the breast cancer cell line MCF-7 (3). Reduction of OFR levels either by using OFR scavengers (1) or by inhibiting enzymes responsible for the production of OFR (2,3) stopped the cellular process they were correlated with; Development of the tumor or DNA fragmentation. One of the hypotheses is that OFR can cause different effects because their effect is concentration dependent. The hypothesis is that high levels of OFR can cause DNA damage and cell death, lower concentrations can cause apoptosis, and even lower concentrations fail to activate the apoptosis signaling and allow cell growth and cancer development. This research proposal suggests testing this theory. The information from this research can be used as a diagnostic tool in cancer detection. It also can provide a scale for the OFR levels and their potential effect on cells.

BODY

The purpose of this research is to show a correlation between the concentrations of oxygen free radicals (OFR) and their effect on cells. The hypothesis is that the effect of OFR is concentration-dependent and that in high concentrations OFR cause cell death, in lower concentrations OFR cause apoptosis, and in even lower concentrations, OFR fail to activate the apoptosis signal transduction pathway and therefore cannot regulate cell growth, which leads to carcinogenesis.
To test this hypothesis, the statement of work divides the period covered by this grant into three phases:

Phase 1 – June 2000 – January 2001(Months 1-8).

1. Establishing work meeting with Dr. O'Connor, which acts as a mentor on this grant. Equip the lab.
2. Hire an undergraduate student.
3. Train the student.
4. Establish breast cell line.
5. Establish primary epithelial cell culture and tissue culture.

These goals have been successfully achieved.

1. My students and I meet with Dr. O'Connor every Wednesday and Dr. O'Connor and I meet with Dr. Jansen once a month or as required.
   I have equipped the laboratory with Biological safety hood, CO_2 incubator, -40^{0}C freezer, Refrigerator, water bath + shaker, analytical balance, pH meter, Centrifuge, Fluorescent microscope, hot plate, and miscellanies that are needed in a tissue culture lab. Xavier university of Louisiana provided me with additional research space (an isolated room to function as a tissue culture room), and with three laptop computers for our use.

From an NSF-EPSCoR grant I have purchased a desk top, colored printer, and a scanner. This equipment allows better analysis and presentation of the results. The fluorescent microscope is hooked to the desktop.

2. I hired Mr. Imani Jones, a Xavier student, as an undergraduate research assistant. He is taking care of the cell lines as well as the tissue culture and operates all equipment in the lab.
   Ms. Terra L. Jones, a Xavier student, is volunteering in my lab and dedicates her time for maintenance of the equipment. She is responsible for the orders, clean-up, and functions as a lab manager.
   Xavier University of Louisiana, through the NIH-MARC program provided me with two students who work on the project too. Ms. Crystal lane and Ms. Christina Griffin work is funded by this grant but the NIH funds their scholarship. Ms. Lane and Ms. Griffin are responsible for the measurements of OFR in cells.
   I have mentored research students through a research class offered in the Chemistry Department at Xavier University (CHEM4083); Tzucanow Cumming, Tamika Tyson, Shalon Babbitt, Shelia Goodmsn, Karachie Ward, and Allison Stephens. These students participated in the data collection. They were exposed to cancer research, which is an important aspect of this grant since they are all African American. A group, which is underrepresented in this area.
3. All students worked in Dr. O'Connor, from Tulane University – Chemical Engineering Department, laboratory in order to master the use of the fluorescence microscope. The students were trained in the tissue culture facility of Dr. Wiese from Xavier University of Louisiana, Pharmacy school, and learned how to maintain cell lines under my supervision. Today, Mr. Jones is responsible for the maintenance of the cell lines and training of new students, in our fully functional tissue and cell culture facility.
   The students also worked in Dr. Zeev Rosenzweig's laboratory at The University of New Orleans (UNO), Chemistry Department in order to learn how to perform the OFR measurements.
4. In the new cell culture facility we have established breast cancer cell line (MCF-7) and normal breast cell line (MCF-10). These cells were used for OFR measurements. We also established murine macrophages (J774). This addition was made because we found it easier to use cells that can do phagocytosis in the OFR measurements. Together with Dr. Rosenzweig's research group, we have developed lipobeads that can be targeted in the cells and perform variety of localized measurements. This is part of Dr. Rosenzweig's research effort to develop tools for single cell analysis. We are collaborating with the group at UNO so we can use their technology to accurately measure OFR in cells. The initial goal of the study was to develop a technique to measure the intracellular level of molecular oxygen, which is closely related to OFR levels in cells. However, we have encountered a problem. The lipobeads, which contain the fluorescence probes could not diffuse to the cells nor could they be transferred to the cells without inducing cell damage. To overcome this problem we started to work with macrophages. These cells can naturally internalize the lipobeads with the dye (sensor) by phagocytosis. It allowed us to test the ability to measure intracellular oxygen; the sensitivity of the method, the stability of the

dye the accuracy of the measurement, and its reversibility. The results of these efforts were published in five papers (4,5,6,9,10,11,12).

5. We were not able to establish primary tissue cultures. The main problem was logistic. In our preliminary experiments we established the need for the tissue to be as fresh as possible in order for the culture to develop in the lab. The nature of my position and the fact that I work with undergraduate students did not provide the flexibility to go to the operation room and get the tissue as it was removed from the patients.

Phase 2 – February 2001 – September 2001 (Months 9-16)

1. Measurements of OFR in breast cell lines and in primary breast cells.
2. Measurements of apoptosis as a function of exposure to H_2O_2 in breast cell lines and primary breast cells.
3. Measurements of growth before and after exposure to H_2O_2.
4. Measurements of immortality in the presence of different concentrations of H_2O_2.
5. Analysis of tumor aggressiveness.

As stated in phase one, the research on primary tissue cultures was not performed due to technical difficulties.

1. Since breast cell lines and primary breast cells cannot do phagocytosis, and in order for the dyes to enter the cells, phagocytosis is required, the preliminary work was done with murine macrophages. We were able to measure oxygen in cells in an accurate, sensitive, and reproducible way. Results of these experiments were published in five different papers (4,5,6,9,10,11,12) and the papers are attached at the end. We used the free dyes, without binding to lipobeads and measured oxygen in the cells after simple diffusion of the dyes into the cells. This work is presented in the appendix under "unpublished data", Figure I. My plan is to present these results in the 2002 Era of Hope Conference.
2. Apoptosis measurements were done in murine macrophages as a model to study the use of the apoptotic commercial kit. The results of these experiments were presented at The ACS meeting in New Orleans (7,8). The apoptosis measurements in breast cells are presented in the appendix under "unpublished data", Figure II A and B. My plan is to present these results in the 2002 Era of Hope Conference. The results show that high concentrations of H2O2 cause cell death that is not associated with apoptosis. Low concentrations cause apoptosis and very low concentrations do not cause apoptosis or cell death.
3. Growth measurements, by the use of Trypan Blue and cell counting was studied and established on murine macrophages and on breast cells. The results of the study on murine macrophages were presented in the ACS meeting (7,8). The results on breast cells are presented in the appendix under "unpublished data", Figures IIIA and B. My plan is to present these results in

the 2002 Era of Hope Conference. The results show that low concentration of H2O2 cause inhibition of growth, very low concentrations of H2O2 cause increase in growth, and high concentrations prevent growth.

4. Immortality study was not performed.
5. Aggressiveness studies were not done.
6. Correlation between Cytochrome P-450 and OFR. This work was done in collaboration with Dr. Foroozesh from Xavier University of Louisiana. Dr. Foroozesh is an organic chemist and synthesizes inhibitors for Cytochrome P-450. We have shown that inhibition of Cytochrome P-450 activity reduces the levels of OFR in breast cancer cells. This work was presented in the 2002 CUR conference in Washington (14).

Phase 3 – October 2001 – November 2001 (Months 17-18)

I have submitted two grant applications to the Breast Cancer Program of the DOD last year. These proposals were not funded.
I have submitted a grant application to the Ovarian Cancer Program of the DOD. This grant application is still pending.
I have submitted a grant application, as a CoPI together with Dr. Zeev Rosenzweig, to the NIH. This grant application is still pending.
I have received funding from the NSF-EPSCoR for a period of three years. This is the first year of funding.

KEY RESEARCH ACCOMPLISHMENTS

- Establishment of research laboratory equipped with cell culture facility and equipment to perform fluorescence measurements.
- Establishment of collaboration with laboratories in research universities at the New Orleans and Xavier vicinity.
- Attracting minority students to the area of breast cancer research.
- Establishment of breast cell lines.
- Establishment of apoptosis measurements.
- Establishment of fluorescence measurements.
- Five peer-reviewed publications.
- Five proposals submitted to federal agencies. One successful and two pending.
- Six presentations by Xavier students in national and international conferences.

REPORTABLE OUTCOMES

Papers

"Synthesis and Application of Submicrometer Fluorescence Sensing Particles for Lysosomal pH Measurements in Murine Macrophages", Jin Ji, Nitsa Rosenzweig, Christina Griffin, and Zeev Rosenzweig, Anal. Chem. (2000), 72: 3497-3503.

"Molecular Oxygen Sensitive Fluorescent Lipobeads for Intracellular Oxygen Measurements in Murine Macrophages", Jin Ji, Nitsa Rosenzweig, Imanie Jones and Zeev Rosenzweig, Anal. Chem. 2001 (published on the internet ACS website June 2001).

"Synthesis, Characterization and Application of Fluorescent Sensing Lipobeads for Intracellular pH Measurements in Single Cells", Kerry McNamara, Thuvan Nguyen, Jin Ji, Gabriela Dumitrascu, Nitsa Rosenzweig and Zeev Rosenzweig, Anal. Chem (2001) 73: 3240-3246.

"Development of A Digital Fluorescence Sensing Technique to Monitor the Response of Macrophages to External Hypoxia", Jacob K Asiedu[1], Jin Ji[1], Mai Nguyen[1], Nitsa Rosenzweig[2], and Zeev Rosenzweig[1]* J Biomed Opt 2001 Apr; 6(2):116-21

"A Novel Fluorescent Oxygen Indicator for Intracellular Oxygen Measurements", Jin Ji[1], Nitsa Rosenzweig[2], Imanie Jones[2] and Zeev Rosenzweig[1]* J. Biomed. Optics, 2002 (in press).

Presentations

"Optochemical Sensors and Probes for Single Cell Analysis. ", Jin Ji, Nitsa Rosenzweig, Imani Jones and Zeev Rosenzweig, ACS Spring 2001.

"Effect of intracerllular sensors on cells" Imani Jones, Crystal Lane, Tzucanow Cummings, Tamika Tyson, and Nitsa Rosenzweig. Presentation at Southeast/Southwest Regional ACS Meeting, January 2001, New Orleans, LA.

"MOLECULAR OXYGEN SENSITIVE FLUORESCENT LIPOBEADS FOR SINGLE CELL ANALYSIS", JIN JI [1] , IMANI JONES [2], NITSA ROSENZWEIG [2], AND ZEEV ROSENZWEIG[1] , Pitcon 2001, New Orleans Louisiana, March 2001
392

"Application of FRET microscopy for real time monitoring of drug delivery into single cells", Dumitrascu, Gabriela; Lane, Crystal; Jones, Imani; Rosenzweig, Nitsa; Rosenzweig, Zeev. 223rd ACS National Meeting, Orlando, FL, United States, April 7-11, 2002

"Fluorescence transfer energy- new analytical tool for the drug delivery follow up", Gabriela Dumitrascu, Imani Jones, Nitsa Rosenzweig, and Zeev Rosenzweig Pitcon Conference, New Orleans, LA, March 17-22, 2002

Correlation Between Oxygen Free Radicals and Cytochrome P-450 Activity in Breast Cancer Keiana Thomas, Tasha Smith, Maryam foroozesh, Nitsa Rosenzweig CUR April 2002.

Funding

"Separation and Molecular Markers Identification of Breast Cancer Cells. Implications for Diagnosis and Prognosis", DoD, 112,252, June 2002 – May 2005. Not funded.

"Career Development – Molecular Markers in Breast Cancer", DoD, $277,047, June 2002 – May 2006. Not funded.

"Neurotechnology Research, Development and Enhancement", NIH, $125,000, 08.01.2002-07.31.2007. Pending.

"Application of Functional Magnetic Nanoparticles for Ultrasensitive Detection of Ovarian Cancer", DOD, $478,601, 06.01.2003-06.30.2005. Pending.

"Louisiana nanotechnology initiative", NSF-EPSCoR, $105,000, June 2001-June 2004. Funded.

Employment

Based on the experience he gained in my lab, Mr. Imani Jones has received a lab technician position at LSU Medical School.
Ms. Griffin is pursuing a Ph.D. at MIT.
Ms. Crystal Lane graduated from Xavier this year and is applying to medical school.

CONCLUSIONS

The data collected in this work show that breast cancer cells have higher levels of OFR than normal breast cells. The results also indicate that OFR effect on growth, apoptosis, and cell death is concentration dependent. This finding provides a clue for breast cancer treatment. We have shown that by changing the concentration of OFR we can force the cells to favor apoptosis over growth.
The measurement of OFR is still imperfect and we continue to work, in collaboration with UNO, through the NSF-EPSCoR fund, on the development of sensor for OFR that will have no toxic effects on the cells.

REFERENCES

1. Cancer chemopreventive and antioxidant activities of pterostilbene, a naturally occurring analogue of resveratrol. Rimando AM, Cuendet M, Desmarchelier C, Mehta RG, Pezzuto JM, Duke SO. J Agric Food Chem 2002 Jun 5;50(12):3453-7

2. Induction of cell death by pro-oxidant action of Moxa smoke. Hitosugi N, Ohno R, Hatsukari I, Nakamura S, Mizukami S, Nagasaka H, Matsumoto I, Satoh K, Negoro T, Hashimoto K, Sakagami H. Anticancer Res. 2002 22:159-

163.

3. Activation of matrix metalloproteinase-2 by overexpression of manganese superoxide dismutase in human breast cancer MCF-7 cells involves reactive oxygen species. Zhang HJ, Zhao W, Venkataraman S, Robbins ME, Buettner GR, Kregel KC, Oberley LW. J. Biol. Chem. 2002 277: 20919-20926.

4. Jin Ji, Nitsa Rosenzweig, Christina Griffin, and Zeev Rosenzweig, "Synthesis and Application of Submicrometer Fluorescence Sensing Particles for Lysosomal pH Measurements in Murine Macrophages", Anal. Chem. (2000), 72: 3497-3503.

5. Jin Ji, Nitsa Rosenzweig, Imanie Jones and Zeev Rosenzweig, "Molecular Oxygen Sensitive Fluorescent Lipobeads for Intracellular Oxygen Measurements in Murine Macrophages", 2001 (published on the Internet ACS website June 2001).

6. Kerry McNamara, Thuvan Nguyen, Jin Ji, Gabriela Dumitrascu, Nitsa Rosenzweig and Zeev Rosenzweig, "Synthesis, Characterization and Application of Fluorescent Sensing Lipobeads for Intracellular pH Measurements in Single Cells", Anal. Chem (2001) 73: 3240-3246.

7. Jin Ji, Nitsa Rosenzweig, Imani Jones and Zeev Rosenzweig, " Optochemical Sensors and Probes for Single Cell Analysis. ", ACS Spring 2001.

8. Imani Jones, Crystal Lane, Tzucanow Cummings, Tamika Tyson, and Nitsa Rosenzweig. "Effect of intracerllular sensors on cells" Presentation at Southeast/Southwest Regional ACS Meeting, January 2001, New Orleans, LA.

9. "Development of A Digital Fluorescence Sensing Technique to Monitor the Response of Macrophages to External Hypoxia", Jacob K Asiedu[1], Jin Ji[1], Mai Nguyen[1], Nitsa Rosenzweig[2], and Zeev Rosenzweig[1]* J Biomed Opt 2001 Apr; 6(2):116-21

10. "A Novel Fluorescent Oxygen Indicator for Intracellular Oxygen Measurements", Jin Ji[1], Nitsa Rosenzweig[2], Imanie Jones[2] and Zeev Rosenzweig[1]* J. Biomed. Optics, 2002 (in press).

11. "MOLECULAR OXYGEN SENSITIVE FLUORESCENT LIPOBEADS FOR SINGLE CELL ANALYSIS", JIN JI [1] , IMANI JONES [2], NITSA ROSENZWEIG [2], AND ZEEV ROSENZWEIG[1] , Pitcon 2001, New Orleans Louisiana, March 2001 392

12. "Application of FRET microscopy for real time monitoring of drug delivery into single cells", Dumitrascu, Gabriela; Lane, Crystal; Jones, Imani; Rosenzweig,

Nitsa; Rosenzweig, Zeev. 223rd ACS National Meeting, Orlando, FL, United States, April 7-11, 2002

13. "Fluorescence transfer energy- new analytical tool for the drug delivery follow up", Gabriela Dumitrascu, Imani Jones, Nitsa Rosenzweig, and Zeev Rosenzweig Pittcon Conference, New Orleans, LA, March 17-22, 2002

14. Correlation Between Oxygen Free Radicals and Cytochrome P-450 Activity in Breast Cancer Keiana Thomas, Tasha Smith, Maryam foroozesh, Nitsa Rosenzweig CUR April 2002.

APPENDICES

APPENDICE 1 – Paper: "Synthesis and Application of Submicrometer Fluorescence Sensing Particles for Lysosomal pH Measurements in Murine Macrophages", Jin Ji, Nitsa Rosenzweig, Christina Griffin, and Zeev Rosenzweig, Anal. Chem. (2000), 72: 3497-3503.

Anal. Chem. **2000**, *72*, 3497–3503

Synthesis and Application of Submicrometer Fluorescence Sensing Particles for Lysosomal pH Measurements in Murine Macrophages

Jin Ji,[†] Nitsa Rosenzweig,[‡] Christina Griffin,[‡] and Zeev Rosenzweig*[,†]

University of New Orleans, Department of Chemistry, New Orleans, Louisiana 70148, and Xavier University of Louisiana, Department of Chemistry, New Orleans, Louisiana 70125

Phagocytosis of bioparticles such as bacteria and viruses by macrophages is a critical component of the immune response against infections. In this paper we describe the synthesis of submicrometer fluorescent particles with pH sensing capability. The particles are used to measure the pH and to monitor the effect of chloroquine, an antimalarial drug, on the pH in the lysosome, the cellular organelle involved in the phagocytosis process. The synthesis of the pH sensing particles is realized by the covalent attachment of amine reactive forms of Oregon Green (pH sensitive dye) and Texas Red (pH insensitive dye) to the surface of amino-modified submicrometer polystyrene particles. The particles are absorbed by J774 Murine Macrophages through phagocytosis and directed to lysosomes. Despite the high lysosomal levels of digestive enzymes and acidity, the absorbed particles remain stable for 12 h in the cells when they are stored in a PBS buffer solution at pH 7.4. The pH dynamic range of the sensing particles is between pH 4.5 and 7 with a sensitivity of 0.1 pH units. Exposure of the cells to chloroquine increases the lysosomal pH from 4.8 to 6.5. The effect is concentration-dependent.

Biological studies at the single-cell level have attracted the attention of researchers from various disciplines for decades. Two of the most popular cellular analysis techniques are fluorescence microscopy and flow cytometry.[1-6] Fluorescence microscopy is used for real-time continuous observation of cells, while flow cytometry is used to rapidly analyze a large number of single cells with a rate of analysis reaching up to 10 000 cells/second. Unlike in fluorescence microscopy, each cell is observed only once as it flows through the detection system of the flow cytometer. A common feature of these two complementary and well-advanced techniques is the employment of molecular fluorescent probes to label the observed cells.

The number of fluorescent probes for cellular analysis has been growing steadily over the last 20 years. Most notable are the numerous fluorescent probes for intracellular pH and free calcium ions.[7,8] Fluorescent probes for other cellular components (reactive oxygen species, inorganic and metal ions) and for cellular properties such as viability, morphology and fluid flow, and membrane potential have also been developed.[9] Nevertheless, the number of cellular constituents that can be quantified using fluorescence microscopy and flow cytometry is limited due to the cytotoxicity of most organic chromophors. Because of their cytotoxicity, it is also impossible to load the entire cell with bioactive molecules such as enzymes and antibodies for selective detection. Other problems associated with cellular labeling include possible alteration of cellular functions, false readings because of the heterogeneous intracellular distribution of fluorophors within the cell, and the possible cross-talk between adjacent cellular zones.

Submicrometer fiber-optic fluorescence-based sensors have been recently developed in an attempt to address the need for nontoxic and noninvasive intracellular measurement techniques.[10-13] To realize true noninvasive intracellular analysis, these sensors are about 100 times smaller than the analyzed cell. To prevent cytotoxicity upon insertion of the sensor into the cell, the sensing reagent is isolated from the cellular environment by a biocompatible matrix. In principle, it is possible to fabricate a sensor that contains several fluorophors and bioactive macromolecules such as enzymes, protein receptors, and antibodies for multiple analyte sensing. The scope of analytes that can be detected with these miniaturized sensors far exceeds the coverage of fluorescence microscopy and flow cytometry. In addition, miniaturized fluores-

[†] University of New Orleans.
[‡] Xavier University of Louisiana.

(1) Ploem, J. S. In *Applications of Fluorescence in the Biomedical Sciences*; Taylor, D. L., Waggoner, A. S., Lanni, F., Murphy, R. F., Birge, R. R., Eds.; Alan R. Liss: New York, 1986; Chapter 13.
(2) Melamed, M. R., Mullaney, P. F., Shapiro, H. M. In *Flow Cytometry and Sorting*, 2nd ed; Melamed, M. R., Lindmo, T., Mendelson, M. L., Eds.; Wiley & Sons: New York, 1990; Chapter 1.
(3) Dunn, K.; Maxfield, F. R. *Methods Cell. Biol.* **1998**, *56*, 217–236.
(4) Bastiaens, P. I. H.; Squire, A. *Trends Cell. Biol.* **1999**, *9*, 48–52.
(5) Darzynkiewicz, Z.; Bedner, E.; Li, X.; Gorczyca, W.; Melamed, M. R. *Exp. Cell. Res.* **1999**, *249*, 1–12.
(6) Oheim, M.; Loerke, D.; Chow, R. H.; Stühmer, W. *Philos. Trans. R. Soc. London, Ser. B* **1999**, *354*, 307–318.
(7) Johnson, I. *Histochem J.* **1998**, *30*, 123–140.
(8) de Silva, A. P.; Eilers, J.; Zlokarnik, G. *Proc. Natl. Acad. Sci. U.S.A.* **1999**, *96*, 8836–8837.
(9) Szucs, S.; Vamosi, G.; Poka, R.; Sarvary, A.; Bardos, H.; Balazs, M.; Kappelmayer, J.; Toth, L.; Szollosi, J.; Adany, R. *Cytometry* **1998**, *33*, 19–31.
(10) Shalom, S.; Strinkovski, A.; Peleg, G.; Druckmann, S.; Krauss, A.; Lewis, A.; Linial, M.; Ottolenghi, M. *Anal. Biochem.* **1997**, *244*, 256–259.
(11) Xin, Q.; Wightman, R. M. *Anal. Chem.* **1998**, *70*, 1677–1681.
(12) Koronczi, I.; Reichert, J.; Heinzmann, G.; Ache, H. J. *Sens. Actuators, B* **1998**, *51*, 188–195.
(13) Rosenzweig, Z.; Kopelman, R. *Anal. Chem.* **1995**, *67*, 2650–2654.

10.1021/ac000080p CCC: $19.00
Published on Web 06/16/2000

cent sensors can be used for site-specific intracellular measurements since problems associated with heterogeneity of the cellular environment and the distribution of fluorescent probes in the cell are eliminated.

The employment of a single fluorescent nanoparticle as an optochemical sensor by Sasaki et al. in 1996[14] marks the emergence of a new type of submicrometer fluorescence sensor. Sasaki et al. entrapped the pH sensitive dye fluorescein in polyacrylamide nanoparticles and used the resulting particles to measure the pH distribution in a water/glass interface. Recently, Kopelman et al. prepared a new type of fluorescent nanosensor named PEBBLEs (Probes Encapsulated by Biologically Localized Embedding).[15-18] In PEBBLEs, the sensing fluorophors are copolymerized or entrapped in hydrogel particles. PEBBLEs ranging from 20 to 200 nm in diameter were applied for pH, calcium ion, and nitric oxide measurements in single cells. These new nanosensors show very high selectivity and reversibility, fast response time, and reversible analyte detection. They were delivered into the observed cells by a variety of minimally invasive techniques, including picoinjection, gene-gun delivery, liposomal incorporation, and natural ingestion. The new technique offers several important advantages over previously described optical fiber nanosensors. First, chemical information can be obtained from a large number of cells simultaneously. Second, because of their small size, the particles can be used to detect analytes in cellular organelles. Third, the technique is truly noninvasive, allowing intracellular measurements while maintaining cellular viability. The confinement of the sensing dyes to the PEBBLE prevents dye compartmentalization and enables the differentiation of the nanosensor location from autofluorescence centers in the observed cells.

This paper describes the synthesis and spectral characterization of new and improved submicrometer fluorescent particles and their application as pH sensors in the lysosomes of Murine Macrophages. Macrophages are a natural target for particle-based fluorescence sensors because of their ability to absorb particles through phagocytosis. Phagocytosis of bioparticles such as bacteria or viruses by macrophages is recognized as a critical component of the immune response to infection.[19] In phagocytosis, the invading pathogens are directed into intracellular lysosomes, which are acidic organelles that are isolated from the cell cytoplasm and other organelles. The macrophages then release digestive enzymes and oxidative agents into the lysosomes to destroy the invading pathogen. The measurement of lysosomal pH can serve as an indication for lysosomal activity. Schlesinger et al. reported lysosomal pH measurements using bacterial or synthetic particles labeled with fluorescein.[20] Straubinger et al.

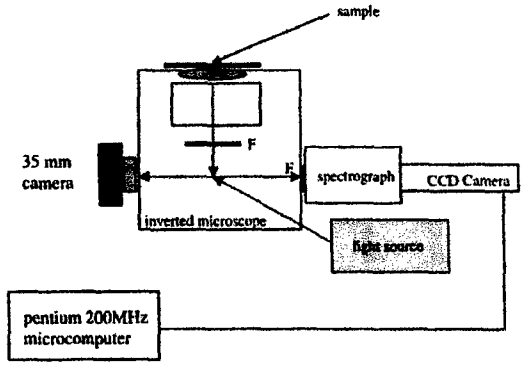

Figure 1. Digital fluorescence imaging microscopy system. The experimental setup consists of an inverted fluorescence microscope with a 40X objective (N.A. 0.9). A scanning spectrograph and a high performance charge coupled device camera (16-bit 512 × 512 chip size) are attached to one detection port. A 35-mm camera is attached to another detection port. A PC compatible microcomputer equipped with digital imaging analysis (Winspec 3.2, Roper Scientific) is used for data analysis.

used particles dually labeled with fluorescein (pH sensitive) and tetramethyl rhodamine (pH nonsensitive) to measure the lysosomal pH. The pH independent fluorescence peak of tetramethyl rhodamine was used as an internal standard to normalize the pH response of the particles.[21] However, spectral overlap between the emission peaks of fluorescein and tetramethyl rhodamine and the fluorescence resonance energy transfer between fluorescein and tetramethyl rhodamine limited the accuracy of the measurement. The sensing particles we fabricated in this study show significant improvement in sensitivity and stability compared with those of previously used particles in the analysis of macrophages. The analytical properties of the particles and their application to monitor the effect of the antimalarial drug chloroquine on the pH in the lysosomes are discussed.

EXPERIMENTAL SECTION

Digital Fluorescence Microscopy. The detection system used for fluorescence measurements of the sensing particles is shown in Figure 1. The system consists of an inverted fluorescence microscope (Olympus IX-70) equipped with three detection ports and with a 100-watt mercury lamp for excitation. The fluorescence is collected by a 40X-microscope objective with a numerical aperture of 0.75. A filter cube containing a 470–490-nm excitation filter, a 500-nm dichroic mirror, and a 515-nm cut-on emission filter is used to ensure spectral purity. The fluorescence signal is dispersed by a 150-mm three-mirror spectrograph (Acton Research, Inc.) equipped with a 600 grooves/mm grating, blazed at an optimum wavelength of 500 nm. The grating can be replaced with a mirror, and the exit slit can be removed from the path of the fluorescence signal signal to allow the image of the particles to pass through the spectrograph without being dispersed by the grating. A high-performance charged-coupled device (CCD) camera (Rupert Scientific, model 256HB) with a 512 × 512 pixel array is used for spectroscopic imaging or for digital fluorescence imaging of the particles. An exposure time of 0.5 s is used to acquire the fluorescence spectra of the particles. A PC micro-

(14) Sasaki, K.; Shi, Z.; Kopelman, R.; Masuhara, H. *Chem. Lett.* **1996**, 141–142.
(15) Clark, H. A.; Barker, S. L. R.; Brasuel, M.; Miller, M. T.; Monson, E.; Parus, S.; Shi, Z.; Song, A.; Thorsrud, B.; Kopelman, R.; Ade, A.; Meixner, W.; Athey, B.; Hoyer, M.; Hill, D.; Lightle, R.; Philbert, M. A. *Sens. Actuators, B* **1998**, *B51*, 12–16.
(16) Clark, H. A.; Hoyer, M.; Philbert, M. A.; Kopelman, R. *Anal. Chem.* **1999**, *71*, 4831–4836.
(17) Clark, H. A.; Kopelman, R.; Tjalkens, R.; Philbert, M. A. *Anal. Chem.* **1999**, *71*, 4837–4843.
(18) Clark, H. A.; Hoyer, M.; Philbert, M. A.; Kopelman, R. *Mikrochim. Acta* **1999**, *131*, 121–128.
(19) Roitt, I. M.; Brostoff, J.; Male, D. K. *Immunology*; Grower Medical Publishing Co.: New York, 1989, 1–4.
(20) Schlesinger, P. H. *Methods Cell. Biol.* **1994**, *45*, 289–311.
(21) Oh, Y. K.; Straubinger, R. M. *Infect. Immun.* **1996**, *64*, 319–325.

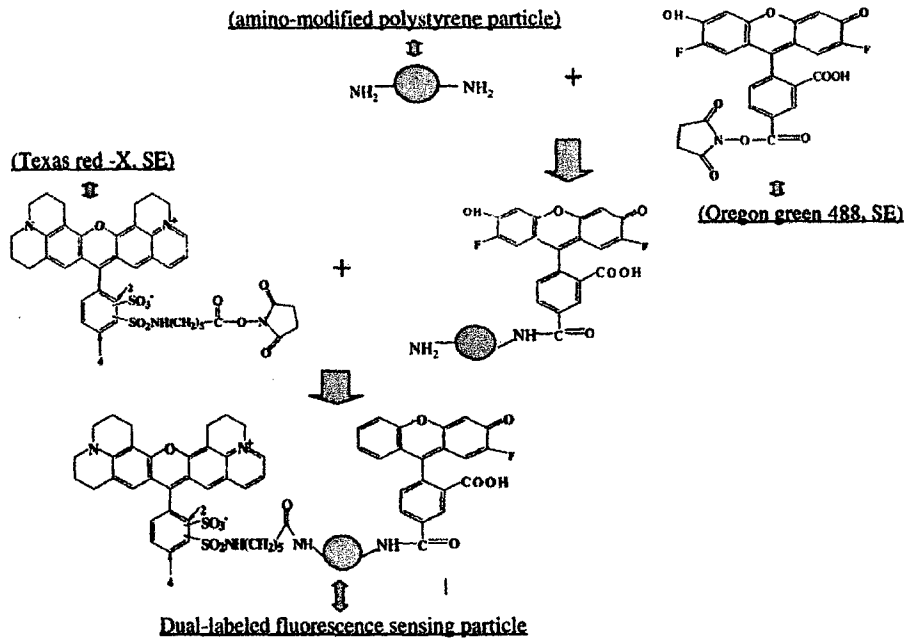

Figure 2. Synthesis of the pH sensing particles. Amino-modified submicrometer polystyrene particles react sequentially with succinimidyl ester derivatives of Oregon Green and Texas Red at room temperature in a light-tight environment.

computer (Gateway 2000, with a 200 MHz Pentium microprocessor) is employed for data acquisition. The Rupert Scientific software WinSpec/32 is used for image analysis.

Synthesis of Dual-Labeled Particles. Synthesis of submicrometer polystyrene particles coated with Oregon Green 488 and Texas Red is achieved by covalent attachment of succinimidyl ester (SE) derivatives of the dyes to the surface of amino-modified polystyrene particles as shown in Figure 2. An alternative coupling technique involves the use of isothiocynate (ITC) derivatives of the fluorophors. However, coupling through the SE functional group leads to the formation of an amide bond, which is more resistant to hydrolysis than the thio-amide bond formed using ITC coupling. Additionally, succinimidyl ester derivatives show higher coupling reactivity to amino-modified polystyrene particles than isothiocynate derivatives.

The preparation of the particles is carried out according to the following procedure: 250 μL of a 5.75% suspension of polystyrene particles is diluted by 6-fold into a 1.5-mL buffer solution of 0.1 M sodium hydrogen bicarbonate (pH 8.3). The diluted particle solution is sonicated in an ice bath for 5 min to ensure monodispersity. Then, a 1.5-mL solution of 300 μM Oregon Green 488, SE, and 0.1 M sodium hydrogen bicarbonate is slowly added to the particle solution under continuous sonication. The mixture is mixed periodically with a Pasteur pipet to avoid aggregation. The gently stirred reaction mixture is incubated for 2 h at room temperature in the dark. Then, a 15-μL solution of 40 μM Texas Red and SE dissolved in Dimethylformamide is slowly added to the particle solution under sonication. The gently stirred reaction mixture is incubated overnight at room temperature in the dark to complete the labeling. The particles are precipitated by slow-speed centrifugation (1000g) for 10 min, washed 3 times, and stored in a buffer solution of 0.1 M sodium hydrogen bicarbonate at pH 8.3. The particle suspension is protected from room light to prevent photo-oxidation. The particles are stable for at least 3 weeks under these storage conditions.

Cell Culture. Cultures of J774 Murine Macrophages are maintained according to a standard protocol.[22] The cells are cultured in Dulbecco's modified Eagle's medium supplemented with 4 mM L-glutamine, 1.5 g/L sodium bicarbonate, 4.5 g/L glucose, 1 mM sodium pyruvate, and 10% fetal bovine serum. The cells are grown at 37 °C in 5% CO_2. The medium is replaced 3 times a week. To prepare subcultures, the cells are scraped in new medium and split into new plates.

Phagocytosis of the pH Sensing Particles by Macrophages. The macrophages are detached from the culture plate surface by scraping. The medium containing cells is centrifuged at 500*g* for 10 min to precipitate the cells. Cells are collected and diluted into $(1-3) \times 10^6$ cells/mL solutions using fresh medium. The concentration of the cells is determined by standard hemacytometry using Trypan Blue to assess cell viability.[23] For phagocytosis experiments, 1 mL of cells ($(1-3) \times 10^6$ cells/mL) is incubated in the dark at 37 °C for 15 min with 200 μL of a 0.5% suspension of fluorescence-sensing particles. The cells are then washed 3 times with a PBS buffer (pH 7.4) to remove particles in excess. A 10-μL sample of cells containing sensing particles is placed between two cover slips on the microscope stage and analyzed by digital fluorescence imaging microscopy.

Fluorescence Spectroscopy Measurements. The excitation and emission spectra of fluorescent dye solutions are obtained using a spectrofluorometer (PTI International, model QM-1), equipped with a 75 Watt continuous Xe arc lamp as a light source.

Materials. Oregon Green 488, Texas Red-X, and succinimidyl ester (SE) are obtained from Molecular Probes, Inc. A 5.75% (solids percentage) suspension of amino-modified particles with an average diameter of 0.9 μm (±1% variation) is obtained from Bangs Laboratory, Inc. Aqueous solutions are prepared with 18 MΩ deionized water produced by a water purification system

(22) Gordon, S. *BioEssays* **1995**, *17*(11), 977–986.
(23) *Biochemicals, Organic Compounds for Research and Diagnostic Reagents*; Sigma Chemical Co.: St. Louis, MO, 1998; pp 1844–1845.

(Barnstead Thermolyne Nanopure). pH buffers are obtained from Fisher Scientific. Sodium hydrogen bicarbonate and dimethylformamide are purchased from Aldrich. J774 Murine Macrophages are purchased from ATCC (American Type Culture Collection). The Dulbecco's modified Eagle's medium and bovine serum albumin are purchased from Sigma. All reagents are used as received without further purification.

RESULTS AND DISCUSSIONS

Choice of Fluorescence Indicators. Fluorescein is frequently used in biological applications because of its high absorptivity and emission quantum yield in the visible range of the electromagnetic spectrum. When derivatized with acetomethyl ester group, fluorescein becomes cell-permeable and can be used for various intracellular applications including pH measurements. As previously mentioned, fluorescein has been used to determine the pH in intracellular lysosomes.[20,21] However, the lysosomal pH of 5 is below the pH range of fluorescein (pK_a = 6.4),[24] preventing accurate pH measurement. Oregon Green 488 is used as a pH indicator in our measurements. Like fluorescein, Oregon Green 488 is excited at 488 nm and its maximum emission is around 520 nm. Oregon Green 488 shows a 2-fold increase in photostability compared with fluorescein. More importantly, the pK_a of Oregon Green 488 is 4.7, which makes it more suitable than fluorescein for site-specific pH determination in intracellular lysosomes.

Texas Red, a pH nonsensitive fluorescent dye is co-immobilized to the surface of the sensing particles, and its fluorescence is used as a reference signal. Texas Red is selected over tetramethyl rhodamine, another commonly used pH nonsensitive fluorescent dye. The two dyes are highly photostable, and like Oregon Green 488, can be excited at 488 nm. They show a strong red shift with a maximum emission wavelength longer than 600 nm. A comparison between the two dyes is shown in Figure 3. Figure 3a shows the fluorescence spectra of solutions containing 0.3 μM Oregon Green 488 and 15 μM carboxytetramethyl rhodamine at (a) pH 4, (b) pH 5, (c) pH 5.5, (d) pH 6 and (e) pH 7, when excited at 488 nm. A spectral overlap between the two emission peaks is noticeable. Furthermore, the fluorescence peak of tetramethyl rhodamine increases by 15% when the pH increases from 4 to 7. The change in the level of the reference signal with increasing pH limits the accuracy of the measurement. Unlike in experiments where Oregon Green is used to measure the pH without the presence of a reference dye, the Oregon Green emission peak increases slightly at pH values higher than 6.5. This increase, and the instability of the emission peak of tetramethyl rhodamine, are partially attributed to spectral overlap between the two emission peaks. It is possible that fluorescence resonance energy transfer (FRET) between Oregon Green 488 (donor) and tetramethyl rhodamine (acceptor) also contributes to the signal change of the reference dye. FRET between fluorescein, which is very similar in its structural and spectral properties to Oregon Green 488, and carboxytetramethyl rhodamine has been previously studied.[25] For example, DNA primers tagged with fluorescein and tetramethyl rhodamine are used in a recently introduced FRET based

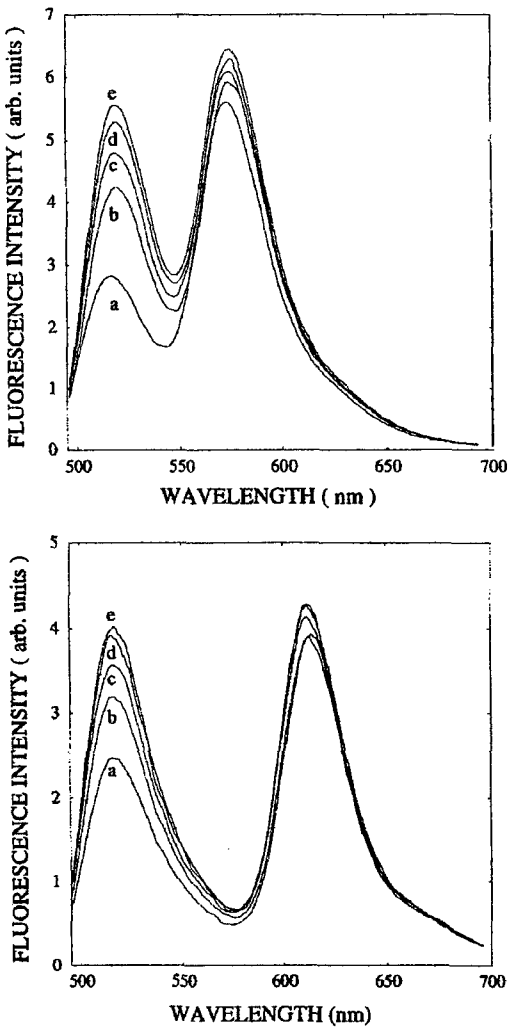

Figure 3. (a) Fluorescence spectra of 0.3 μM Oregon Green 488 and 15 μM carboxyltetramethyl rhodamine solutions of pH values ranging from 4 to 7. (b) Fluorescence spectra of 0.3 μM Oregon Green and 15 μM Texas Red solutions of pH values ranging from 4 to 7. The samples are excited at 488 nm.

4-fluorophore DNA sequencing technique.[26] Figure 3b shows the fluorescence spectra of solutions containing 0.3 μM Oregon Green 488 and 15 μM Texas Red at (a) pH 4, (b) pH 5, (c) pH 5.5, (d) pH 6, and (e) pH 7 (pH 4–7) when excited at 488 nm. A baseline separation between the fluorescence peaks is observed. While the optimal excitation wavelength of Texas Red is 595 nm, it can still be excited at 480 nm with 16-fold lower excitation efficiency. Increasing the density of Texas Red on the surface of the particles negates the loss of fluorescence signal due to the low excitation efficiency.

A digital fluorescence image of the submicrometer dually labeled fluorescent sensing particles is shown in Figure 4a. The particles are spherical in shape and average 0.9 micrometer in diameter. They are evenly coated with the fluorophors. The signal-to-noise ratio of the fluorescent particles is about 200. Figure 4b shows the emission spectrum of the dually labeled particles. The

(24) Vergne, I.; Constant, P.; Laneelle, G. *Anal. Biochem.* **1998**, *255*, 127–132.
(25) Mergny, J. L. *Biochemistry* **1999**, *38*(5), 1573–1581.
(26) Ju, J.; Kheterpal, I.; Scherer, J. R.; Ruan, C.; Fuller, C. W.; Glazer, A. N.; Mathies, R. A. *Anal. Biochem.* **1995**, *231*(1), 131–140.

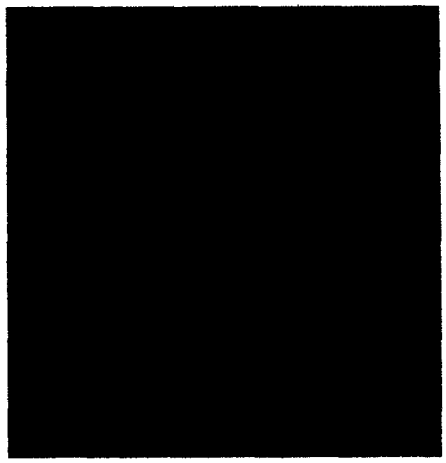

(a)

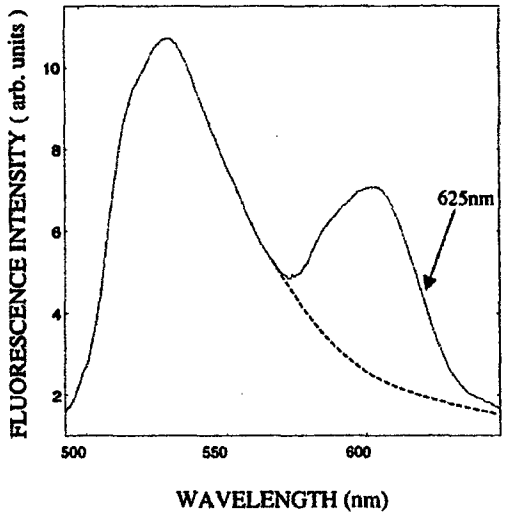

(b)

Figure 4. (a) Digital fluorescence image of 0.9-μm dually labeled fluorescent sensing particles. The sensing particles are suspended in a PBS buffer solution at pH 6. A 470–490-nm excitation filter, a 505-nm dichroic mirror, and a 515-nm cut-on emission filter are used to collect the image through a 40X microscope objective. The exposure time is 0.5 s. (b) Fluorescence spectrum of the dually labeled particles at pH 6. Despite the partial overlap between the emission peaks, the contribution of Oregon Green to the peak height at 625 nm is negligible.

spectrum is obtained using the digital fluorescence imaging spectroscopy system described in Figure 1. A partial spectral overlap between the emission peaks of Oregon Green and Texas Red is observed. This spectral overlap is attributed to the covalent attachment of the dye molecules to the surface of the particles. To increase the accuracy of the pH measurements, the reference signal is measured at 625 nm, 20 nm red-shifted from the maximum emission peak of Texas Red. It can be seen that the contribution of the Oregon Green to the peak height at 625 nm is less than 10%. As a result, the peak height at 625 nm shows only a 5% variation when the pH of the sample solution is changed from 4 to 7.

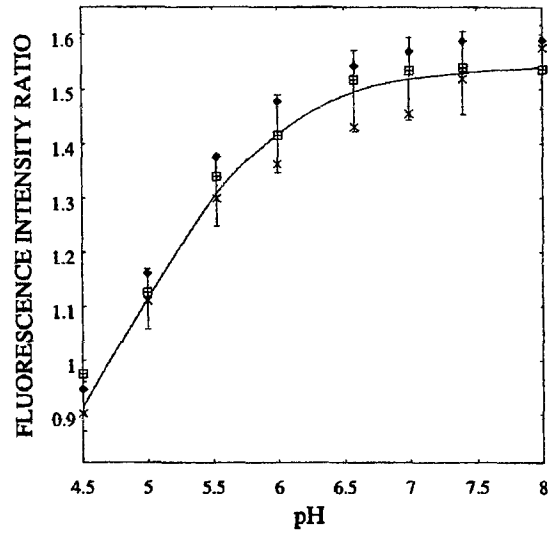

Figure 5. A pH calibration curve of the pH sensing particles. The ratio between the fluorescence intensities of Orgeon Green at 525 nm and Texas Red at 625 nm is plotted against the pH of standard buffer solutions.

Photostability of the pH Sensing particles. To test the photostability of the particles, samples of particles were placed on the microscope stage and illuminated continuously at 480 nm. The fluorescence intensity of Oregon Green 488 decreases by approximately 10% during 30 min of continuous illumination, while the fluorescence intensity of Texas Red does not change under these illumination conditions. During our kinetic measurements, the particles are exposed to the excitation light for less than 1 s in each measurement. Each experiment lasts 30 min, and images are taken in 30-s intervals. We therefore conclude that under our illumination conditions the particles remain photostable throughout the experiment.

Calibration of the pH Sensing Particles. The pH sensing particles are calibrated against standard solutions of pH 4–7. The particles are immobilized to the negatively charged surface of a glass cover slip by spin-coating. The particles adsorb strongly to the glass surface at acidic and natural pHs, allowing replacement of solutions over the immobilized particles. To calibrate single particles, a diluted solution of pH sensing particles is visualized through the microscope. A particle is then positioned at the center of the field of view. The field of view is imaged through a slit, allowing only the fluorescence of one particle to be dispersed by the attached spectrograph. A CCD camera collects the fluorescence spectrum of the particle. The pH is determined on the basis of the ratio between the emission peaks of Oregon Green at 515 nm and the emission peak of Texas Red at 625 nm. Figure 5 describes the pH dependence of the ratio between the fluorescence signals of Oregon Green 488 and Texas Red obtained from 10 pH sensing particles. A variation of about 5% in the signal ratio of different particles at a given pH is observed. The dynamic range of the particles is found to be between pH 4.5 and 7, with a pH sensitivity of 0.1 pH unit. The response time of the particles is less than 1 s.

Intracellular pH Measurements. As previously mentioned, the particles are internalized by the macrophages and directed to intracellular lysosomes. A bright-field image and a digital

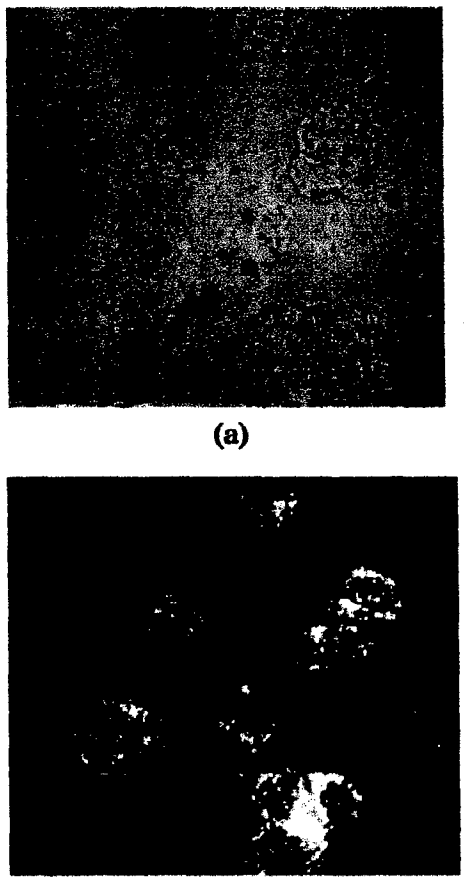

Figure 6. (a) Bright field transmission image and (b) Digital fluorescence image of 0.9-μm fluorescent particles internalized by macrophages. The particles remain stable in the cells up to 12 h after ingestion.

fluorescence image taken through a 40X-microscope objective of 0.9-μm fluorescent particles internalized by macrophages are shown in Figure 6. The bright-field image shows that individual particles are isolated from each other in the cell. The signal-to-noise ratio in the fluorescence image is about 100. The lysosomal pH is determined by comparing the ratio between the fluorescence signal of Oregon Green 488 at 525 nm and the fluorescence signal of Texas Red at 625 nm to the pH calibration curve (Figure 5). We assume that the pH calibration curve constructed from data obtained in aqueous solution can be used to determine the lysosomal pH. Since it is impossible to calibrate the pH probe inside the cell, one must interpolate the results obtained in aqueous solution to the cellular environment. To test this interpolation, we measured the effect of bovine serum albumin (BSA), a major cellular constituent, on the fluorescence intensity of the pH sensing beads. BSA is a hydrophobic protein that is likely to adsorb to the surface of the particles. A slight decrease of less than 10% in the fluorescence intensity of Oregon Green and Texas Red was observed. The ratio between the fluorescence intensities of the indicators shows only a marginal change, which is lower than the ±5% error of our digital fluorescence imaging and spectroscopy system.

The lysosmal pH, measured immediately after phagocytosis of the particles, is measured in a large number of Murine

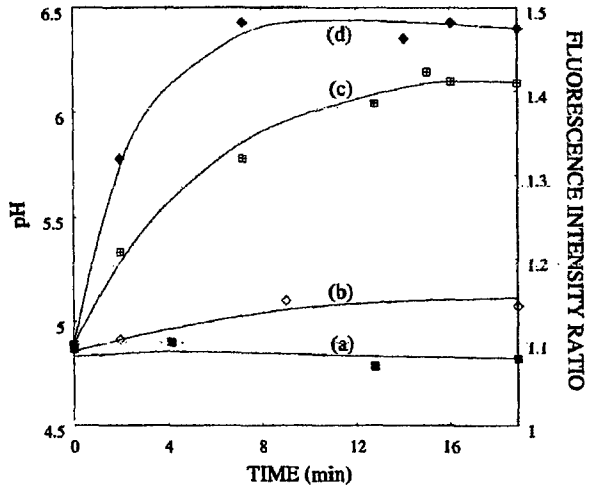

Figure 7. Effect of chloroquine on lysosmal pH. The ratio between the fluorescence intensities of Oregon Green and Texas Red (right) and the lysosomal pH (left) are plotted against a time coordinate at increasing chloroquine concentrations. Curve a represents a control experiment in chloroquine-free solution. Curves b, c, and d represent the effect of 10, 50, and 100 μM chloroquine, respectively, on the lysosomal pH. The lysosomal pH increase due to exposure to chloroquine is concentration-dependent.

Macrophages to be 4.8 ± 0.1. It increases to 5.2 ± 0.1 when the cells are kept for 1 h in a PBS solution of pH 7.4. This result is in agreement with previous studies that use flow cytometry to analyze the pH in the lysosomes of macrophages.[27,28] The particles maintain their structural integrity and fluorescence intensity for 12 h, indicating that the conditions in the lysosomes do not chemically affect the polystyrene particles. To demonstrate the utility of the newly synthesized fluorescence-sensing particles, we use them to monitor the lysosomal pH when the cells are exposed to increasing concentrations of the antimalarial drug, chloroquine.[29] Chloroquine has been shown to induce a lysosomal pH increase in macrophages,[30] which may be related to its antimalarial activity. Figure 7 describes the effect of increasing chloroquine concentrations on the lysosomal pH of individual macrophages. Curve a is a control experiment performed in a chloroquine-free solution. It shows that the fluorescence-intensity ratio between the emission peaks of Oregon Green and Texas Red remains constant in the absence of chloroquine throughout the experiment. This observation clearly indicates that the ratio between the fluorescence intensities of the indicators is not affected by the lysosomal environment during the experiment. Curves b, c, and d describe the effect of 10, 50, and 100 μM chloroquine on the pH in the lysosomes. A concentration of 10 μM does not cause a noticeable pH increase, while a concentration of 100 μM increases the pH from 4.8 to 6 in about 2 min. The pH further increases to 6.5 in 10 min of chloroquine exposure.

SUMMARY AND CONCLUSIONS

Submicrometer pH sensing fluorescent particles were prepared and applied for lysosomal pH measurements in Murine Macro-

(27) Lukas, G. L.; Rotstein, O. D.; Grinstein, S. *J. Biol. Chem.* **1991**, *266*, 24540–24548.
(28) Bassoe, C. F.; Laerum, O. D.; Glett, J.; Hopen, G.; Haneberg, B.; Solberg, C. O. *Cytometry* **1983**, *4*, 254–262.
(29) Homewood, C. A.; Warhurst, D. C.; Peters, W.; Baggaley, V. C. *Nature (London)* **1972**, *235*(5332), 50–52.
(30) Ohkuma, S.; Poole, B. *Proc. Natl. Acad. Sci. U.S.A.* **1978**, *7*, 3327–3331.

phages. The development of particle-based intracellular sensors represents a new trend in the application of fluorescence in cellular biological studies, addressing the need for miniaturized, site-specific, and noninvasive intracellular measurement techniques. Like in previous studies, the fluorescent particles are used for noninvasive cellular analysis. However, the use of a high-resolution digital fluorescence imaging and spectroscopy system allows us to monitor in real time a dynamic pH change in macrophages when they are charged with increasing concentrations of chloroquine. Using this system, we have been able to quantitatively measure the fluorescence of the same particles and the same living cells during experiments that last 20 min. We have clearly shown that the pH response of macrophages to external stimuli (chloroquine charge) is concentration-dependent. Moreover, we have been able to monitor this dynamic event in a number of cells simultaneously. Additionally, our pH sensing particles show a significant improvement in analytical properties over previous studies because of several reasons. First, the dye molecules are covalently immobilized to the surface of the particles. The covalent immobilization of the dye molecules to the surface of the particles shortens their response time because the analyte ions do not need to diffuse into the bulk of the synthetic or bioparticles to interact with the sensing fluorophors. The covalent immobilization of dyes to the surface of the particles prevents dye leaking. Leaking of fluorescent dyes is a common problem in sensors fabricated by physically entrapping hydrophilic sensing reagents like pH indicators in a polymer matrix. A disadvantage of the covalent approach is the exposure of the fluorescence indicators to the lysosomal environment. Unlike in the newly fabricated PEBBLEs,[16-18] the fluorescence dyes are not encapsulated in the polymeric matrix of the particles and are not protected from the cellular environment. However, our results show that the emission properties of the particles remain constant for 20 min when the dually labeled fluorescent particles are loaded into macrophages that are suspended in chloroquine-free solution. Moreover, the particles are not affected by levels of bovine serum albumin (BSA) in solution of up to 50 μM. Second, we use surface-modified polystyrene particles as the polymer support for the sensing reagents. Polystyrene particles show higher chemical stability than bioparticles or hydrogels and are better suited to the lysosomal conditions characterized by high acidity and high concentration of digestive enzymes. Third, we use a unique pair of dye molecules for the pH measurements. The particles are dually labeled with Oregon Green 488 (pH sensitive dye) and Texas Red (pH nonsensitive dye). Oregon Green 488 proves to be a better lysosomal pH indicator than fluorescein, which was previously used as a pH indicator in lysosomal pH measurements. This is due to its lower pK_a and higher photostability. Texas Red proves to be a better reference dye than carboxytetramethyl rhodamine, which was previously used as an internal standard in lysosomal pH measurements. The improvement in the stability of the reference peak is attributed to greater spectral separation between the emission peaks of Texas Red and Oregon Green 488 and to lower probability for fluorescence resonance energy transfer between the dyes. It also leads to a marked improvement in the sensitivity of lysosomal pH measurements with a pH sensitivity of ± 0.1 pH unit.

Currently we are investigating ways to synthesize fluorescence-sensing particles for lysosomal measurement of hydrogen peroxide. These particles will be used to study the effect of oxidative agents and antioxidants on the level of reactive oxygen species (ROS) and oxidative activity in the lysosomes.

ACKNOWLEDGMENT

This work is supported by the National Science Foundation through CAREER Grant CHE-9874498 and by a Research Grant from the Cancer Association of Greater New Orleans (CAGNO). The authors thank Tom Weise from Xavier University of Louisiana School of Pharmacy for the use of his cell culture laboratory.

Received for review January 24, 2000. Accepted May 6, 2000.

AC000080P

APPENDICE 2 – Paper: "Molecular Oxygen Sensitive Fluorescent Lipobeads for Intracellular Oxygen Measurements in Murine Macrophages", Jin Ji, Nitsa Rosenzweig, Imanie Jones and Zeev Rosenzweig, Anal. Chem. 2001 (published on the internet ACS website June 2001).

Molecular Oxygen-Sensitive Fluorescent Lipobeads for Intracellular Oxygen Measurements in Murine Macrophages

Jin Ji,[†] Nitsa Rosenzweig,[‡] Imanie Jones,[‡] and Zeev Rosenzweig*,[†]

Department of Chemistry, University of New Orleans, New Orleans, Louisiana 70148, and Department of Chemistry, Xavier University of Louisiana, New Orleans, Louisiana 70125

Intracellular oxygen concentration is of primary importance in determining numerous physiological and pathological processes in biological systems. This paper describes the development and application of micrometer-sized oxygen-sensitive fluorescence lipobeads for intracellular measurements of molecular oxygen in J774 murine macrophages. A ruthenium diimine complex $[Ru(bpy\text{-}pyr)(bpy)_2]Cl_2$ (bpy = 2,2′-bipyridine, bpy-pyr = 4-(1″-pyrenyl)-2,2′-bipyridine) is used as the oxygen indicator. The indicator exhibits high chemical and photostability and high sensitivity to oxygen. The indicator molecules are immobilized in a phospholipid membrane that coats polystyrene microparticles. The fluorescence of the lipobeads is effectively quenched by molecular oxygen. The fluorescence intensity of the oxygen-sensitive lipobeads is 3 times higher in a nitrogenated solution than in an oxygenated solution. The lipobeads are internalized by murine macrophages through phagocytosis. They maintain their spectral properties for 24 h in living cells when the cells are stored in phosphate-buffered saline at pH 7.4. The photostability, reversibility, and effect of hypoxia, hyperoxia, and oxidative stress on the intracellular level of oxygen in J774 murine macrophages are described.

Intracellular oxygen concentration is a key indicator of numerous physiological and pathological processes in biological systems. In cells, excess oxygen leads to overproduction of the extremely reactive and unstable reactive oxygen species (ROS), which oxidize lipids, carbohydrates, DNA, and proteins, altering their structure and function.[1,2] The determination of oxygen concentration is of particular importance in tumor cells since it may enable the prediction of the response of the tumor to radiation and chemotherapy.[3-5] The development of a real-time measurement technique for the determination of intracellular oxygen concentrations would be highly valuable for studies aiming to reveal how oxygen imbalance affects normal and cancerous cells.

Despite the significance of intracellular oxygen in various biochemical processes, there are surprisingly few analytical methods to measure its levels.[6,7] The role of oxygen in cellular processes is mostly assessed by indirect data derived from the measurement of extracellular oxygen concentration. This approach is ambiguous, as there is a difference between intracellular and extracellular oxygen concentrations.[8,9] Clark electrodes have been widely used to measure extracellular oxygen levels in cell culture media.[6,10] However, when applied to intracellular studies, the electrodes may cause structural damage to the cell membrane due to penetration. The use of oxygen microelectrodes only enables the measurement of molecular oxygen in one cell at a time and is not suitable for applications that require fast cell screening. Furthermore, the technique often gives misleading information due to the abundance of interfering species in the cytoplasm. The consumption of oxygen by the electrodes can alter the cellular oxygen level near the electrode and lead to false readings as well.

Nuclear magnetic resonance (NMR) spectroscopy provides a noninvasive method for intracellular oxygen concentration measurements.[5,11] However, in NMR, the concentration of oxygen is analyzed indirectly from measurements of oxygen-dependent metabolic species. The technique is limited in temporal resolution due to the relatively long relaxation time of biologically relevant nuclei and in spatial resolution due to the size of NMR probes. Electron spin resonance (ESR) spectroscopy has also been used for intracellular and extracellular oxygen measurements.[12-15] This

[†] University of New Orleans.
[‡] Xavier University of Louisiana.

(1) Tortora, G.; Funke, B.; Case, C. L. *Microbiology*. 5th ed.; The Benjamin/Cummings Publishing Co. Inc.: Reading, MA, 1995; pp 413–414.
(2) Martínez-Cayuela, M. *Biochimie* **1995**, *77*, 7–161.
(3) Lo, Y. Y.; Cruz, T. F. *J. Biol. Chem.* **1995**, *270* (20), 11727–11730.
(4) McIlroy, B. W.; Curnow, A.; Buonaccorsi, G.; Scott, M. A.; Brown, S. G.; MacRobert, A. *J. Photochem. Photobiol. B: Biol.* **1998**, *43*, 47–55.
(5) Glickson, J. J., Wehrle, J. P., Rajan, S. S., Li, S. J., Steen, R. G., Pettegrew, J. W., Eds. NMR spectroscopy of tumors. In *NMR: Principles and Applications to Biomedical Research;* Springer-Verlag: New York, 1990; pp 255–309.
(6) Lau, Y. Y.; Abe, T.; Ewing, A. G. *Anal. Chem.* **1992**, *64* (15), 1702–1705.
(7) Chen, K.; Ng, C. E.; Zweier, J. L.; Kuppusamy, P.; Glickson, J. D.; Swartz, H. M. *Magn. Reson. Med.* **1994**, *31* (6), 668–672.
(8) Robiolio, M.; Rumsey, W. L.; Wilson, D. F. *Am. J. Physiol.* **1989**, *256* (6 pt 1), C1207–1213.
(9) Glockner, J. F.; Swartz, H. M.; Pals, M. A. *J. Cell. Physol.* **1989**, *140* (3), 505–511.
(10) Titovets, E. *Anal. Biochem.* **1987**, *166* (1), 79–82.
(11) Long, R. C.; Papas, K. K.; Sambanis, A.; Constantinidis, I. *J. Magn. Reson.* **2000**, *146* (1), 49–57.
(12) Glockner, J.; Norby, S. W.; Swartz, H. M. *Magn. Reson. Med.* **1993**, *29* (1), 12–18.
(13) Santini, M. T., Morelli, G.; Fattorossi, A.; Malorni, W.; Rainaldi, G.; Indovina, P. L. *Free Radical Biol. Med.* **1996**, *20* (7), 915–924.

10.1021/ac010344n CCC: $20.00
Published on Web 00/00/0000

technique is based on the interaction between molecular oxygen and paramagnetic materials such as nitroxides. Oxygen broadens the ESR spectral lines of paramagnetic probes via Heusenberg spin exchange in a concentration-dependent manner. The use of these paramagnetic probes combined with recent instrumental developments extends the use of ESR to large water-containing specimens and enables the measurement of oxygen in the same type of samples used for NMR studies of cells. However, the technique is susceptible to electromagnetic interference and lacks real-time measurement capability.

Fluorescence microscopic techniques have been used widely for the measurement of pH and ion levels in single cells.[16,17] The measurements are based on the interaction of fluorophors with the ions of interest, which results in a concentration-dependent change in their fluorescence intensity. Recently, we reported the use of the fluorophore tris(1,10-phenanthroline)ruthenium chloride ($Ru(phen)_3$) for the measurement of the effect of external hypoxia on the molecular oxygen level in J774 murine macrophages. The measurement was based on the fluorescence quenching of $Ru(phen)_3$ by molecular oxygen. However, these measurements had limited sensitivity due to instability of the fluorescence intensity of $Ru(phen)_3$ in the cellular environment. A continuous negative signal drift observed in these experiments was attributed to the interaction of $Ru(phen)_3$ with cellular components such as proteins, DNA, and ROS. Fiber-optic oxygen sensors have also been fabricated for oxygen measurements in cells.[18,19] In these sensors, the fluorescence indicator is immobilized in a polymer matrix that is attached covalently to the distal end of the fiber. The polymer matrix protects the dye from the effect of intracellular macromolecules and ROS. Unlike oxygen electrodes, fiber-optic oxygen sensors do not consume oxygen during measurements. However, invasion or penetration of the sensor into the observed cell still occurs and structural damage to the cell membrane is a concern. Similarly to electrodes, the application of fiber-optic oxygen sensors for cellular analysis has been also limited by their low throughput.

To overcome the low throughput of electrodes and fiber-optic sensors, Kopelman et al. developed a new type of nanosensor named PEBBLEs (*p*robes *e*ncapsulated *b*y *b*iologically *l*ocalized *e*mbedding). PEBBLEs (ranging from 20 to 200 nm in diameter) were fabricated and applied for intracellular measurements of pH, molecular oxygen, calcium ions, glucose, and nitric oxide in single cells.[20-22] These new nanosensors show very high selectivity and reversibility, fast response time, and reversible analyte detection. They are delivered into the observed cells by a variety of minimally invasive techniques, including picoinjection, gene gun delivery, liposomal incorporation, and natural ingestion. The new technique offers several important advantages. First, as in cellular labeling techniques, chemical information can be obtained from a large number of cells simultaneously. Second, because of their small size the particles can be used to detect analytes in cellular organelles. Third, the technique is truly noninvasive, allowing intracellular measurements while maintaining cellular viability. Last, embedding the fluorescence sensing dyes in the PEBBLEs avoids dye compartmentalization and enables the differentiation of the nanosensor location from autofluorescence centers in the observed cells. However, PEBBLE-based fluorescence sensors have some structural problems that limit their quantitative power. Hydrophobic particles do not disperse in aqueous samples and tend to aggregate. As a result, hydrophilic PEBBLEs, where the sensing indicator is embedded in hydrophilic polymers, e.g., hydrogels, have been prepared and used to measure analyte levels in aqueous samples and cells. This approach limits the sensing technique to hydrophilic indicators. Furthermore, unless the indicators are covalently bound to the polymer network, a high leaking rate is expected, which decreases the stability and sensitivity of the sensor.

Recently we reported the synthesis and application of micrometric phospholipid-coated polystyrene particles named lipobeads as intracellular pH sensors.[23,24] In lipobeads, the sensor is composed of a polymer particle coated with a phospholipid membrane. The fluorescence-sensing molecules are immobilized in the membrane. The interaction between the dye and cellular components is minimized, as well as the toxicity of the dye. This paper describes the preparation, characterization, and application of oxygen-sensitive lipobeads for real-time intracellular oxygen measurements in J774 murine macrophages. A highly hydrophobic ruthenium metal complex, $Ru(bpy\text{-}pyr)(bpy)_2$, (bpy = 2,2′-bipyridine, bpy-pyr = 4-(1″-pyrenyl)-2,2′-bipyridine) is used as the oxygen indicator.[24] The indicator displays strong emission via metal-to-ligand charge transfer (MLCT) with an excited-state lifetime of 1.3 μs. It exhibits a high molar absorption coefficient of $2 \times 10^4\ M^{-1}\ cm^{-1}$ at 456 nm and an emission quantum yield of 0.1 at 632 nm, which presents a preferable large Stoke shift. The oxygen-sensitive lipobeads show significant improvement in stability and biocompatibility compared to previously used sensors in intracellular studies. The analytical properties of the lipobeads and their application for oxygen measurements in murine macrophages under conditions of hypoxia, hyperoxia, and oxidative stress are discussed.

EXPERIMENTAL SECTION

Digital Fluorescence Microscopy. The experimental setup used for fluorescence measurements of the oxygen-sensitive lipobeads is shown in Figure 1. The system consists of an inverted fluorescence microscope (Olympus IX-70) equipped with three detection ports. A 100-W mercury lamp is used as the light source for excitation. The fluorescence is collected by a 20× or 40× microscope objective with a numerical aperture 0.5 or 0.9,

(14) Povich, M. J. *Anal. Chem.* **1975**, *47* (2), 346–347.
(15) Lai, C. S.; Hopwood, L. E.; Hyde, J. S.; Lukiewicz, S. *Proc. Natl. Acad. Sci. U.S.A.* **1982**, *79* (4), 1166–1170.
(16) Radosevic K.; de Grooth, B. G.; Greve, J. *Cytometry* **1995**, *20* (4), 281–289.
(17) Muallem, S.; Zhang, B. X.; Loessberg, P. A.; Star, R. A. *J. Biol. Chem.* **1992**, *267* (25), 17658–17664.
(18) Stefansson, E.; Peterson, J. I.; Wang, Y. H. *Am. J. Physiol.* **1989**, *256* (4 Pt 2), H1127–1133.
(19) Zhao, Y.; Richman, A.; Storey, C.; Radford, N. B.; Pantano, P. *Anal. Chem.* **1999**, *71*, 3887–3893.
(20) Clark, H. A.; Marion, H.; Martin, A. P.; Kopelman, R. *Anal. Chem* **1999**, *71*, 4831–4836.
(21) Clark, H. A.; Kopelman, R.; Tjalkens, R.; Philbert, M. *Anal. Chem* **1999**, *71*, 4837–4843.
(22) Clark, H. A.; Barker, S. L. R.; Brasuel, M.; Miller, M. T.; Monson, E.; Parus, S.; Shi, Z. Y.; Song, A.; Thorsrud, B.; Kopelman, R.; Ade, A.; Meixner, W.; Athey, B.; Hoyer, M.; Hill, D.; Lightle, R.; Philbert, M. A. *Sens. Actuators B* **1998**, *51*, 12–16.
(23) McNamara, K. P.; Rosenzweig, N.; Rosenzweig, Z. *Proc. SPIE BiOS 2000 Symp.* **2000**, *3922*, 148–157.
(24) Simon, J. A.; Curry, S. L.; Schmehl, R. H.; Schatz, T. R.; Piotrowiak, P.; Jin, X. Q.; Thummel, R. P. *J. Am. Chem. Soc.* **1997**, *119*, 11012–11022.

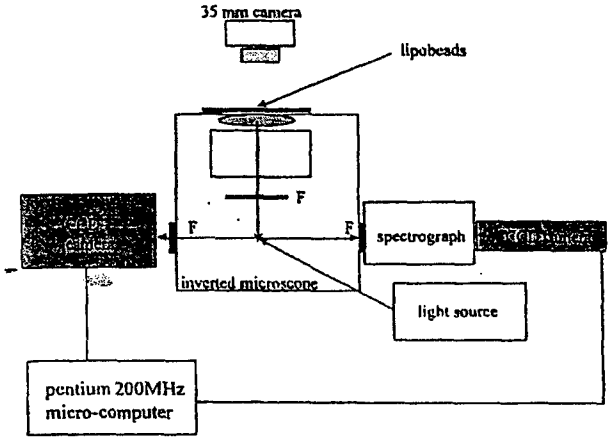

Figure 1. Digital fluorescence imaging microscopy system. The experimental setup consists of an inverted fluorescence microscope with a 20× or 40× objective (NA = 0.5 or 0.9) and a high-performance charge-coupled device camera (16-bit resolution, 512 × 512 chip size). A PC-compatible microcomputer equipped with digital imaging analysis (Winview 3.2, Roper Scientific) is used for data analysis.

respectively. A filter cube containing a 480-nm narrow band excitation filter, 500-nm dichroic mirror, and 515-nm long-pass emission filter is used to ensure spectral purity. A high-performance charge-coupled device (CCD) camera (Rupert Scientific, model 256HB) with a 512 × 512 pixel array is used for digital fluorescence imaging of the samples. The Rupert Scientific software Winview 3.2 is used for image analysis.

Synthesis of Oxygen-Sensitive Lipobeads. Four milligrams of polystyrene microspheres is dispersed in 100 μL of ethanol/hexane (v/v 1:1) mixture by sonication using a 47-kHz, Bransonic sonicator. A lipid stock solution (50 mM) is prepared with a 5:4:1 molar ratio of dimyristoylphosphatidylcholine, cholesterol, and dihexadecyl phosphate in chloroform. A 100-μL aliquot of of 0.1 mM $[(bpy)_2Ru(bpy\text{-}pyr)]Cl_2$ in $CHCl_3$ is added to the lipid solution. The solution is briefly vortexed to ensure homogeneity. A 100-μL aliquot of the microsphere suspension is then slowly added while the mixture is sonicated in an ice bath. The solution is kept at room temperature for 1 h to allow the indicator and the phospholipid molecules to absorb onto the surface of the particles. The sample is then dried overnight under nitrogen. The dried beads are resuspended in 1 mL of phospahte-buffered saline (PBS) solution at pH 7.4. The lipobeads solution is sonicated for 30 min in an ice bath to break formed aggregates, remove loosely bound indicator molecules, and ensure even phospholipid coating of the particles. Excess phospholipids, indicator, and uncoated beads are removed by centrifugation (1000*g*, 15 min). Lipobeads evenly coated with indicator and phospholipids are collected at the bottom of the glass centrifuge tube while the supernatant and floating beads are decanted. The low-speed centrifugation is necessary to minimize leakage of the indicator from lipobeads. The lipobeads are resuspended and stored in 2 mL of PBS (pH 7.4) at 4 °C. Under these storage conditions, the lipobeads maintain their oxygen sensitivity for at least two weeks.

Photostability Measurements of Ru(bpy-pyr)(bpy)$_2$. Solutions of $Ru(bpy\text{-}pyr)(bpy)_2$ and $Ru(phen)_3$ were continuously exposed to a 765-W xenon lamp in a Sunbox (Suntest CPS$^+$, Atlas Electric Devices Co.). The fluorescence intensity of the solutions was acquired every 5 min using a spectrofluorometer (PTI, Quantmaster).

Immobilization of Lipobeads on the Surface of a Chambered Cover Glass for Calibration Measurements. To immobilize the lipobeads, a chambered cover glass (borosilicate, Nalge Nunc International) is rinsed with 70% ethanol/water, followed by a thorough wash with deionized water. The chambered cover glass is incubated overnight in a 200-μL solution of 0.01% poly(L-lysine). It is then rinsed with deionized water and PBS solution at pH 7.4. A 200-μL lipobead suspension is then placed in the chambered cover glass for 1 h. The unimmobilized lipobeads are then rinsed out with a PBS solution at pH 7.4.

Cell Culture. Cultures of J774 murine macrophages are maintained according to a protocol described by Gordon et al.[25] The cells are cultured in Dulbecco's modified Eagle's medium supplemented with 4 mM L-glutamine, 1.5 g/L sodium bicarbonate, 4.5 g/L glucose, 1.0 mM sodium pyruvate, and 10% fetal bovine serum. The cells are grown at 37 °C under 5% CO_2. The medium is replaced three times a week. To prepare subcultures, the cells are scraped in new medium and split into new plates.

Cell Culture on the Surface of a Chambered Cover Glass. The macrophages are detached from the surface of a tissue culture plate by scraping. The cells are mixed with the growth medium by a glass pipet. A 5-μL aliquot of the cell suspension (~1 × 10^6 cells/mL) is then placed in a chambered cover glass. A total of 950 μL of fresh medium is added to the chamber. The cells are incubated to attach and grow on the chambered cover glass at 37 °C under 5% CO_2. Typically 80% confluency is achieved in 3 days.

Phagocytosis of Lipobeads by Macrophages. A solution of 150 μL of medium containing 0.5 mg/mL lipobeads is briefly sonicated and added to a chambered cover glass covered with cells at 80% confluence. The cells are incubated with the lipobead suspension at room temperature for 1 h to allow the phagocytosis of lipobeads to take place. The excess lipobeads are washed out with PBS solution at pH 7.4.

Materials and Reagents. Trisbipyridine-4-(1''''-pyrenyl)-2,2'-bipyridineruthenium chloride $(Ru(bpy\text{-}pyr)(bpy)_2]Cl_2)$ was a gift from Dr. Russell Schmehl of Tulane University. $Ru(phen)_3$ was purchased from Aldrich. 1,2-Dimyristoyl-*sn*-glycero-3-phosphocholine (DMPC) was purchased from Avanti Polar Lipids. Glucose, glucose oxidase from *Aspergillus niger* with enzymatic activity of 10 000 units/mL, 0.1% poly(L-lysine), menadione, Dulbecco's modified Eagle's medium, and bovine serum albumin were purchased from Sigma. J774 murine macrophages were purchased from American Type Culture Collection (ATCC). Lab-Tek II chambered cover glass used for microscopy and pH buffers were purchased from Fisher Scientific. Aqueous solutions were prepared with a 18-MΩ deionized water purification system (Barnstead Thermolyne Nanopure). PBS solutions at pH 7.4 were prepared from PBS tablets (Amresco). All reagents were used as received without further purification.

RESULTS AND DISCUSSION

Choice of Indicator. $Ru(II)(L)_3^{2+}$ complexes (L = 2,2'-bipyridine, 1,10-phenanthroline, or substituted derivatives) have been used frequently as indicators for oxygen level determination in gas samples and aqueous solutions due to their strong visible

(25) Gordon, S. *BioEssays* **1995**, *17* (11), 977–986.

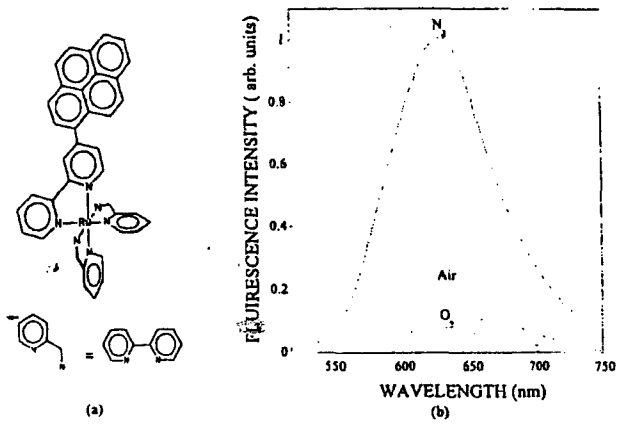

Figure 2. (a) Structure of Ru(bpy-pry)$(bpy)_2$. bpy = 2,2′-bipyridine, bpy-pyr = 4-(1″-pyrenyl)-2,2′-bipyridine). (b) Response of free [(bpy)-2Ru(bpy-pry)] to different oxygen levels in PBS at pH 7.4. The experiments are conducted in a spectrofluorometer.

absorption, high photochemical stability, high fluorescence quantum yield, and relatively long excited-state lifetimes. However, most of these complexes are hydrophilic. We have previously prepared and used lipobeads containing tris(1,10-phenanthroline)-ruthenium chloride for oxygen measurements in aqueous samples. However, because of the high leaking rate of $Ru(phen)_3$ from the lipobeads, the sensors show poor stability. In this study, a ruthenium(II) diimine−pyrene complex, Ru(bpy-pyr)$(bpy)_2$ (structure shown in Figure 2a), is used for the first time as an oxygen indicator for cellular oxygen measurements. In addition to the strong visible absorption, high photochemical stability, efficient fluorescence, and relatively long-lived MLCT excited state, this indicator is hydrophobic and has low solubility in aqueous solutions. It adsorbs strongly to the membrane of the lipobeads, showing insignificant leakage rate during two weeks storage in PBS solution at pH 7.4. Figure 2b shows the fluorescence spectra of Ru(bpy-pyr)$(bpy)_2$ in nitrogen, air, and oxygen-saturated solutions. Due to dynamic quenching by molecular oxygen, the fluorescence intensity of Ru(bpy-pyr)$(bpy)_2$ in a nitrogen-saturated solution is 13 times higher than the fluorescence of the dye in an oxygen-saturated solution. The dependence of the fluorescence intensity of the dye on the concentration of dissolved oxygen is determined by the Stern−Volmer equation.[26] The indicator responds more efficiently to a lower range of oxygen concentration.

Formation of Lipobeads. The phospholipid-coated polystyrene beads, lipobeads, are formed through physical adsorption. When a hydrophobic dye such as Ru(bpy-pyr)$(bpy)_2$ is added to the lipobead suspension, the dye molecules are trapped in the hydrophobic regions of the phospholipid membrane coating of the particles. The phospholipid membrane formed on the surface of the polystyrene core is not only biocompatible but also provides protection for the sensing fluorophore from the intercellular environment. Interaction between the dye and proteins is minimized, as well as intracellular sequestration and toxicity of the dye. A digital fluorescence image of fluorescent lipobeads averaging 2.1 μm in diameter is shown in Figure 3. It can be seen that the lipobeads are evenly coated with the indicator and exhibit bright fluorescence with a signal-to-noise ratio of 20. Photostability study of the new indicator is conducted by comparing its photobleaching property with that of the highly photostable Ru-$(phen)_3$ complex. The two dyes are exposed to a 765-W senon lamp in a Sunbox continuously for 1 h. Both dyes show a 50% fluorescence decrease in 30 min of continuous exposure to light (data not shown). The photobleaching rates are comparable. To minimize the photobleaching rate of the dye and the effect of cellular autofluorescence, excitation light at the nonoptimum excitation wavelength of 480 nm is used for oxygen measurements instead of the optimum excitation wavelength of 460 nm. Additionally, a neutral density filter of 1.0 is used to reduce the excitation intensity of the 100-W mercury light source. We also limit the exposure time to 0.5 s and the number of exposures during kinetic measurements to 20 in order to protect the fluorescent lipobeads from photobleaching. Under these conditions, the lipobeads are photostable during experiments that last up to 1 h.

Figure 3. Digital fluorescence image of 2.1-μm oxygen-sensitive lipobeads: Light source, 100-W mercury lamp; excitation filter, D480/30X; dichroic mirror, 500 nm; emission filter, BA 515 nm; objective:, 20× with NA = 0.5; neutral density, 1.0; exposure time, 0.5 s. The imaging conditions remain the same through the experiments unless otherwise stated.

Analytical Properties of the Oxygen-Sensitive Lipobeads in Aqueous Solution. The fluorescence intensity of the lipobeads is ~3 times higher in nitrogenated solutions than in oxygenated ones. The analytical range of the lipobeads is governed by the respective quenching curve and the Stern−Volmer constant. The variation in the fluorescence intensity as a function of dissolved oxygen concentration is given by the Stern−Volmer equation: $I_0/I_c = 1 + K_{sv}[O_2]$, where I_0 is the fluorescence intensity of Ru(bpy-pyr)bpy_2 in a nitrogenated solution, I_c is the fluorescence intensity of Ru(bpy-pyr)bpy_2 in a solution of given dissolved oxygen concentration, and K_{sv} is the Stern−Volmer quenching constant. In principle, higher quenching constants result in higher accuracy at low levels of oxygen. This is due to the larger signal change

(26) Stern, O.; Volmer, M. *Z. Phys.* **1919**, *20*, 183−189.

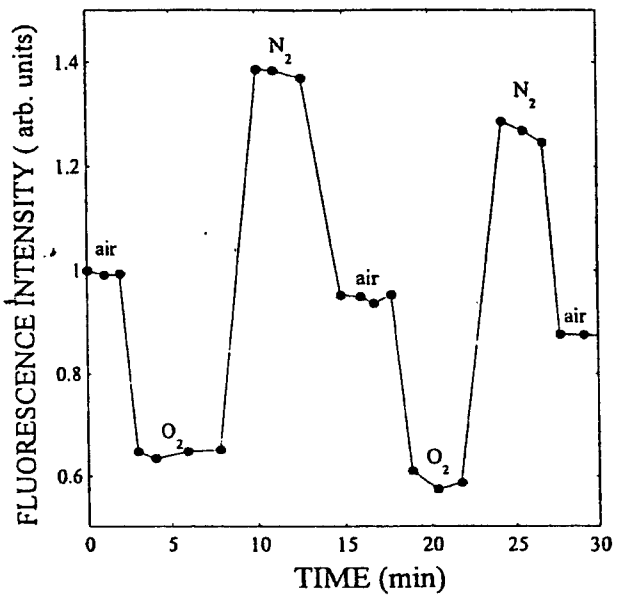

Figure 4. Reversibility of oxygen-sensitive Ru(bpy-pry)$(bpy)_2$-containing lipobeads. The lipobeads are repeatedly exposed to oxygenated or nitrogenated solutions. The experiments are conducted using a digital fluorescence microscopy system.

per oxygen concentration interval. However, high quenching constants result in a more limited linear dynamic range. K_{sv} for Ru(bpy-pyr)$(bpy)_2$ containing lipobeads is 4730 ± 5% M^{-1}. The linear dynamic range is between 0.1 and 12 ppm molecular oxygen with a correlation coefficient of 0.991. We found a standard deviation of ~4% between 10 consecutive fluorescence measurements in air-saturated solutions. The standard deviation increases at high oxygen levels where the signal is low up to 10%. To test the reversibility of the lipobeads, lipobeads are immobilized on the surface of a chambered cover glass coated with poly(L-lysine). The lipobeads are then exposed to oxygen-, air-, and nitrogen-saturated solutions repeatedly. Figure 4 describes the fluorescence intensity, normalized to the fluorescence intensity in air-saturated solution, of the immobilized lipobeads. The fluorescence of the lipobeads decreases by ~40% when the cells are incubated in an oxygen-saturated PBS solution, indicating an increase of the oxygen level over 12 ppm, the upper linear limit of the lipobead-based sensor. The fluorescence of the lipobeads increases instantly by 2.5-fold when the oxygenated buffer is replaced with a nitrogenated PBS solution. Replacing the nitrogenated solution with an air-saturated solution restores the fluorescence signal to its original level. It can be seen that the oxygen-sensing lipobeads are reversible and their response and recovery times are in the seconds time scale.

Intracellular Oxygen Measurements Using Oxygen-Sensing Lipobeads. The lipobeads are applied to monitor intracellular oxygen level changes in J774 murine macrophages. Lipobeads are internalized by the macrophages and directed to intracellular lysosomes through phagocytosis. A bright-field image and a digital fluorescence image taken through a 40× microscope objective of the lipobeads internalized by macrophages are shown in Figure 5. The lipobeads maintain their structural integrity, spectral properties, and oxygen sensitivity for over 24 h following phagocytosis. When the cells are exposed to extreme conditions of hyperoxia or hypoxia, they appear to resist the rapid gas diffusion before they are overwhelmed. However, such treatment leads to irreversible changes in the physical shape of the cells and eventually to cell death as confirmed by a standard Trypan Blue staining method.

To test the sensitivity of the lipobeads under less destructive conditions, we applied the oxygen-sensitive lipobeads to monitor the cellular response of individual macrophages to hypoxia caused by enzymatic oxidation of glucose in the medium. When a glucose/glucose oxidase solution is added into the cell medium, glucose oxidase catalyzes the oxidation of glucose. This enzymatic oxidation reaction consumes molecular oxygen. The rate of the oxidation and the steady-state level of oxygen in the medium depend on the glucose concentration and glucose oxidase activity. Figure 6 describes the response of cells to hypoxia caused by different concentrations of glucose/glucose oxidase. The response is observed by monitoring the signal change of Ru(byp-pyr)$(bpy)_2$-containing lipobeads in the macrophages. Curve c is the control experiment, conducted in a glucose- and glucose oxidase-free solution. It shows that the signal of lipobeads remains constant in the absence of glucose and glucose oxidase throughout the experiment. Curves a and b describe the cellular response of macrophages to 1.5 mM glucose with 5 units/mL glucose oxidase and 2.5 units/mL, respectively, in the solution. A 40 (a) and 30% (b) fluorescence increase is obtained in 4 min, indicating a decrease in the oxygen level in the intracellular lysosomes to 4 and 4.8 ppm, respectively. It is interesting to note that the variation between the fluorescence of the lipobeads in different cells increases with decreasing oxygen level. This results in an unusual situation where the error in the experiments increases with an increase in the fluorescence signal and signal-to-noise ratio. The number of dead cells increases with decreasing oxygen concentration. The large variation in the fluorescence of the lipobeads in cells under conditions of extreme hypoxia may be attributed to a difference in their fluorescence intensity in viable and dead cells. When the glucose/glucose oxidase solution is replaced with a PBS solution at pH 7.4 10 min after the start of the enzymatic reaction, the fluorescence intensity of the lipobeads drops back to its original value in ~5 min, indicating that a normal intracellular oxygen level has been restored. Trypan Blue staining shows that ~85% of the cells survive this treatment. However, when the glucose/glucose oxidase solution is replaced with a PBS solution at pH 7.4 20 min after the start of the enzymatic reaction, only 50% of the cells survive these conditions of hypoxia.

The oxygen-sensitive lipobeads are also applied to assess the effect of the oxidative agent menadione on the intracellular oxygen level in macrophages. Menadione is known to generate a large quantity of ROS when it enters cells.[27] It is believed that the semiquinone radicals that are generated through the one-electron reduction of quinines can rapidly reduce dioxygen to form superoxide anion radicals and, subsequently, hydrogen peroxide, hydroxyl radical, and other ROS.[27,28] Because of its prooxidant quality, menadione is often used to induce oxidative stress and study its effect on cells. Figure 7 describes the fluorescence intensity of lipobeads internalized in macrophages when the cells are exposed to the oxidizing agent menadione. Curve a is a control

(27) Thor, H.; Smith, M. T.; Hartzell, P.; Bellomo, G.; Jewell, S. A.; Orrenius, S. *J Biol Chem*, **1982**, *257*, 12419–12425.
(28) DeGroot, H.; Littauer, A. *Free Radical Biol. Med.* **1989**, *6*, 541–551.

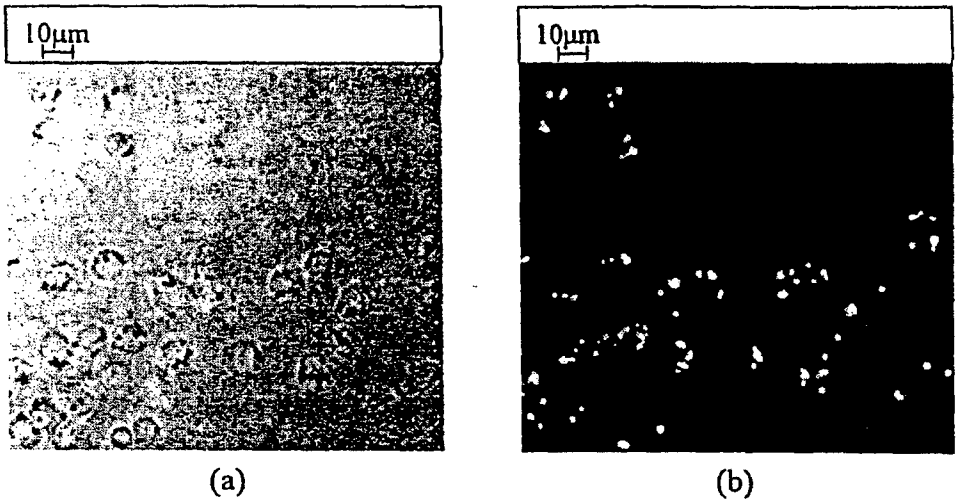

Figure 5. Phagocytosis of 2.1-μm [(bpy)$_2$Ru(bpy-pyr)] lipobeads. (a) A transmission image; (b) a digital fluorescence image of lipobeads internalized by macrophages. Objective: 40× with NA = 0.9.

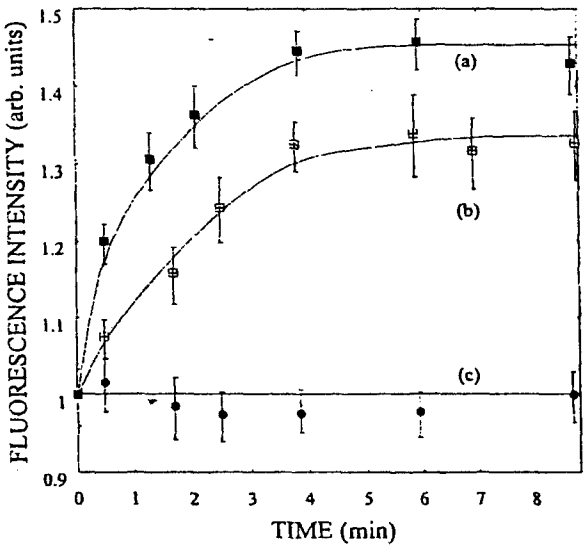

Figure 6. Intracellular oxygen level changes monitored by Ru(bpy-pry)(bpy)$_2$-containing lipobeads in macrophages. Curves a and b describe the response of the Ru(bpy-pry)(bpy)$_2$ lipobeads to a solution containing 1.5 mM glucose and (a) 2.5 and (b) 5 units/mL glucose oxidase. Curve c is a control experiment in a glucose/glucose oxidase-free solution. Error bar, 4%.

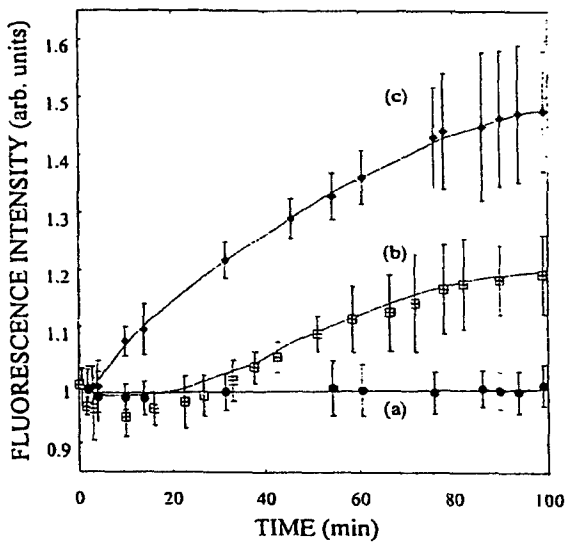

Figure 7. Response of (bpy)$_2$Ru(bpy-pry) lipobeads in macrophages to oxygen level changes induced by menadione. Curve a is the control experiment. The cells are incubated in PBS at pH 7.4 in the absence of menadione. Curves b and c describe the response of the lipobeads to solutions containing (b) 500 μM and (c) 1 mM menadione.

experiment showing that the fluorescence intensity of the lipobeads remain constant in a menadione-free solution. Curves b and c describe the fluorescence intensity of the internalized lipobeads when the cells are exposed to 1 (b) and 0.5 mM (c) menadione solutions. When the cells are exposed to 1 mM menadione, the fluorescence intensity of the lipobeads increases by 50% in ~2 h, indicating a decrease of the intracellular oxygen level to ~3.2 ppm. Treatment of the cells with 500 μM menadione results in a lower and slower change in the fluorescence intensity of the lipobeads. The decrease in oxygen level in the cells results from reduction of molecular oxygen by semiquinone radicals to form ROS. This leads to an increase in the fluorescence intensity of the lipobeads.

To evaluate the necessity of protecting the dye by immobilization in the phospholipid coating of the particles, we also measured the effect of menadione on cells loaded with free Ru(bpy-pyr)-(bpy)$_2$. We observed a 2-fold decrease in the fluorescence of the oxygen-sensitive dye when the cells were exposed to 1 mM menadione. Removal of menadione restored the signal of the dye to ~80% of its original value (data not shown). This experiment supports our prediction that, without protection, the sensing dye is prone to be affected by a variety of interfering species. In this case, the targeted agent itself, menadione, quenches the fluorescence intensity of the dye and leads to its partial degradation.

SUMMARY AND CONCLUSIONS

Oxygen-sensitive fluorescence lipobeads were prepared and used for the first time for intracellular oxygen measurements. A new oxygen indicator, Ru(bpy-pyr)(bpy)$_2$, was chosen as the oxygen indicator because of its high hydrophobicity, high oxygen sensitivity, large Stoke shift, and high photo- and chemical stability. The fluorescence intensity of single oxygen-sensing lipobeads in

nitrogenated solutions was 3 times higher than their fluorescence in oxygenated solutions. The oxygen-sensitive lipobeads enabled us to monitor noninvasively and in real time the level of molecular oxygen in cells. We were also able to monitor the kinetic response of murine macrophages to hypoxia induced by the enzymatic oxidation of glucose by glucose oxidase and to oxidative stress applied by the oxidative agent menadione. Moreover, we were able to monitor these processes in a large number of cells simultaneously. Our studies show that the protection of the oxygen-sensitive fluorescence indicator is necessary to prevent its destruction or false readings because of interaction of the indicator with cellular macromolecules or ROS. Fluorescent-sensing lipobeads offer significant improvement in analytical properties compared to previously used particle-based intracellular sensors. The charge properties of the particles are easily controlled to prevent aggregation. The unique hydrophobic core–hydrophilic shell structure enables the use of hydrophobic indicators in aqueous samples. The dye molecules are protected from the cellular environment by a membrane rather than being bound or adsorbed to the surface or the bulk of the particles. This shortens the response and recovery time of the particles. Currently, we are developing fluorescence-sensing lipobeads for glucose and for zinc and calcium ions. Fabrication of lipobeads through covalent attachment between the phospholipid membrane, the indicator, and the core surface of the particles is also being developed in our laboratory.

ACKNOWLEDGMENT

This work is supported by the National Science Foundation through CAREER grant CHE-9874498. The authors thank Dr. Russell Schmehl from Tulane University Department of Chemistry for providing us with the oxygen indicator Ru(bpy-pyr)(bpy)$_2$. The authors also thank Tom Weise from Xavier University of Louisiana School of Pharmacy for the use of his cell culture laboratory.

Received for review March 21, 2001. Accepted May 24, 2001.

AC010344N

APPENDICE 3 – Paper: "Synthesis, Characterization and Application of Fluorescent Sensing Lipobeads for Intracellular pH Measurements in Single Cells", Kerry McNamara, Thuvan Nguyen, Jin Ji, Gabriela Dumitrascu, Nitsa Rosenzweig and Zeev Rosenzweig, Anal. Chem (2001) 73:3240-3246.

Anal. Chem. 2001, *73*, 3240–3246

Synthesis, Characterization, and Application of Fluorescence Sensing Lipobeads for Intracellular pH Measurements

Kerry P. McNamara,[†] Thuvan Nguyen,[†] Gabriela Dumitrascu,[†] Jiri Ji,[†] Nitsa Rosenzweig,[‡] and Zeev Rosenzweig*,[†]

Department of Chemistry, University of New Orleans, New Orleans, Louisiana 70148, and Department of Chemistry, Xavier University of Louisiana, New Orleans, Louisiana 70125

This paper describes the synthesis and characterization of micrometric phospholipid-coated polystyrene particles, named lipobeads, with pH-sensing capability and their application for intracellular pH measurements in murine macrophages. The phospholipids used to coat the particles are labeled with fluorescein (a pH-sensitive dye) and tetramethylrhodamine (a pH-insensitive dye), which serves as a referencing fluorophore for increased accuracy of the pH measurements. The synthesis of the pH-sensing lipobeads is realized by the covalent attachment of the fluorescent phospholipids to the surface of carboxylated polystyrene particles. The pH dynamic range of the sensing particles is between 5.5 and 7.0 with a sensitivity of 0.1 pH unit. The excitation light intensity is reduced to minimize photobleaching of the fluorescein–phospholipid conjugates. The fluorescent lipobeads are used to measure the pH in single macrophages. The lipobeads are ingested by the macrophages and directed to lysosomes, which are the cellular organelles involved in the phagocytosis process. Despite the high lysosomal levels of digestive enzymes and acidity, the absorbed particles remain stable for over 6 h in the cells when they are stored in a phosphate-buffered saline solution at pH 7.4.

The development of optochemical sensors for use in biological samples has made remarkable advances in recent years. Cellular labeling, using fluorescent dyes sensitive to a given analyte of interest, has been able to give strong fluorescent signals that can be calibrated to determine specific levels of analytes.[1-3] However, cellular labeling is invasive and may chemically or physically damage the observed cells due to the high levels (μM to mM) of fluorophors required to obtain measurable signals. Additionally, cellular measurements using cellular labeling techniques provide average information about the observed cells. Miniaturized probes must be developed in order to decrease the invasiveness of fluorescence microscopic techniques and enable the interrogation of specific organelles in the cellular environment.

Phospholipid vesicles (liposomes) that form upon injection of phospholipids into water can encapsulate water-soluble materials.[4-6] Previously, we showed that encapsulated water-soluble fluorescence-sensing dyes display sensing properties similar to those observed in free solution.[7] Additionally, the liposome bilayer membrane can protect the dye from potentially quenching species likely to attenuate a fluorescent signal of the same dyes in free solution by up to 90%.[8] We prepared dye-encapsulating liposomes sensitive to pH,[9] Ca^{2+},[8] and O_2[10] and applied them successfully in volume-limited aqueous samples with resolution limited only by the imaging capabilities of the microscope used and the diffraction limit. Liposomes have also been shown capable of delivering encapsulated therapeutic and genetic material to specific biological areas, both in vitro[11] and in vivo ,[12] using ligand–receptor strategies for targeting specific cells or tissues. Normally in such approaches, the bilayer liposome membrane undergoes fusion and phospholipid exchange with the bilayer membrane of a cell, thereby delivering the liposome contents by passive uptake and avoiding acute damage to the cell.[13,14] However, the same process that enables drug or gene delivery into cells becomes an obstacle when liposome-based sensors are applied for intracellular or extracellular measurements. When incubated with cells, liposomes fuse with the cell membrane and deliver the encapsulated fluorescent dyes into the cytoplasm in a diffuse, nonspecific manner.[15] The result is an averaged analytical signal (with an associated decrease in resolution) for each cell, similar to that

† University of New Orleans.
‡ Xavier University of Louisiana.

(1) McNamara, K. P.; Yeung, E. S.; Rosenzweig, N.; Rosenzweig, Z. *Anal. Chim. Acta* **1997**, *356*, 75–83.
(2) Hedley, D. W.; Chow, S. *Cytometry* **1994**, *15*, 349–358.
(3) Kosower, E. M.; Kosower, N. S. *Methods Enzymol.* **1995**, *251*, 133–148.
(4) Batzri, S.; Korn, E. D. *Biochim. Biophys. Acta* **1973**, *298*, 1015–1019.
(5) Kremer, J. M. H.; Esker, M. W. J.; Pathmamanoharan, C.; Wiersema, P. H. *Biochemistry* **1977**, *16*, 3932–3935.
(6) Hope, M. J.; Bally, M. B.; Webb, G.; Cullis, P. R. *Biochim. Biophys. Acta* **1985**, *812*, 55–65.
(7) McNamara, K. P.; Rosenzweig, Z. *Anal. Chem.* **1998**, *70*, 4853–4859.
(8) McNamara, K. P.; Rosenzweig, Z. *Anal. Chem.*, submitted for publication.
(9) McNamara, K. P.; Rosenzweig, N.; Rosnezweig, Z. *Mikrochim. Acta* **1999**, *131*, 57–64.
(10) Floch, V.; Le Bolc'h, G.; Audrezet, M.-P.; Yaouanc, J.-J.; Clement, J.-C.; des Abbayes, H.; Mercier, B.; Abgrall, J.-F.; Ferec, C. *Blood Cells, Mol., Dis.* **1997**, *23*, 69–87.
(11) Bugelski, P. J.; Gennaro, D. E.; Poste, G.; Hoffstein, S. T. *J. Histochem. Cytochem.* **1989**, *37*, 843–851.
(12) Barber, K.; Mala, R. R.; Lambert, M. P.; Qiu, R.; MacDonald, R. C.; Klein, W. L. *Neurosci. Lett.* **1996**, *207*, 17–20.
(13) Struck, D. K.; Pagano, R. E. *J. Biol. Chem.* **1980**, *255*, 5404–5410.
(14) Muller, W. J.; Zen, K.; Fisher, A. B., Shuman, H. *Am. J. Physiol.* **1995**, *269*, L11–L19.
(15) Linseisen, F. M.; Hetzer, M.; Brumm, T.; Bayerl, T. M. *Biophys. J.* **1997**, *72*, 1659–1667.

10.1021/ac0102314 CCC: $20.00
Published on Web 06/14/2001

seen in cellular-labeling techniques. Clearly, for effective, site-specific cellular analysis, there is a need for a sensing geometry that can maintain mechanical stability as it passes through the cell membrane and cytoplasm and also preclude damage to the cell upon uptake or placement.

Kopelman et al. recently prepared a new type of nanosensors named PEBBLEs (*p*robes *e*ncapsulated by *b*iologically *l*ocalized *e*mbedding). PEBBLEs ranging from 20 to 200 nm in diameter for pH, molecular oxygen, calcium ions, glucose, and nitric oxide were fabricated and applied for intracellular measurements in single cells.[16-18] These new nanosensors show very high selectivity and reversibility, fast response time, and reversible analyte detection. They were delivered into the observed cells by a variety of minimally invasive techniques, including picoinjection, gene gun delivery, liposomal incorporation, and natural ingestion. The new technique offers several important advantages. First, as in cellular-labeling techniques, chemical information can be obtained on a large number of cells simultaneously. Second, because of their small size, the particles can be used to detect analytes in cellular organelles. Third, the technique is truly noninvasive, allowing intracellular measurements while maintaining cellular viability. Last, the confinement of the sensor reporter dyes to the PEBBLE avoids dye compartmentalization and enables the differentiation of the nanosensor location from autofluorescence centers in the observed cells. PEBBLE-based fluorescence sensors have some structural problems that limit their quantitative power. Hydrophobic particles do not disperse in aqueous samples and tend to aggregate. As a result, hydrophilic PEBBLEs, where the sensing indicator is embedded in hydrophilic polymers, e.g., hydrogels, have been prepared and used to measure analyte levels in aqueous samples. This approach limits the sensing techniques to hydrophilic indicators. Furthermore, unless the indicators are covalently bound to the polymer network, a high leaking rate is expected, which decreases the stability and sensitivity of the sensor.

The objective of this study is to prepare new sensing particles where hydrophilic or hydrophobic indicators are strongly immobilized to the particles. This will improve the chemical stability of particle-based fluorescence nanosensors and enable the use of hydrophobic indicators for sensing applications in aqueous samples. The study focuses on the preparation of core–shell structured particles in which a hydrophobic core is coated with a hydrophilic shell. Several research groups have previously described the synthesis of large polymer particles ranging in diameter from 20 to 100 μm that are coated with a monolayer or bilayer of phospholipids and their application as drug delivery vehicles.[19-23] In this work, we describe the synthesis and characterization of miniaturized phospholipid coated polystyrene particles with pH-sensing capability. These particles, termed "lipobeads" because they combine the mechanical stability of polymer beads and the unique spectroscopic properties and biocompatibility of liposomes, are applied for pH measurements in murine macrophages.

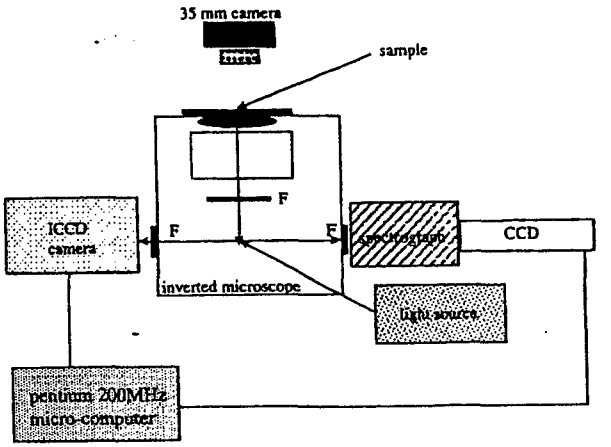

Figure 1. A digital fluorescence-imaging system for the measurement of micrometric fluorescent lipobeads. The instrument consists of an inverted fluorescence microscope equipped with continuous mercury light source. A slow-scan high-performance ICCD camera is used for imaging while a second high-performance CCD camera is coupled to a scanning spectrograph and used for fluorescence spectroscopy measurements. A microcomputer is used for data acquisition and analysis.

EXPERIMENTAL SECTION

Digital Fluorescence-Imaging Microscopy and Spectroscopy System. A schematic diagram of the experimental setup used to characterize the spectral properties of fluorescent lipobeads is shown in Figure 1. It consists of an inverted fluorescence microscope (Olympus IX70) equipped with a 100-W mercury lamp as a light source. The fluorescence image of the lipobeads may be collected using a 20× microscope objective with NA = 0.5, a 40× microscope objective with NA = 0.9, or an oil immersion 100× microscope objective with NA = 0.95. Two filter cubes are used to ensure spectral imaging purity. The filter cube for fluorescein imaging contains a 480-nm narrow band-pass excitation filter, a 500-nm dichroic mirror, and a 525 ± 15 nm narrow band-pass emission filter. The filter cube for rhodamine imaging contains the same excitation filter and dichroic mirror and a 580 ± 20 nm emission filter. A high-performance ICCD camera (Princeton Instruments, model BH2RFLT3) is employed for digital imaging of the lipobeads. A second high-performance CCD camera (Rupert Scientific, model 256HB) is used for spectral fluorescence imaging of the particles. The camera is coupled to a 150-mm three-mirror spectrograph (Acton Research Inc.) equipped with a 600 grooves/mm grating, blazed at an optimum wavelength of 500 nm. An exposure time of 0.1 s is used to acquire the fluorescence spectra of the particles. A PC microcomputer (Gateway 2000, with a 200-MHz Pentium microprocessor) is employed for data acquisition. The Rupert Scientific software WinSpec/32 is used for image analysis. The software Adobe PhotoShop v3.0 is used for the enhancement of presented images.

Synthesis of Fluorescent Lipobeads. Fluorescent lipobeads are synthesized based on a modified procedure originally de-

(16) Clark, H. A.; Hoyer, M.; Philbert, M. A.; Kopelman, R. *Anal. Chem.* **1999**, *71*, 4831–4836.
(17) Clark, H. A.; Kopelman, R.; Tjalkens, R.; Philbert, M. A. *Anal. Chem.* **1999**, *71*, 4837–4843.
(18) Clark, H. A., Barker, S. L. R., Brasuel, M., Miller, M. T., Monson, E., Parus, S., Shi, Z. Y., Song, A.; Thorsrud, B.; Kopelman, R.; Ade, A.; Meixner, W.; Athey, B.; Hoyer, M.; Hill, D.; Lightle, R.; Philbert, M. *Sens. Actuators B* **1998**, *51*, 12–16.
(19) Kim, Y.; Lichtenbergova, L.; Snitko, Y.; Cho, W. *Anal. Biochem.* **1997**, *250*, 109–116.
(20) Heiati, H.; Phillips, N. C.; Tawashi, R. *Pharm. Res.* **1996**, *13*, 1406–1410.
(21) Major, M.; Prieur, E.; Tocanne, J. f.; Betbeder, D.; Sautereau, A. M. *Biochim. Biophys. Acta* **1997**, *1327*, 32–40.
(22) Jin, T.; Pennefather, P.; Lee, P. I. *FEBS Lett.* **1996**, *397*, 70–74.
(23) Oh, Y. K.; Straubinger, R. M. *Infect. Immunol.* **1996**, *64*, 319–325.

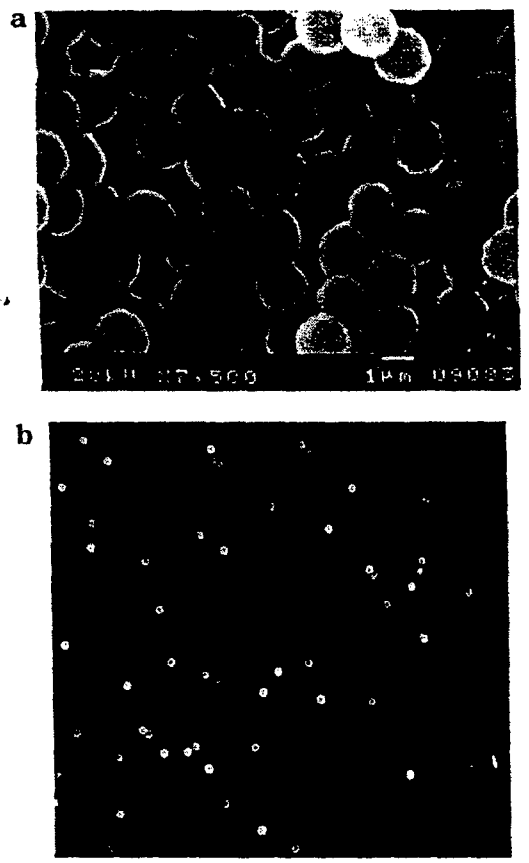

Figure 2. (a) Scanning electron micrograph of lipobeads averaging 1.6 μm in diameter. (b) A 40× digital fluorescence image of a washed sample of fluorescent lipobeads. The fluorescent lipobeads are spherical, uniform in size, and evenly coated. No aggregation is observed.

scribed by Kim et al.[19] The 1.6-μm polystyrene beads (40 mg/mL) are suspended in a 1:1 (v/v) ethanol/hexane solution. A 50 mM phospholipid (4:0.01:0.1:4:1 molar ratio) is prepared with dimyristoylphosphatidylcholine, fluorescein-DHPE, tetramethylrhodamine-DHPE, cholesterol, and dihexadecyl phosphate in chloroform. The excess of rhodamine DHPE over fluorescein-DHPE is due to the use of a 480-nm light for the excitation of the lipobeads. At this wavelength, the emission quantum yield of fluorescein is ~10 times larger than the emission quantum yield of tetramethylrhodamine. To prepare pH sensing lipobeads, 500 μL of the 50 mM phospholipid mixture is added to 200 μL of the particle suspension and sonicated for 10 min. The suspension is incubated at room temperature for 2 h and dried overnight under nitrogen stream at room temperature. The dried particles are then resuspended in 2 mL of phosphate buffer at pH 7 and sonicated for 15 min to ensure an even coating of phospholipids on the particles and to prevent the formation of multiple phospholipid layers. During the coating step, there is a simultaneous formation of liposomes in addition to the coated particles. The formed liposomes and uncoated particles are washed 3 times in a buffer solution using low-speed centrifugation of 1000 rpm for 15 min until the background is clean. A scanning electron microscopy (SEM) micrograph of the fluorescent lipobeads is shown in Figure 2a. The particles are spherical and average 1.6 μm in diameter with a narrow size distribution of ±1%. A digital fluorescence image of a washed sample of fluorescent lipobeads is shown in Figure 2b. It can be seen that the particles are evenly coated with the fluorophors. However, a 35% variation in the fluorescence intensity of the lipobeads is observed, suggesting that multilamellar films form on some of the polystyrene particles. The signal-to-noise ratio of the fluorescence measured from these particles is ~200. The fluorescent lipobeads are stored in a glass test tube covered with aluminum foil under nitrogen at room temperature until use.

Cell Culture of Murine Macrophages. Cultures of J774 murine macrophages are maintained according to a standard protocol.[24] The cells are cultured in Dulbecco's modified Eagle's medium (DMEM) supplemented with 4 mM L-glutamine, 20 mM sodium bicarbonate, 25 mM glucose, 1 mM sodium pyruvate, and 10% fetal bovine serum. The cells are grown at 37 °C in 5% CO_2. The medium is replaced 3 times a week. To prepare subcultures the cells are scraped in new medium and split into new plates. Before use, cells were scraped from the Petri dish and characterized for viability using Trypan Blue. Cells were then stored at 37 °C in 15 mL disposable tubes in a fresh DMEM solution until use. Cells were ~100 μm in diameter, although no precise sizing measurements were made.

pH Measurements in Macrophages Loaded with Fluorescence-Sensing Lipobeads. A sample of macrophages is detached from a culture plate surface by scraping. The medium containing cells is centrifuged at 500*g* for 10 min to precipitate the cells. Cells are collected and diluted into (1−3) × 10^6 cells/mL solutions using fresh medium. The concentration of the cells is determined by standard hemacytometry using Trypan blue to determine cell viability.[25] For phagocytosis experiments, 1 mL of cells ((1−3) × 10^6 cells/mL) are incubated in the dark at 37 °C for 15 min with 200 μL of a 0.5% suspension of fluorescence-sensing lipobeads. The cells are then washed 3 times with a PBS buffer (pH 7.4) to remove particles in excess. A 10-μL sample of cells containing sensing particles is placed between two cover slips on the microscope stage and analyzed by the digital fluorescence-imaging microscopy system.

Materials and Reagents. Amino-modified polystyrene particles (mean diameter, 1.6 μm, ± 0.5%) were purchased from Seradyn Instruments, Inc. (Indianapolis, IN) in dry form. *N*-(Fluorescein-5-thiocarbomyl)-1,2-dihexadecanoyl-*sn*-glycero-3-phosphoethanolamine (fluorescein-DHPE) and *N*-6-tetramethylrhodamine-thiocarbamoyl-1,2-dihexadecanoyl-sn-glycero-3-phosphoethanolamine (TRITC-DHPE) were obtained from Molecular Probes, Inc. (Eugene, OR). 1,2-Dimyristoyl-sn-glycero-3-phosphocholine (DMPC) was purchased from Avanti Polar Lipids. Sodium hydroxide and hexane were purchased from EM Sciences and used without further purification. Spectroscopic grade ethanol was purchased from Aldrich Chemical Co. (Milwaukee, WI). All aqueous preparations were made using Nanopure distilled water. Murine macrophages were purchased from the American Type Culture Collection (Manassas, VA) and cultured for growth in sterile Petri dishes using DMEM and glucose (Sigma). L-Glutamine was provided by Gibco.

(24) Verkman, A. S.; Takla, R.; Sefton, B.; Basbaum, C.; Widdicombe, J. H. *Biochemistry* **1989**, *28*, 4240−4244.
(25) Sigma Catalog; Sigma Chemical Co., St. Louis, MO, 2000; pp 1848−1849.

RESULTS AND DISCUSSION

Choice of Fluorescence Indicators. Fluorescein and tetramethylrhodamine are used frequently in cellular applications because of their high absorbance and emission quantum yield in the visible range of the electromagnetic spectrum. In our study, fluorescein is used as a pH indicator while tetramethylrhodamine serves as a reference dye to correct the observed fluorescein intensities for the heterogeneity in the excitation field, which is a common problem in fluorescence microscopes. It is also used to correct the data for fluctuations in the signal collection efficiency. The dyes are excited at 480 nm and show significant red shifts with maximum emission wavelengths of 525 and 575 nm. In lipobeads, the dyes are covalently attached to the polar headgroup or to the alkyl backbone of the phospholipid membrane coating the polystyrene beads. The peak maximums of the fluorescent lipobeads are similar to that of the dyes in solution. Additionally, the pH sensitivity of fluorescein and the pH insensitivity of tetramethylrhodamine are preserved when the dyes are bound to the phospholipid membrane.

Photostability of the pH-Sensing Lipobeads. To test the photostability of the fluorescent lipobeads, samples are placed on the microscope stage and illuminated continuously at 480 nm. The fluorescence intensity of fluorescein decreases by ~30% during 10 min of illumination while the fluorescence intensity of tetramethylrhodamine does not change under these illumination conditions. Because of the large difference in the photobleaching rate, tetramethylrhodamine cannot be used to correct the data for a decrease in the fluorescence of fluorescein due to photobleaching. To overcome the inherent instability of fluorescein, we limit the exposure time and the number of exposures of the fluorescent lipobeads to the excitation light during our kinetic measurements. The lipobeads are exposed to the excitation light for 0.1 s in each measurement. The number of exposures of the lipobeads is limited to 100. Under these illumination conditions, the fluorescein- and tetramethylrhodamine-containing lipobeads remain photostable throughout the experiment.

pH-Sensitivity Measurements. The pH-sensing lipobeads are calibrated against standard solutions of pH 5.0–8.0. The lipobeads are immobilized to a glass cover slip coated with a layer of poly(L-lysine). The lipobeads adsorb strongly to the coated glass surface, allowing replacement of measured solutions. To calibrate single lipobeads, a diluted solution of pH-sensing lipobeads is visualized through the microscope. A single lipobead located at the center of the field of view is imaged through a slit allowing only the fluorescence of the selected lipobead to be dispersed by the attached spectrograph. A CCD camera collects the fluorescence spectrum of the lipobead. The pH is determined based on the ratio between the emission peaks of fluorescein at 525 nm and tetramethylrhodamine at 575 nm. Figure 3a describes the fluorescence spectra of fluorescein- and tetramethylrhodamine-containing lipobeads in solutions of pH between 5.0 and 8.0. The pH dependence of the ratio between the fluorescence signals of fluorescein and tetramethylrhodamine obtained from 50 pH-sensing lipobeads is shown in Figure 3b. As previously mentioned, there is a variation of 35% in the fluorescence intensity of the lipobeads. In contrast, the variation in the ratio between the fluorescence intensities of fluorescein and tetramethylrhodamine in the different beads is only 10%. This observation suggests that

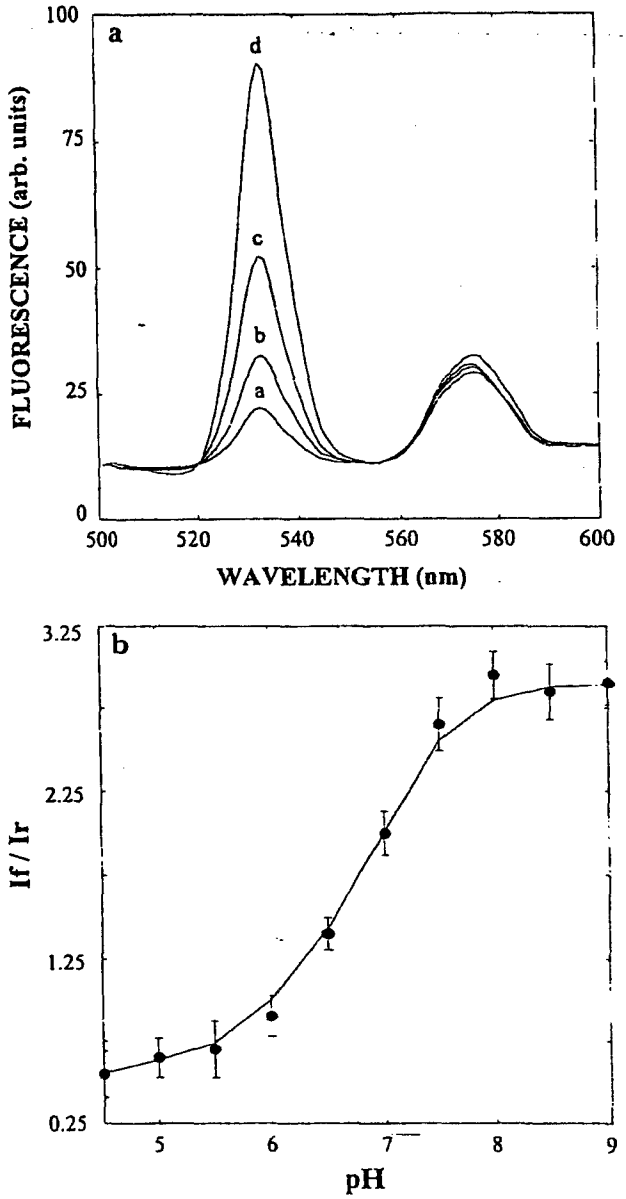

Figure 3. (a) Fluorescence spectra of individual fluorescein- and teramethylrhodamine-containing lipobeads in solutions of increasing pH: (a) pH 5, (b) pH 6, (c) pH 7, and (d) pH 8. (b) A pH calibration curve of the fluorescent lipobeads. The ratio between the fluorescence intensities of fluorescein (If) at 525 nm and tetramethylrhodamine (Ir) at 575 nm is plotted against the pH of standard buffer solutions.

the possible formation of multilamellar films around the beads does not significantly alter their pH sensitivity. The dynamic range of the particles is found to be between pH 5.5 and 7.5 with a pH sensitivity of 0.1 pH unit. The response time of the pH-sensing lipobeads is less than 1 s.

Effect of Quenchers on the Sensing Capability of Lipobeads. The interaction between macromolecules, e.g., proteins, and fluorescence or electrochemical sensors is a major concern, especially when the sensors are used to measure analyte levels in biological samples. Protection of the indicator from quenching species is particularly imperative in miniaturized particle-based sensors due to the limited number of fluorescence-sensing molecules, which ranges from 1000 to 10 000 molecules. The

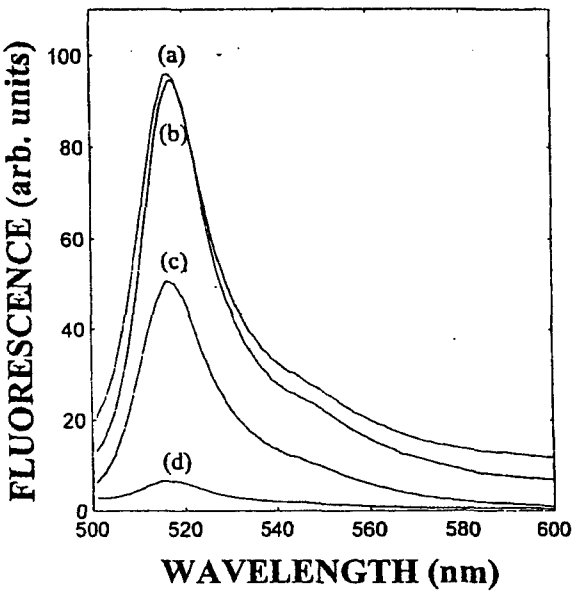

Figure 4. Fluorescence spectra of solutions containing the following: (a) 50 nM fluorescein; (b) lipobeads in which fluorescein is bound to the alkyl backbone of the phospholipid membrane; (c) lipobeads in which fluorescein is bound to the alkyl backbone of the phospholipid membrane and 1 μg/mL antifluorescein; (d) 50 nM fluorescein and 1 μg/mL antifluorescein. It can be seen that the membrane provides significant protection to fluorescein from quenching species such as anti-fluorescein.

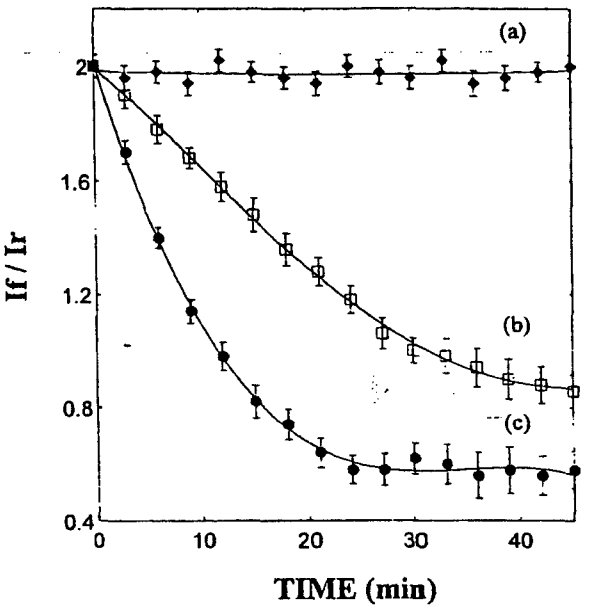

Figure 5. Temporal dependence of the ratio between the fluorescence intensities of fluorescein (If) and tetramethylrhodamine (Ir) in individual lipobeads monitoring the pH decrease during the enzymatic oxidation of glucose catalyzed by glucose oxidase. Curve a describes a control experiment where the lipobeads are suspended in a 10 mM oxygenated glucose solution in the absence of glucose oxidase. Curves b and c describe the fluorescence intensity of individual lipobeads in (b) air-saturated and (c) oxygen-saturated 10 mM glucose solutions containing 0.1 aunit/mL glucose oxidase. The fluorescence decrease is due to the accumulation of gluconic acid near the lipobead.

newly prepared lipobeads are coated with a phospholipid membrane that could protect the sensing molecules from quenching species. Figure 4 describes the fluorescence spectra of solutions containing the following: (a) 50 nM fluorescein, (b) lipobeads in which fluorescein is bound to the alkyl backbone of the phospholipid membrane, (c) lipobeads in which fluorescein is bound to the alkyl backbone of the phospholipid membrane and 1 μg/mL antifluorescein, and (d) 50 nM fluorescein and 1 μg/mL antifluorescein. The concentration of the fluorescein-containing lipobeads (curve b) is adjusted to a level that leads to a fluorescence intensity similar to the fluorescence intensity of the 50 nM flurescein solution (curve a). Since no autoquenching of the lipobeads' bound fluorescein is observed, we assume that there is a similar number of fluorophors in the fluorescein solution (curve a) and the fluorescein-containing lipobead solution (curve b). The effect of adding 1 μg/mL antifluorescein to solutions a and b is profoundly different. This level of antifluorescein quenches the fluorescence intensity of the free fluorescein solution by over 90%. The same level of antifluorescein quenches the fluorescence of the fluorescein-containing lipobeads solution by only 30%. Furthermore, increasing the concentration of antifluorescein to 5 μg/mL does not increase the quenching efficiency of the lipobeads. On the basis of these observations, it can be concluded that the phospholipid membrane provides significant protection to fluorescein from anti-fluorescein. The decrease in the fluorescence-quenching efficiency is attributed to the inability of the large anti-fluorescein molecules to penetrate the phospholipid membrane in order to form the antibody−antigen complex with fluorescein. Furthermore, the protection efficiency in lipobeads in which the fluorescein molecules are immobilized to the alkyl backbone of the phospholipid membrane is slightly higher than the protection efficiency in lipobeads in which the fluorescein molecules are bound to the phospholipid headgroups. Because of the significant protection efficiency, lipobeads in which the fluorescein molecules are bound to the alkyl backbone of the phospholipid membrane have been used to measure the pH in single cells and biological samples.

Measurement of a pH Change in a Volume-Limited Sample Using Single Lipobeads. The experiment described in this section demonstrates the capability of single lipobeads to monitor a pH change due to a chemical reaction in volume-limited samples containing only few microliters. A sample of lipobeads labeled with fluorescein and tetramethylrhodamine is added to a 100 μL of 10 mM glucose solution at pH 7.4. A 5-μL aliquot of glucose oxidase of 2.5 active units is then added to this solution and mixed by vortexing the sample. A 5-μL sample is then placed between two cover slips and continuously observed using the digital fluorescence-imaging system. The oxidation of glucose is catalyzed by glucose oxidase to form gluconic acid and hydrogen peroxide. The formation of gluconic acid leads to a decrease in the pH of the solution, which decreases the fluorescence of the observed lipobeads. Figure 5 describes the average temporal dependence of the ratio between the fluorescence intensities of fluorescein and tetramethylrhodamine in 10 individually analyzed lipobeads during the enzymatic reaction. Curve a describes a control experiment monitoring the fluorescence intensity of the lipobeads in an oxygenated aqueous solution at pH 7.4. It can be seen that the lipobeads are photostable under these conditions despite the high level of oxygen. Curve b describes the fluores-

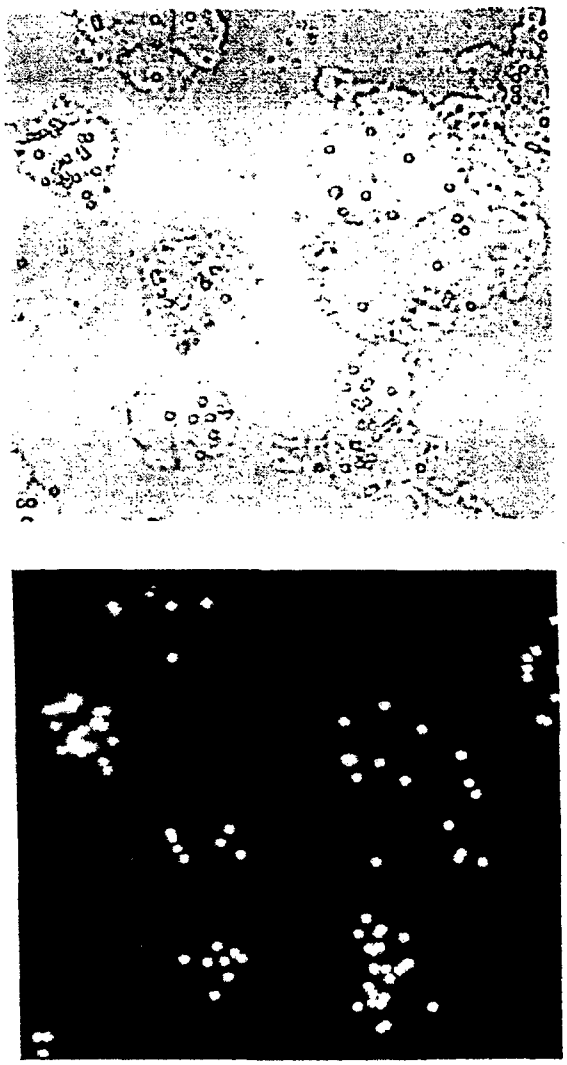

Figure 6. Bright-field image (a) and digital fluorescence image (b) of murine macrophages loaded with 1.6-μm fluorescent lipobeads taken through a 40× microscope objective. The lipobeads maintain their structural integrity and fluorescence properties for up to 6 h following ingestion.

cence intensity of the lipobeads during the enzymatic oxidation of glucose (10 mM) by glucose oxidase (0.1 aunit/mL) in an air-saturated solution. Curve c describes the fluorescence intensity of the lipobeads following the same reaction in an oxygen-saturated solution. As expected, the rate of the reaction increases with increasing the initial oxygen concentration. The shape of the pH response is consistent with the pH dependence of glucose oxidase activity that peaks at pH 6–8.[26] The response of the pH-sensitive lipobeads decreases at pH below 4, which is the lower limit for fluorescein linear pH range. It is also consistent with the reported decrease of glucose oxidase activity at a pH below 4.[26] The enzymatic oxidation of glucose by glucose oxidase results in the formation of hydrogen peroxide at millimolar levels. Our studies indicate that, in the absence of horseradish peroxidase, exposure of the lipobeads to millimolar levels of hydrogen peroxide for several hours does not affect their structural integrity and pH response.

(26) Burrin, J. M.; Price, C. P. *Ann. Clin. Biochem.* **1985**, *22*, 327–342.

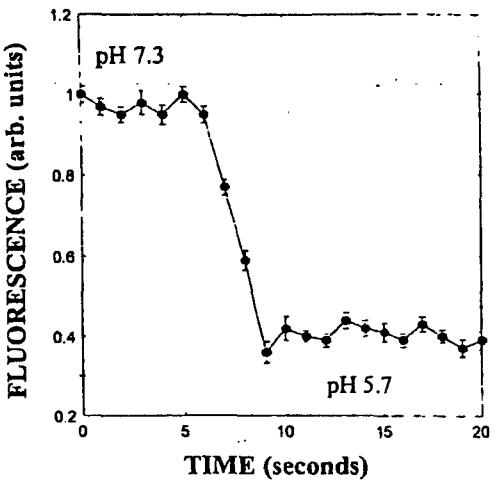

Figure 7. pH change during the phagocytosis process of a single pH-sensing lipobead by a single macrophage. A sharp drop in the fluorescence of the lipobead is observed when the cell ingests the lipobead.

Fluorescence-Imaging and pH-Sensing Measurements of Lipobeads in Macrophages. Typical bright-field and digital fluorescence images taken through a 40× microscope objective of 1.6-μm fluorescent lipobeads internalized by single macrophages are shown in Figure 6. The bright-field image shows that individual particles are isolated from each other in the cell. The signal-to-noise ratio in the fluorescence image is ~200. The lysosomal pH is determined by comparing the ratio between the fluorescence signals of fluorescein at 525 nm and the fluorescence signal of tetramethylrhodamine at 575 nm to the pH calibration curve. The extracellular pH is determined from fluorescence measurements of lipobeads outside the cells to be 7.3, indicating an experimental error of ±0.1 pH unit as the cells are suspended in PBS at pH 7.4. The lysosomal pH is measured from lipobeads that are ingested by the cells to be 5.7 ± 0.1. To enhance the rate of phagocytosis, the cells are kept for 1 h in a PBS solution of pH 7.4 at 37 °C. Figure 7 describes the pH change during the phagocytosis process of a single pH-sensing lipobead by a single macrophage. A sharp drop in the fluorescence of the lipobead is observed when the cell ingests the lipobead. In our cellular experiments, the lipobeads maintain their structural integrity and fluorescence intensity for 6 h, indicating that the conditions in the lysosomes do not cause a fast chemical degradation of the fluorescent lipobeads.

SUMMARY AND CONCLUSIONS

Micrometric pH-sensing fluorescent lipobeads were synthesized, characterized, and applied to monitor pH changes in microliter-volume samples and for lysosomal pH measurements in murine macrophages. The development of particle-based intracellular sensors represents a new trend in the application of fluorescence in cellular biological studies, addressing the need for miniaturized, site-specific, and noninvasive intracellular measurement techniques. The fluorescent lipobeads show a significant improvement in analytical properties over currently used particles for several reasons. First, the dye molecules are covalently attached to phospholipids that are strongly attached to the surface of the particles. This prevents leaking of dye molecules from the

particles to the observed environment, which is a common problem in fluorescence sensors fabricated by physically entrapping hydrophilic-sensing reagents such as pH indicators in a polymer matrix. The covalent immobilization of the dye molecules to the surface of the particles shortens their response time because the analyte ions do not need to diffuse into the bulk of the synthetic or bioparticles to interact with the sensing fluorophors. The use of labeled phospholipids may have an additional advantage over direct coupling of the fluorescent dyes to the surface of the particles. While direct coupling may alter the spectroscopic and sensing properties of the fluorescent dyes, the phospholipids provide a bridge between the dyes and the surface of the particles. This inert bridge weakens the interaction between the dye and the particle surface, resulting in a solution-like behavior of the fluorescent molecules. Second, surface-modified polystyrene particles are used as the polymer support for the fluorescent phospholipids. Polystyrene particles show higher chemical stability than bioparticles or hydrogels and are better suited to the lysosomal conditions that are characterized by high acidity and high concentration of digestive enzymes. Third, the coating membrane protects the fluorescence indicators from quenching species particularly when the dyes are immobilized to the alkyl backbone of the phospholipid molecules. Last, our fluorescent lipobeads are dually labeled with fluorescein (pH-sensitive dye) and tetramethylrhodamine (pH-nonsensitive dye). The use of teramethylrhodamine as a reference dye increases the accuracy of the pH measurements in comparison to previous studies. This study shows that the pH sensitivity of the fluorescent lipobeads is ±0.1 pH unit throughout the pH working range between pH 5.5 and 7.5. The pH-sensing lipobeads are used successfully to monitor pH changes, resulting from a glucose oxidation reaction catalyzed by glucose oxidase in a sample of only 5 μL. The lipobeads are also used to determine the pH in the lysosomes of single macrophages, which is measured to be 5.7 when the cells are stored in a PBS solution of pH 7.4.

Currently we are investigating ways to synthesize fluorescence-sensing lipobeads for lysosomal measurements of hydrogen peroxide. These lipobeads will be used to study the effect of oxidative agents and antioxidants on the level of oxidative activity in the lysosomes. We are also investigating whether coating the polymer particles with phospholipids affects the phagocytosis efficiency of macrophages in comparison to the phagocytosis of uncoated particles. It is expected that coating the polymer particles with membranelike materials would increase their biocompatability, which may result in decreasing phagocytosis efficiency and decreasing cytotoxicity.

ACKNOWLEDGMENT

This work is supported by the National Science Foundation through Career Grant CHE- 9874498 and by a research grant from the Cancer Association of Greater New Orleans (CAGNO). The authors thank Tom Weise from Xavier University of Louisiana School of Pharmacy for the use of his cell culture laboratory.

Received for review February 23, 2001. Accepted May 6, 2001.

AC0102314

APPENDICE 4 – Abstract of the lecture: "Optochemical Sensors and Probes for Single Cell Analysis.", Jin Ji, Nitsa Rosenzweig, Imani Jones and Zeev Rosenzweig, ACS Spring 2001.

OPTOCHEMICAL SENSORS AND PROBES FOR SINGLE CELL ANALYSIS

Ji, Jin, Nitsa Rosenzweig, Imani Jones and Zeev Rosenzweig

The field of single cell analysis has generated increasing attention during the last decade. Rapid analysis of single cells can identify a disease state at the ultimate early stage of its formation, the single cell level. However, many approaches used for single cell analysis, such as capillary electrophoresis, mass spectrometry, and patch-clamp techniques, are destructive to the cells studied. In addition, these techniques are not suitable for real time kinetic studies of cellular processes.

Fluorescence probes and miniaturized optochemical sensors, combined with fluorescence microscopy, are non-destructive means for single cell analysis. The observed cells remain viable during the analysis, and the kinetics of many cellular processes may be observed in real time. During the last four years, my research focused on a number of sensing techniques searching for an optimum sensor design for single cell measurements. Cellular dimensions dictate that the sensor should be miniaturized to sub-micrometric size. It is also required that the sensor would be highly biocompatible, show high chemical and photo-stability, and high throughput. Research accomplishments described in this presentation include the use of free fluorescent molecules for cytoplasmic oxygen measurements in cells, the fabrication and application of fiber optic sensors for simultaneous measurements of calcium ion and pH levels in volume limited samples, and the development of particle-based sensors for pH and molecular oxygen in the lysosomes of murine macrophages. The development of these sensors, their advantages and limitations, as well as their application in monitoring the effect of physical and chemical stimulation of cells and kinetic studies of biological processes at the single cell level are discussed.

APPENDICE 5 – Poster Presentation: "Effect of intracerllular sensors on cells" Imani Jones, Crystal Lane, Tzucanow Cummings, Tamika Tyson, and Nitsa Rosenzweig. Presentation at Southeast/Southwest Regional ACS Meeting, January 2001, New Orleans, LA.

The Effect of Intracellular Sensors on Cells

Imani Jones, Tzucanow Cummings and Nitsa Rosenzweig
Xavier University of Louisiana

pH sensing particles consisting of complex of Amino-modified polystyrene particle, Texas red-X,SE, and Oregon green 488,SE were introduced to murine macrophages (J774). The cells were internalized through phagocytosis process. We show the cells with the sensing particles in the cytoplasm. The particles maintained their ability to respond to pH changes. After internalization, the effect of the sensors on the cells was tested. Measurements of markers for apoptosis, cell growth, and markers for carcinogenesis were performed. The sensors had no effect on the expression of apoptotic and cancer markers. The sensors did have an effect on cell growth. An inhibition of 30% in the growth of cells with sensors was detected over 20 days compared to un treated cells. The inhibition was observed in cells that were exposed to sensors chronically. Cells that were treated with sensors for three hours, washed and allowed to grow without addition of sensors to medium did not exhibit growth inhibition.

APPENDICE 6 – Paper: "Development of A Digital Fluorescence Sensing Technique to Monitor the Response of Macrophages to External Hypoxia", Jacob K Asiedu[1], Jin Ji[1], Mai Nguyen[1], Nitsa Rosenzweig[2], and Zeev Rosenzweig[1]* J Biomed Opt 2001 Apr; 6(2):116-21

Development of A Digital Fluorescence Sensing Technique to Monitor the Response of Macrophages to External Hypoxia

Jacob K Asiedu[1], Jin Ji[1], Mai Nguyen[1], Nitsa Rosenzweig[2], and Zeev Rosenzweig[1]*

1) University of New Orleans, Department of Chemistry, New Orleans, LA 70148
2) Xavier University of Louisiana, Department of Chemistry, New Orleans, LA 70125

J Biomed Opt 2001 Apr; 6(2):116-21

* zrosenzw@uno.edu

ABSTRACT

Oxygen plays a very important role in living cells. The intracellular level of oxygen is under tight control, as even a small deviation from normal oxygen level affects major cellular metabolic processes and is likely to result in cellular damage or cell death. This paper describes the use of the oxygen sensitive fluorescent dye tris (1,10-phenanthroline) ruthenium chloride [$Ru(phen)_3$] as an intracellular oxygen probe. $Ru(phen)_3$ exhibits high photostability, a relatively high excitation coefficient at 450 nm (18000 M^{-1} cm^{-1}), high emission quantum yield (~0.5) and a large Stoke shift (peak emission at 604 nm). It is effectively quenched by molecular oxygen due to its long excited state lifetime of around 1μsec. The luminescence of $Ru(phen)_3$ decreases with increasing oxygen concentrations and the oxygen levels are determined using the Stern Volmer equation. In our studies, J774 Murine Macrophages are loaded with $Ru(phen)_3$, which passively permeates into the cells. Fluorescence spectroscopy and digital fluorescence imaging microscopy are used to observe the cells and monitor their response to changing oxygen levels. The luminescence intensity of the cells decreases when exposed to hypoxia and recovers once normal oxygen conditions are restored. The analytical properties of the probe and its application in monitoring the cellular response to hypoxia are described.

INTRODUCTION

Oxygen is one of the key metabolites in aerobic systems. The rate of oxygen uptake is a good indicator of metabolic activity of cells. The oxygen concentration inside cells is of primary importance in determining numerous physiological and pathological processes in biological systems. Intracellular level of oxygen is under tight control, as even a small deviation from normal oxygen levels would cause major cellular damage or even cell death. The determination of oxygen in tumor cells for instance may lead to the treatment and prediction of the response of the tumor to therapy [1]. The level of intracellular analytes including molecular oxygen can be significantly altered when cells are exposed to hypoxia since the condition of hypoxia induces the production of intracellular reactive oxygen species (ROS) [2,3].

ROS are extremely reactive and display a short half-life and low steady state concentration. Examples of ROS are Superoxide radical ($O^{2-\cdot}$), hydrogen peroxide (H_2O_2), singlet oxygen ($^1O_2$), hydroxyl radical ($OH^{\cdot}$) and nitrogen oxide radical ($NO^{\cdot}$) [4]. ROS attack most cellular components including lipids, carbohydrates, DNA and proteins. When produced in excess ROS damage these components. Normally, the cells enzymatic systems and chemical scavengers remove the ROS formed in the cells. ROS therefore only becomes dangerous when the aforementioned systems are overwhelmed by production of excessive ROS. It has been suggested that multiple exposure of cells to ROS may alter gene expression to produce a cancerous tumor [5]. The level of molecular oxygen is directly proportional to the level of ROS in the cells. The probability for cellular damage or cell death increases with increasing levels of ROS and molecular

oxygen [6]. It is therefore expected that exposure of cells to hypoxia would alter the intracellular oxygen balance and lead to an increase in intracellular oxygen tension. It should be noted that production of ROS does not always damage cells, since it is part of the cells defense mechanism against pathogens. However, an excessive production of ROS is believed to be the cause of many diseases [7].

The area of cellular analysis using fluorescence microscopy has grown in the last decade resulting in the development of a large number of cell permeable fluorescent probes [8]. Recent strides in the development of highly sensitive and relatively inexpensive charge couple device (CCD) cameras [9-11] have led to a dramatic improvement in the accuracy, reliability and sensitivity of fluorescence microscopy measurements. The employment of laser scanning confocal microscopy has increased the spatial resolution of these measurements down to the diffraction limit ($\lambda/2$) [12]. With these improvements, digital fluorescence imaging microscopy has become a method of choice in cellular analysis. This paper describes a digital fluorescence imaging microscopy technique to monitor the response of murine macrophages to hypoxia, particularly the level of molecular oxygen in the cells. The number of analytical methods to measure oxygen levels in cells is surprisingly limited. Ewing et al used a Clark oxygen microelectrode to measure intracellular levels of molecular oxygen in neuron cells (13). Clark electrodes have also been used to measure extracellular levels of molecular oxygen in cell culture media (14). However, microelectrodes often fail in biological systems due to interfering electroactive species. Furthermore, the technique is not suitable in applications where a large number of cells need to be analyzed in real time. In our study, the oxygen sensitive luminescent

indicator tris (1,10 phenanthroline) ruthenium (II) chloride [$Ru(phen)_3$] is used for the first time, to measure in real time the level of molecular oxygen in cells. The luminescence properties of $Ru(phen)_3$ have been studied extensively by Demas et al [15-18]. The dye displays strong emission via metal-to-ligand charge transfer (MLCT) with a decay time of about 1 μs. It exhibits high molar absorption coefficient of 1.80×10^4 $M^{-1}cm^{-1}$ at 450 nm and high emission quantum emission yield (~ 0.5) at 604 nm (19), which presents a large Stokes shift. Additionally, $Ru(phen)_3$ shows high photostability, high chemical stability and water solubility, all of which lend to the usefulness of this dye in fluorescence quenching-based oxygen level measurements. $Ru(phen)_3$ has been used extensively as a luminescent oxygen indicator in fiber optic oxygen sensors and oxygen sensing films [20-24]. These sensors have been applied in aqueous samples [25,26] and biological fluids [27,28] but not for cellular imaging of oxygen. The employment of high performance digital fluorescence imaging technique enables the study of the response of a large number of cells simultaneously to hypoxia on a cell-by-cell basis. The hypoxia conditions are applied by suspending a cekll sample in a glucose/glucose oxidase solution. Glucose oxidase catalyzes the oxidation of glucose. The reaction consumes oxygen, thus inducing conditions of external hypoxia.

EXPERIMENTAL

Digital Fluorescence Imaging Microscopy - The detection system used to measure the fluorescence of the oxygen sensitive dye, $Ru(phen)_3$, loaded into the cells is shown in Figure 1. The system consists of an inverted fluorescence microscope (Olympus IX70) equipped with a 100 W mercury lamp as a light source. The fluorescence image of the cells is collected by a 20X-microscope objective with a numerical Aperture of 0.5. A 450-nm narrow-band excitation filter, a 500-nm dichroic mirror, and a 590-nm long-pass emission filter are used to ensure spectral imaging purity. The fluorescence signal is dispersed by a 150-mm three-mirror spectrograph (Acton Research Inc., Acton, MA, USA) equipped with a 600 groves/mm grating blazed at an optimum wavelength of 500 nm. The grating can be replaced with a mirror, and the exit slit can be removed from the path of the fluorescence signal to allow the image of the cells to pass through the spectrograph without being dispersed by the grating. A high-performance charged-couple device (CCD) camera (Roper Scientific, Princeton, NJ,USA, model 256HB) with a 512 X 512 pixel array is used for spectroscopic imaging or for digital fluorescence imaging of the cells. An exposure time 0.5 sec is used for image collection. A PC microcomputer (Gateway 2000, Pentium 200 MHz) is employed for data acquisition and the Rupert Scientific software WinSpec/32 is used for image analysis.

Fluorescence Spectroscopy Measurements - Excitation and emission spectra, as well as kinetic measurements are carried out using a PTI model QM-1 fluorometer, (PTI, London, Ontario, Canada) equipped with a 75-W continuous Xe arc lamp as a light source.

Cell Culture - Cultures of J774 Murine Macrophages are maintained according to a standard protocol [29]. The cells are cultured in Dulbecco's modified Eagle's medium supplemented with 4 mM L-glutamine, 10mM sodium bicarbonate, 25mM glucose, 1 mM sodium pyruvate, and 10% fetal bovine serum. The cells are grown at 37 ^{0}C in 5% CO_2. The medium is replaced 3 times a week. To prepare subcultures, the cells are scraped in a new medium and split into new plates.

Loading of Cells with $Ru(phen)_3$ - The macrophages are detached from the culture plate surface by scraping with a rubber policeman. The medium containing cells is centrifuged at 500g for 10 min to precipitate the cells. Cells are collected and diluted to a concentration of about 10^6 cells/ml using a fresh medium. The concentration of the cells is determined by standard hemacytometry using Trypan Blue to assess cell viability. For the loading of the dye, 1 ml of cells ((1-3) x 10^6 cells/ml) is incubated in the dark at 37 ^{0}C for 15 min with the appropriate volume of $Ru(phen)_3$ solution such that the dye concentration is 10^{-4}M in the solution. The cells are then washed 3 times with PBS buffer (pH 7.2) to remove excess free dye from the solution and from the surface of the cells.

Generation of Hypoxia Conditions using the Glucose/Glucose Oxidase System - An aliquot of glucose oxidase of 10 units/ml is added to 100 μL of a PBS buffer (pH 7.2) that contains 20-mM glucose and 10^6 cell/ml $Ru(phen)_3$ loaded cells. A 20-μL sample of this solution is placed between two microscope cover slips for fluorescence imaging. The sample is excited at 450-nm and the cells are imaged through a 20X objective. The first image is taken approximately 3 min after the reaction starts when movement of the cells

stops. Subsequent images are taken every 4-min. An exposure time of 0.5 second is used for fluorescence image collection.

Materials and Reagents - Glucose and Glucose Oxidase (from Aspergillus niger) with enzymatic activity of 10,000 units/ml were purchased from Sigma. Tris (1,10-phenanthroline) ruthenium chloride ($Ru(phen)_3$) was purchased from Aldrich Chemical Company. Corning glass cover slips used for microscopy and pH buffers were purchased from Fisher Scientific. Aqueous solutions were prepared with 18 MΩ deionized water purification system (Barnstead Thermolyne Nanopure). J774 Murine Macrophages were purchased from ATCC (American Type Culture Collection). The Dulbecco's modified Eagle's medium and bovine serum albumin were purchased from Sigma. All reagents were used as received, without further purification.

RESULTS AND DISCUSSION

Spectroscopic Properties of $Ru(phen)_3$ - As previously mentioned ruthenium diimine complexes have been widely used as oxygen indicators in gas and aqueous samples. In this study the fluorescence properties of $Ru(phen)_3$ are used to monitor changes in J774 Macrophages as a result of external hypoxia. $Ru(phen)_3$ shows a strong absorption in the visible region (λ_{max} = 450 nm, ε = 18100 $M^{-1}cm^{-1}$), a high-emission quantum yield of ~0.5 at 604 nm, and a long excited-state lifetime (~ 1 μs). A concentration dependence of the fluorescence intensity of $Ru(phen)_3$ at 600 nm (λ_{ex} = 450 nm) in aqueous solution using a fluorometer, is shown in figure 2. The fluorescence intensity of the free dye increases with increasing dye concentrations. However, at concentrations higher than 1x 10^{-4}M, the fluorescence intensity decreases with increasing concentrations, a phenomenon that is attributed to self-quenching of the fluorescence signal (26).

Oxygen Sensitivity of $Ru(phen)_3$ - The fluorescence spectra of $Ru(phen)_3$ in a nitrogen, air and oxygen saturated solutions are shown in Figure 3. The fluorescence measurements are performed using a spectrofluorometer. Due to dynamic quenching by molecular oxygen, the fluorescence intensity of $Ru(phen)_3$ in nitrogen saturated solution, I (N_2), is higher than that in air saturated solution, I(air), which is also higher than the fluorescence intensity of the oxygen saturated solution, I(O_2). The response factor, I (N_2)/I (O_2) = 7.
The analytical range of an oxygen probe is governed by the respective quenching curve and the Stern-Volmer constant. The variation in the fluorescence intensity as a function of the dissolved oxygen concentration is given by the Stern-Volmer equation:

$$I_0/I_c = 1 + Ksv [O_2]$$

where I_0 is the fluorescence intensity of $Ru(phen)_3$ in a nitrogen-saturated solution, Ic is the fluorescence intensity of $Ru(phen)_3$ in a given dissolved oxygen concentration and Ksv is the Stern-Volmer quenching constant. In principle, higher quenching constants result in higher accuracy at low levels of oxygen. This is due to the larger signal change per oxygen concentration interval. However, high quenching constants result in a more limited linear dynamic range. In a previous article we described oxygen concentration dependent fluorescence measurements of $Ru(phen)_3$ in aqueous media (26). We found that that Ksv for $Ru(phen)_3$ is about 5420 M^{-1}. We also found a linear dynamic range between 0.1 and 12 ppm of molecular oxygen with a correlation coefficient of 0.996. We found a standard deviation of around 4% between 10 consecutive fluorescence measurements in air saturated solutions. The standard deviation increases at lower oxygen levels when two large fluorescence intensities are subtracted from each other to obtain a small intensity difference. The accuracy of the oxygen measurement is governed by the uncertainties in the determination of I_0 (nitrogen saturated solution), Ksv and Ic. An accurate determination of I_0 is essential for obtaining sufficiently accurate calibration curve and Ksv value.

Stability of loaded cells with Respect to leaking and Photobleaching - Under our experimental conditions a 10^{-4} M $Ru(phen)_3$ solution is used for loading $Ru(phen)_3$ into the cells. Since the dye passively diffuses into the cells, the efficiency of permeation is nearly 100 %. Transmission and Fluorescence images of cells loaded with $Ru(phen)_3$ are shown in figure 4. Figure 4a shows a transmission image of the cells taken with an exposure time of 3 msec. Figure 4b shows the fluorescence image of the same cells taken

with an exposure time of 0.5 sec. The images are taken using a 20X microscope objective (NA = 0.5). Monitoring the fluorescence intensity of the cells for 1 hour shows a minimal leakage of $Ru(phen)_3$ from the cells.

The photobleaching rate of $Ru(phen)_3$ has previously been studied in our laboratory [22]. To monitor the rate of photobleaching of $Ru(phen)_3$ loaded-cells under our experimental conditions, a 10 μL sample of the solution is placed between two microscope cover slips. The sample is then placed on the microscope stage and illuminated continuously at 450 nm. The fluorescence intensity of the cells decreases by approximately 5% during 30 minutes of continuous illumination. During our kinetic measurements the cells are exposed to the excitation light for less than 1 second in each measurement. Each experiment lasts 30 minutes and images are taken in 3-5 minutes intervals. We therefore conclude that under our experimental conditions the loaded cells remain photostable throughout the experiment.

Response of Single Cells to hypoxia - Since our samples are volume limited (~10 μl) it is practically impossible to physically change the extracellular concentrations of oxygen in the observed samples. The response of individual cells to conditions of hypoxia is therefore demonstrated by monitoring the enzymatic oxidation of glucose when a glucose/glucose oxidase solution is added to a microscope cover slip covered with cells. Glucose Oxidase catalyses the oxidation of glucose as follows:

$$\text{Glucose} + O_2 \rightarrow \text{Gluconic acid} + H_2O_2$$

Molecular oxygen is consumed during this enzymatic oxidation. Figure 5a shows the fluorescence image of loaded cells taken five minutes after the start of the enzymatic reaction. The signal to noise ratio between the fluorescent cells and the background signal is found to be 80. Figure 5b shows the fluorescence images of loaded cells taken at 30 minutes after the start of the enzymatic reaction. The signal to noise ratio is 50. The cells maintain their structural integrity. There is about 30% variation in the fluorescence intensity of the $Ru(phen)_3$ loaded cells. This variation is due to the heterogeneity of the cellular sample, which contains viable cells at different growth stages and even dead cells. Viability measurements using a standard Trypan Blue method shows that the percentage of viable cells in a typical cellular sample is around 70%. Nevertheless, the variation in the relative decrease in signal of individual loaded cells as the enzymatic reaction progress is only 10%. The dye molecules distribute evenly in the cells and there is no evidence of compartmentalization. In figure 6 the fluorescence intensity of single loaded cells is plotted against the enzymatic reaction time coordinate at different levels of glucose oxidase activity and cell viability. Each curve represents the average response of 10 cells. Curve (a) describes the results of a control experiment in which the cells are suspended in a solution of 10mM glucose in the absence of gluocose oxidase. Curve (b) describes a control experiment in which the $Ru(phen)_3$ loaded cells were left for 24 hours in a PBS buffer solution under ambient conditions. Unlike under normal storage conditions in a cell culture medium, 5% CO_2 atmosphere and 37°C, the cells stop growing and die. Trypan Blue measurements show that under these conditions only about 10% of the cells remain viable after 24 hours. These cells were suspended in a solution containing 10mM glucose and 10 units/ml glucose oxidase. Both curves (a) and

(b) show no noticeable change in the signal level due to hypoxia. Curves (c) and (d) describe the fluorescence intensity of viable cells when suspended in solutions containing 10mM glucose and 10 units/ml (c) and 20 units/ml (d) of glucose oxidase. A 30% decrease in the fluorescence intensity of the cells is observed, indicating a production of molecular oxygen in macrophages when subjected to conditions of external hypoxia. The overproduction of oxygen continues as long as the cells are exposed to external hypoxia. Once the glucose/glucose oxidase solution is removed and replaced with glucose oxidase free buffer solution, the fluorescence intensity of the cells recovers to about 90% of its original value in about 20 minutes. This result supports our observation that the cellular fluorescence signal changes follow the production or depletion of molecular oxygen in the cells.

SUMMARY AND CONCLUSIONS

A high-resolution digital fluorescence imaging microscopy is used for the first time to follow the response of the oxygen sensitive fluorescent dye $Ru(phen)_3$ loaded into Murine Macrophages to hypoxia in real time. $Ru(phen)_3$ shows high photostability in cells, minimal dye leakage, a high emission quantum yield, and a large stokes shift, which eliminates interference by cellular autoflourescence. Because of the high photostability of the dye, we have been able to quantitatively measure the fluorescence of the same living cells during experiments that last 30 minutes without noticeable photobleaching. Control experiment in which the loaded cells were continuously exposed to the excitation light for 30 minutes show that the fluorescence intensity of the dye remains constant in living cells. The fluorescence of the loaded cells decreases by 30% when exposed to external hypoxia. The fluorescence decrease is attributed to the cellular production of molecular oxygen when the cells are exposed to hypoxia. The fluorescence intensity recovers to about 90% of its original fluorescence intensity once normal conditions are restored. This study offers a simple and direct way to monitor changes in oxygen levels in cells when they are exposed to external hypoxia. It is however possible that other processes contribute to the decrease in the fluorescence intensity of the dye when the cells are exposed to hypoxia. For example, it is possible that other quenching species are expressed when the cells are exposed to hypoxia. It is also possible that the increasing levels of reactive oxygen species leads to oxidation of Ru(phen)3 which results in a decrease in the fluorescence intensity. The reversibility of the process suggest that any oxidized form of Ru(phen)3 is unstable and readily reduced back to Ru(phen)3 once normal oxygen conditions are restored.

ACKNOWLEDGMENTS

This work is supported by the National Science Foundation CAREER grant CHE-9874498 and by the Louisiana Board of Regents Support Fund research grant LEQSF (1997-00)-RD-A-29.

References

1. McIlroy, B. W.; Curnow, A.; Buonaccorsi, G.; Scott, M. A.; Brown, S. G.; MacRobert, A. " Spatial Measurement of Oxygen Levels During Photodynamic Therapy Using Time-Resolved Optical Spectroscopy." J. Photochem. Photobio. B: Biology **1998**, 43, 47-55.
2. Kelley, J. "Cytokines of the Lung." Am. Rev. Respir. Dis. **1990**, 141, 765-788.
3. Kienast, K.; Knorst, M.; Lubjuhn, S.; Muller-Quernheim, M.; Ferlinz, R. "Nitrogen Dioxide-Induced Reactive Oxygen Intermediates Production by Human Alveolar Macrophages and Peripheral Blood Mononuclear Cells." Arch. Environ. Health **1994**, 49, 246-250.
4. Tortora, G., Funke, B.; Case CL (1995) Microbiology (5th ed) The Benjamin/Cummings Publishing Co Inc: p413
5. Armstrong, R. S.; Sohal, R. G.; Cutler, R. G.; Slater, T.F., Eds. Free Radicals in Molecular Biology, Aging and Disease", (1984) Raven, New York.
6. Martinez-Cayuela, M. "Oxygen Free Radicals and Human Disease." 1995, Biochimie, 147-161.
7. Reddy, V. M. "Mechanism of Mycobacterium Avium Complex Pathogenesis." Frontiers in Bioscience **1998**, 3, 525-531.
8. Haugland, R. P.; Handbook of Fluorescent Probes and Research Chemicals, 6th Ed, Molecular Probes Inc., Eugene, Chap 15, 16, 21.
9. Sweedler, J. V.; Bilhorn, R. B.; Epperson, G. R. S.; Denton, M. B. "High Performance Charge Transfer Device Detectors." Anal. Chem. **1988**, 60, 282A – 291A.

10. Sweedler, J. V.; Bilhorn, R. B.; Epperson, G. R. S.; Denton, M. B. "Applications of Charge Transfer Devices in Spectroscopy." Anal. Chem. **1988**, 60, 327A –335A.

11. Hanley, Q. S.; Earle, C. W.; Pennebaker, F. M.; Madden, S. P.; Denton, M. B. "Charge Transfer Devices in Analytical Instrumentation." Anal. Chem. **1996**, 68, 661A-667A.

12. . Georgiou, G. N.; Ahmet, M. T.; Houlton, A.; Silver, J.; Cherry, J. "Measurement of the Rate of Uptake and Subcellular Localization of Porphyrins in cells using Fluorescence Digital Imaging Microscopy." Photochem. Photobiol. **1994**, 59(4), 419.

13. . Lau, Y. Y.; Abe T.; Ewing A.G.;" Voltammetric Measurement of Oxygen in Single Neurons Using Platinized Carbon Ring Electrodes." Anal. Chem **1992,** 64(15),1702-1705

14. Connoly P.; Clark P.; Curtis A. S.; Dow J. A.; Wilkinson C. D. "An Extracellular Microelectrode Array for Monitoring Electrogenic Cells in Culture." Biosens. Bioelectron. **1990**, 5(3), 223-234.

15. Carraway, E. R.; Demas, J. N.; DeGraff, B. A.; Bacon, J. R. "Photophysics and Photochemistry of Oxygen Sensors Based on Luminescent Transition-Metal Complexes." Anal. Chem. **1991**, 63, 337-342.

16. Demas, J. N.; DeGraff, B. A. "Design and Applications Of Highly Luminescent Transition Metal Complexes." Anal. Chem. **1991**, 63, 829A-837A.

17. Sacksteder, L.; Demas, J. N.; DeGraff, B. A. "Design of Oxygen Sensors Based on Quenching of Luminescent Metal Complexes: Effect of Ligand Size on Heterogeneity." Anal. Chem. **1993**, 65, 3480-3483.

18. Xu, W.; McDonough, R.C., III; Langsdorf, B.; Demas, J. N.; DeGraff, B. A., "Oxygen Sensors Based on Luminescence Quenching: Interactions of Metal Complexes with the Polymer Supports." Anal. Chem. **1993**, 66, 4133-4141.

19. Hartmann, P., "Photochemically Induced Energy-Transfer Effects on the Decay Times of Ruthenium Complexes in Polymers", **2000**, 72, 2828-2834.

20. Wolfbeis, O. S., Ed. Fiber Optic Chemical Sensors and Biosensors; CRC Press: Boca Raton, 1991.

21. Rosenzweig, Z.; Kopelman, R. "Development of A Submicrometer Optical Fiber Oxygen Sensor." Anal. Chem. **1995**, 67, 2650-2654.

22. McNamara, K. P.; Rosenzweig, Z. "Dye-Encapsulating Liposomes as Fluorescence-Based Oxygen Nanosensors." Anal. Chem. **1998**, 70, 4853-4859.

23. . McNamara, K. P.; Rosenzweig, Z. "Liposome-Based Optochemical Nanosensors", Mikrochim Acta **1999**, 131, 57-64.

24. Clark, H. A.; Hoyer, M.; Philbert, M. A.; Kopelman, R. "Optical Nanosensors for Chemical Analysis inside Single Living Cells. 1. Fabrication, Characterization, and Methods for Intracellular Delivery of PEBBLE Sensors." Anal. Chem. **1999**, 71, 4831-4836.

25. Rosenzweig, Z.; Kopelman, R. "Analytical Properties and Sensor Size Effects of a Micrometer-Sized Optical Fiber Glucose Biosensor." Anal. Chem., **1996**, 68, 1408-1413.

26. Rosenzweig, Z.; Kopelman, R. "Analytical Properties of Miniaturized Oxygen And Glucose Fiber Optic Sensors." Sens. Actuators **1996**, B35-36, 475-483.

27. Papkovsky, D. B.; O'Riordan, T. C.; Guilbault, G. G "An Immunosensor Based on the Glucose Oxidase Label and Optical Oxygen Detection." Anal Chem. **1999**, 71, 1568-1573.

28. Ruffolo, R., Evans, C. E. B; Liu, X.; Ni, Y.; Pang, Z.; Park, P.; McWilliams, A. R.; Gu, X.; Yekta, A.; Winnik, M. A.; Manners, I. "Phosphorescent Oxygen Sensors Utilizing Sulfur-Nitrogen-Phosphorus Polymer Matrixes: Synthesis, Characterization, and Evaluation of Poly(thionylphosphazene)-b-Poly(tetrahydrofuran) Block Copolymers." Anal. Chem. **2000**, 72, 1894-1904.

29. Gordon, S. "The macrophage." BioEssays **1995**, 17(11), 977-986.

Figure Captions

Figure 1: Digital fluorescence imaging microscopy system. The experimental setup consists of an inverted fluorescence microscope with a 20X objective (NA = 0.5), a high-performance charge-coupled device camera (Roper Scientific, 16-bit resolution, 512 x 512 chip size), and a microcomputer for image analysis.

Figure 2: Fluorescence intensity of $Ru(phen)_3$ in solution as a function of its concentration. A 450 nm light is used for excitation. Self-quenching occurs at concentrations greater than 1×10^{-4} M.

Figure 3: Spectral response of $Ru(phen)_3$ of nitrogen, air and oxygen saturated solutions when excited at 450 nm. Emission maximum is obtained at 604 nm.

Figures 4: Digital transmission (a) and fluorescence (b) images of $Ru(phen)_3$ loaded cells. A 10μL sample is placed between two microscope slips, and fluorescence is detected and imaged by a CCD camera. A fluorescence filter cube consisting of a 450±10 nm excitation filter, a 500 nm dichroic mirror and a 515 nm long band emission filter is used for imaging.

Figures 5: Digital Fluorescence images of $Ru(phen)_3$ loaded cells taken (a) 5 minutes and (b) 30 minutes respectively after enzymatic reaction begins. A 10μL sample is placed between two microscope slips, and fluorescence is detected and imaged by a CCD camera. A fluorescence filter cube consisting of a 450±10 nm excitation filter, a 500 nm dichroic mirror and a 515 nm long band emission filter is used for imaging.

Figure 6: The response of macrophages to hypoxia. Curve (a) describes the fluorescence intensity of the cells in the absence of glucose oxidase (normal conditions). Curve (b) describes the fluorescence intensity of dead cells in the presence of glucose and glucose oxidase. Curve (c) and (d) show a decrease in the fluorescence intensity of the cells

when incubated with a solution containing 10 mM glucose and 10 units/ml (c) and 20 units/ml (d) glucose oxidase.

Figure 1

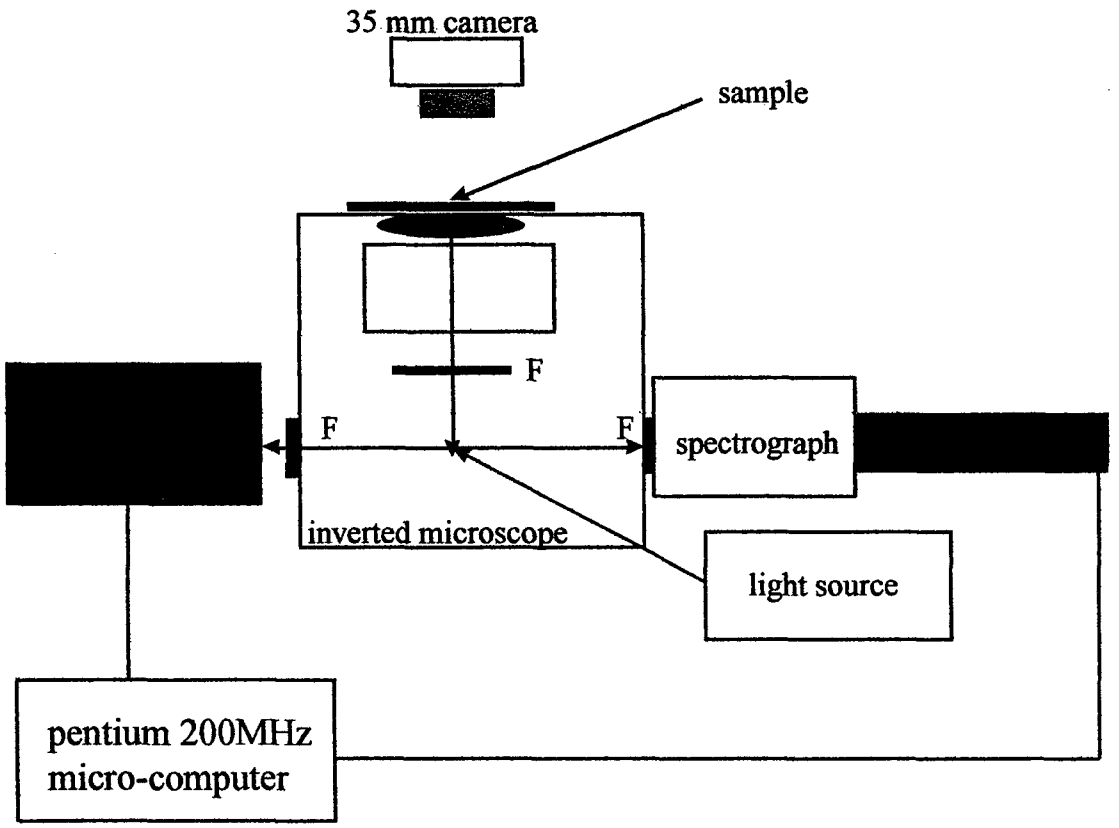
35 mm camera
sample
F
F
F
spectrograph
inverted microscope
light source
pentium 200MHz
micro-computer

Figure 2

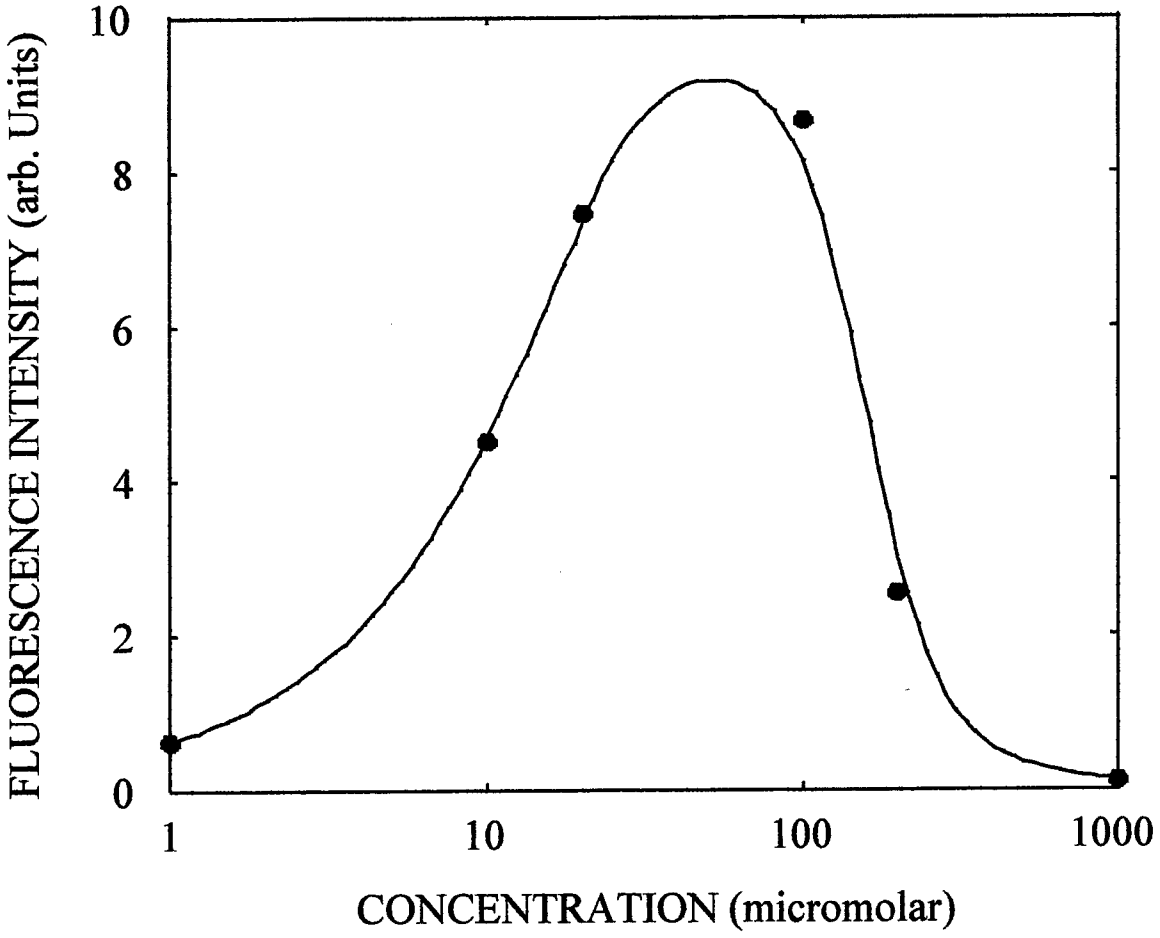
FLUORESCENCE INTENSITY (arb. Units)
10
8
6
4
2
0
1
10
100
1000
CONCENTRATION (micromolar)

Figure 3

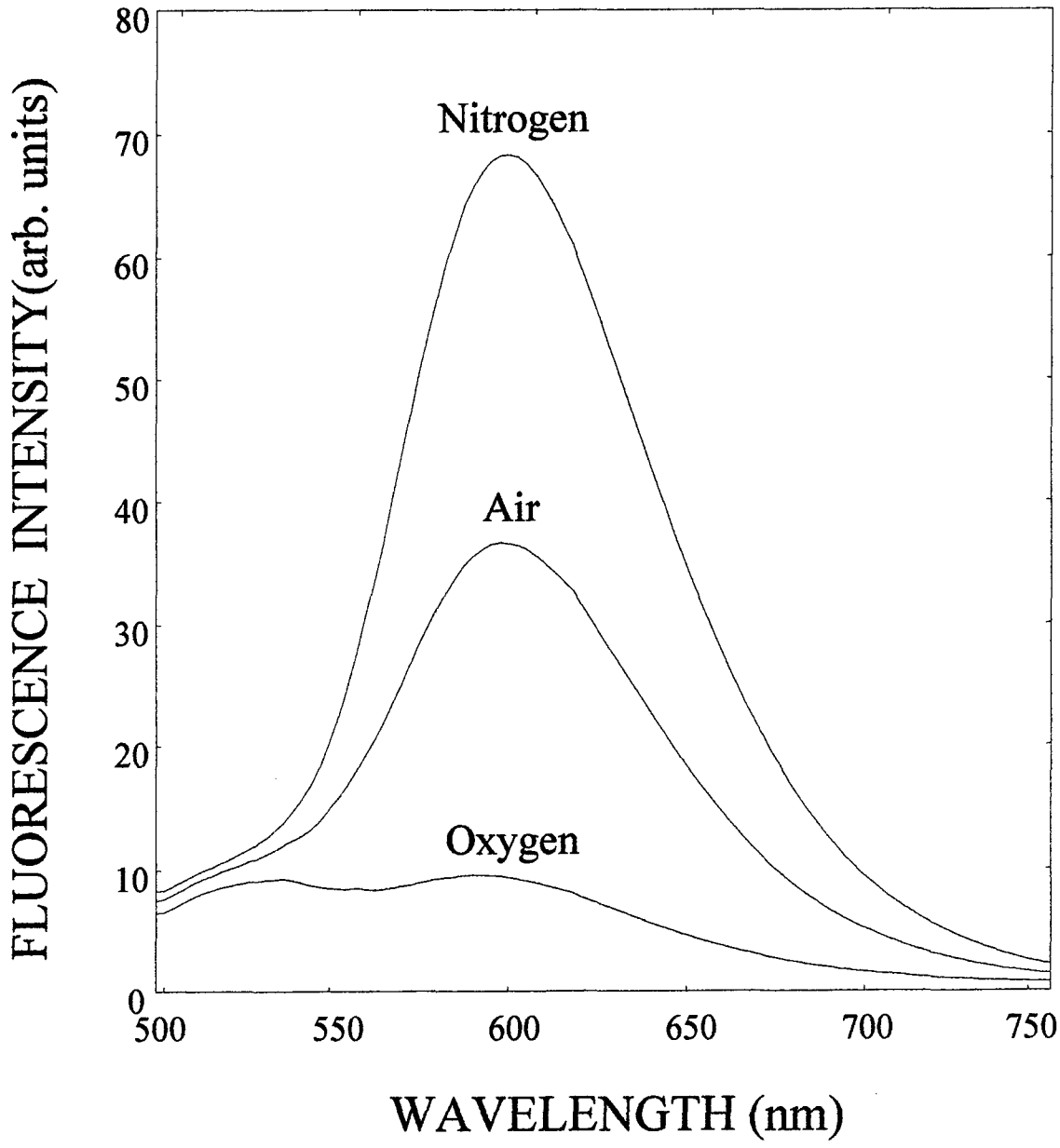
FLUORESCENCE INTENSITY(arb. units)
80
70
60
50
40
30
20
10
0
500
550
600
650
700
750
Nitrogen
Air
Oxygen
WAVELENGTH (nm)

Figure 4

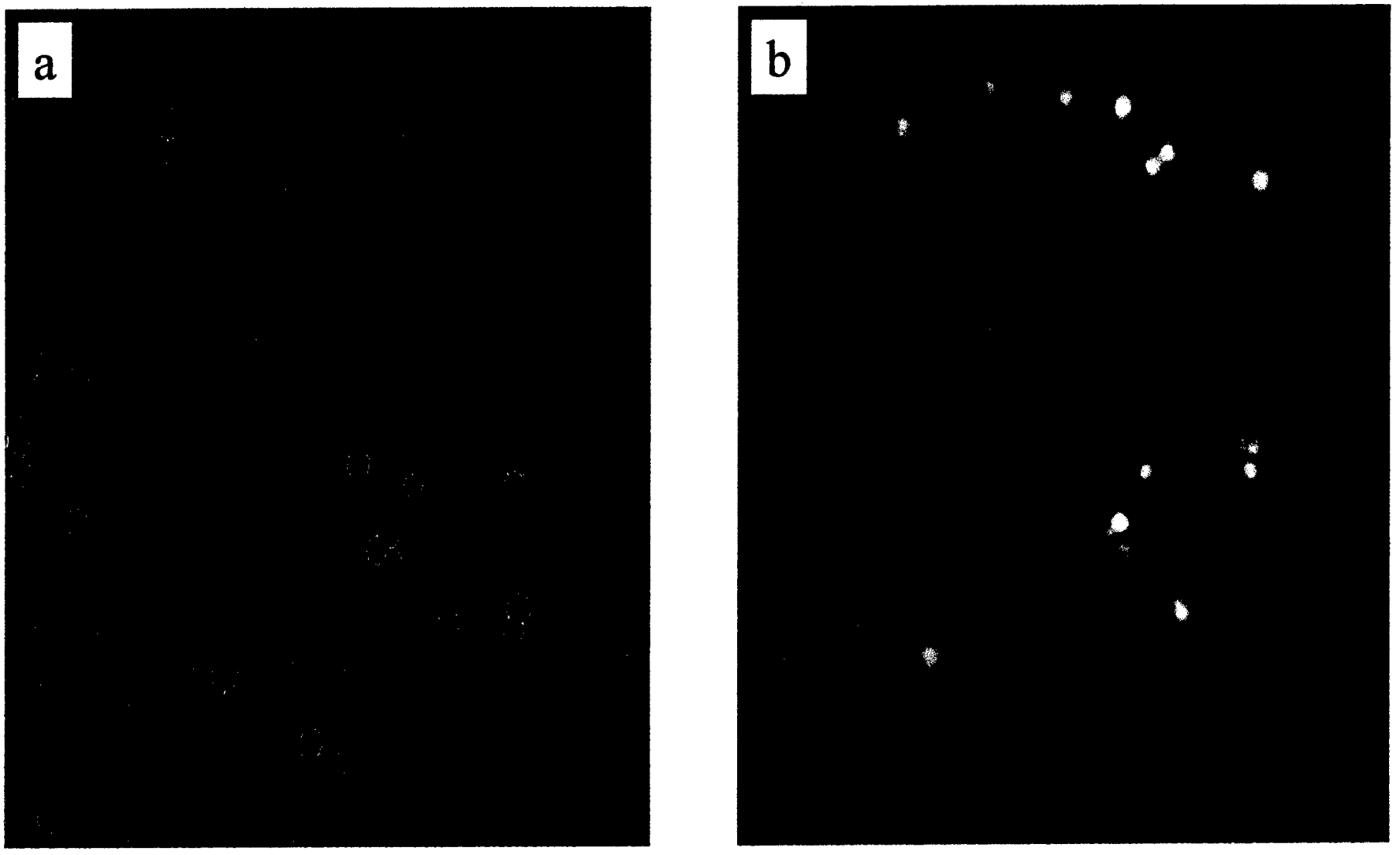

Figure 5

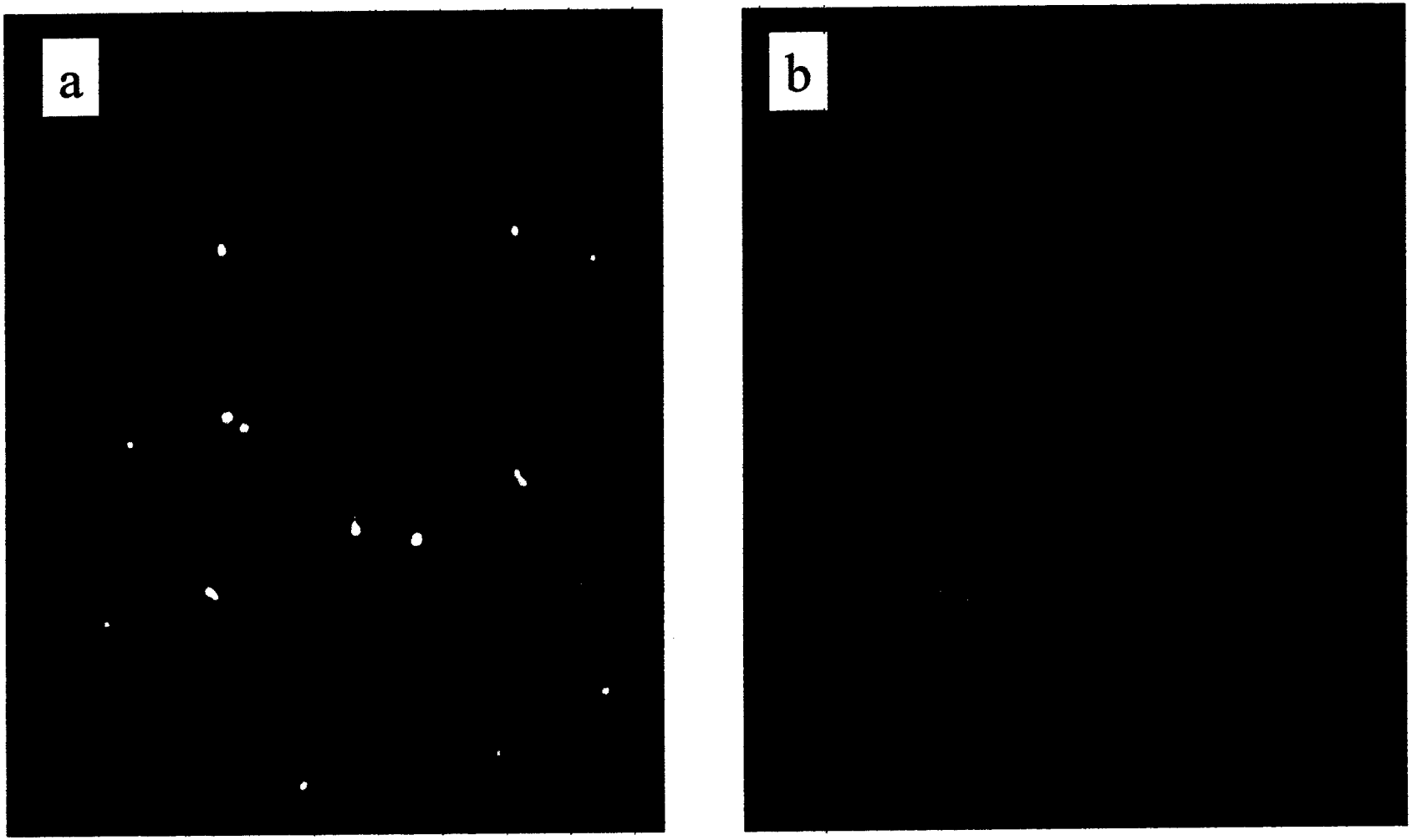

Figure 6

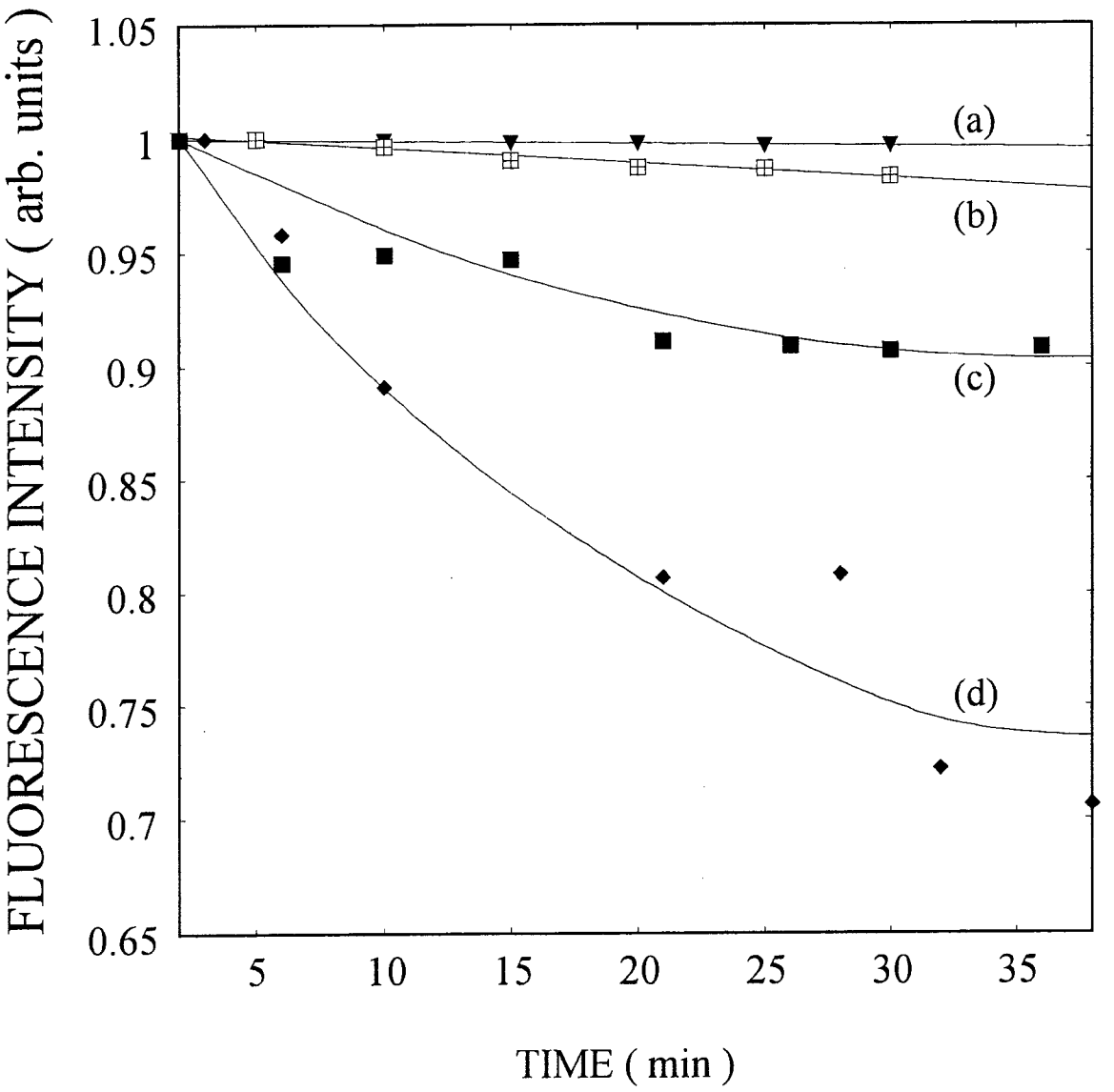
FLUORESCENCE INTENSITY (arb. units)
1.05
1
0.95
0.9
0.85
0.8
0.75
0.7
0.65
5
10
15
20
25
30
35
TIME (min)
(a)
(b)
(c)
(d)

APPENDICE 7 – Paper: "A Novel Fluorescent Oxygen Indicator for Intracellular Oxygen Measurements", Jin Ji[1], Nitsa Rosenzweig[2], Imanie Jones[2] and Zeev Rosenzweig[1]* J. Biomed. Optics, 2002 (in press).

A Novel Fluorescent Oxygen Indicator for Intracellular Oxygen Measurements

Jin Ji[1], Nitsa Rosenzweig[2], Imanie Jones[2] and Zeev Rosenzweig[1]*

1) University of New Orleans, Department of Chemistry, New Orleans, LA 70148

2) Xavier University of Louisiana, Department of Chemistry, New Orleans, LA 70125

J. Biomed. Optics, 2002 (in press).

ABSTRACT

Intracellular oxygen concentration is of primary importance in determining numerous physiological and pathological processes in biological systems. In this paper, we describe the application of the oxygen sensing indicator, ruthenium dibipyridine 4-(1"-pyrenyl)-2,2'-bipyridine chloride, $Ru(bpy\text{-}pyr)(bpy)_2$, for molecular oxygen measurement in J774 murine macrophages. $Ru(bpy\text{-}pyr)(bpy)_2$ exhibits strong visible absorption, efficient fluorescence, long excited state lifetime, large Stokes shift, and high photo and chemical stability. The fluorescence of $Ru(bpy\text{-}pyr)(bpy)_2$ is efficiently quenched by molecular oxygen. It is 13 fold higher in a nitrogenated solution than in an oxygenated one. The dye passively permeates into cells and maintains its oxygen sensitivity for at least 5h when the cells are stored in a phosphate buffered saline (PBS) solution at pH 7.4. The oxygen sensitivity, photostability and chemical stability of the indicator and the effect of hypoxia and hyperoxia on the intracellular oxygen level in single macrophages are discussed.

INTRODUCTION

In spite of the significance of intracellular oxygen levels in numerous cellular processes, there are surprisingly few analytical methods to measure intracellular oxygen levels. The role of oxygen in cellular processes is mostly assessed by indirect data derived from measurements of the concentration of extracellular oxygen (1,2). This approach is ambiguous, as there is a difference between the intracellular and extracellular oxygen concentration (3, 4). Clark electrodes have been widely used to measure extracellular oxygen level in cell culture media (1, 5). However, when applied in intracellular studies, the electrodes may injure the cell due the penetration. A Clark microelectrode can only measure the oxygen level in one cell at a time and is not suitable in applications that require fast cell screening. Furthermore, the technique often gives misleading data due to the abundance of interfering species in cytoplasm. Additionally, the consumption of oxygen by the Clark electrodes can alter the oxygen level near the surface of the electrode and cause an error in the oxygen measurement.

Fluorescence microscopy and spectroscopy are widely used techniques for cellular analysis. In 1970, Vaughan and Webber observed that oxygen concentrations in the physiological range quench the fluorescence of pyrenebutyric acid in solution (6). The observation led to the use of pyrenebutyric acid for intracellular oxygen measurements in isolated rat liver cells (7-9). The technique offered several advantages: First, the dye detected the intracellular oxygen concentration directly without consuming oxygen. Second, electromagnetic interference or changes due to stirring or fluid currents did not affect the accuracy of the technique. Third, loading of the indicator into cells was less

invasive than the penetration of electrodes. Furthermore, chemical information was obtained from a large number of cells simultaneously and in real time. However, the lack of a suitable indicator limited the quantitative power of the technique. The excitation and emission of pyrene and its derivatives are in the UV, overlapping with cellular auto-fluorescence. This resulted in high background that complicated the data interpretation. Additionally, these dyes show poor photostability and poor chemical stability in the cellular environment.

Wilson et al. introduced phosphorescence quenching as an alternative to fluorescence quenching of pyrene for intracellular and tissue measurements of molecular oxygen (9-11). The method dramatically extends the oxygen sensitivity range down to nanomolar scale, a parameter that no other techniques have achieved. The technique was applied to study oxygen distribution in perfused tissue (12), oxygen consumption by suspensions of mitochondria (13) and cellular energetics in cardiac myocytes (14). However, the long lifetime of the phosphorescent probes allows interactions between the probes and the environment. Most of the few available phosphorescent probes are pH and temperature sensitive, which limits the accuracy of the technique. In addition, due to the inefficient intersystem crossing rate, quantum yield of the indicators is low which requires a highly sensitive detection system.

Ruthenium diimine complexes represent an important class of fluorescence-based oxygen indicators. The photophysics and photochemistry of these complexes have been extensively studied by Demas et al (15-19). They show great photo-stability and high

fluorescence quantum yield (0.1-0.6). Unlike pyrene and its derivatives the excitation wavelength of these complexes is in the visible range of the elctromagnetic spectrum (450-460 nm). The emission maximum of these complexes is at 610 nm. This large Stokes Shift increases the signal to noise ratio of the fluorescence measurements in biological samples because no cellular autofluorescence is observed at this wavelength. Additionally, the background scattering is lower than the background scattering observed when pyrene is used for oxygen measurements. This is because the scattering intensity decreases with the forth power of the excitation wavelength. Ruthenium diimine complexes are particularly suitable for oxygen measurements because of their long excited state lifetime in the microseconds time scale. Molecular oxygen effectively quenches the fluorescence intensity and decreases the excited state lifetime of these complexes. In the last decade, tris (1,10 phenanthroline) ruthenium (II) chloride [$Ru(phen)_3$] and tris (4,7 diphenyl, 1,10 phenanthroline) ruthenium (II) Chloride [$Ru(dpp)_3$] have been applied successfully in fiber optic sensors for oxygen and glucose (20-23) in the gas phase (oxygen) and in solution (dissolved oxygen and glucose). Recently, we utilized tris(1,10-phenanthroline) ruthenium chloride ($Ru(phen)_3$), a commonly used oxygen indicator for gas and aqueous samples, to monitor the effect of external hypoxia on J774 murine macrophages (23). The measurements were limited in sensitivity due to the chemical instability of $Ru(phen)_3$. A constant negative signal drift was observed and explained by the degradation of $Ru(phen)_3$ by cellular components like protein and DNA. A more chemically stable visible indicator for intracellular oxygen measurement is desired.

In 1997, Schmehl et al. reported the synthesis of a new ruthenium metal complex, ruthenium dibipyridine 4-(1"-pyrenyl)-2,2'-bipyridine chloride ($[(bpy)_2Ru(bpy\text{-}pyr)]Cl_2$) (25). The complex is a ruthenium(II) diimine (donor) - pyrene (acceptor) complex linked by a single C-C bond. It was synthesized to understand the photophysical behavior of $[(bpy)_2Ru(L)]^{2+}$ complexes. The complex displays strong emission via metal to ligand charge transfer (MLCT) with an excited state lifetime of 1.3μsec. It exhibits high molar absorption coefficient of $2\times10^4\ M^{-1}cm^{-1}$ at 456nm and an emission quantum yield of 0.5 at 632nm. In this paper, we study the oxygen sensing properties of $[(bpy)_2Ru(bpy\text{-}pyr)]Cl_2$ in aqueous solutions and living cells. The application of this new indicator for intracellular oxygen measurements in J774 murine macrophages under the condition of hypoxia and hyperoxia is discussed.

EXPERIMENTAL

Digital Fluorescence Imaging Microscopy - The experimental setup used for fluorescence measurements of macrophages loaded with the indicator is shown in figure 1. The system consisted of an inverted fluorescence microscope (Olympus IX-70) equipped with 3 detection ports. A 100 W mercury lamp was used for excitation. The fluorescence was collected by a 20 X microscope objective with a numerical aperture (NA) of 0.50. A filter cube containing 480nm narrow band excitation filter, 500nm dichroic mirror and 515nm long pass emission filter was used to ensure spectral purity. A high performance charge-coupled device (CCD) camera (Rupert Scientific, model 256HB) with a 512 x 512 pixel array was used for digital fluorescence imaging of the samples. The Rupert Scientific software Winview 3.2 was used for image analysis.

Spectrofluorometry Experiments – Excitation and emission spectra, as well as the spectral response of $[(bpy)_2Ru(bpy\text{-}pyr)]Cl_2$ in solution to different oxygen levels were conducted using a PTI model QM-1 spectrofluorometer (PTI, London, Ontario, Canada), equipped with a 75W continuous Xe arc lamp as the light source.

Photostability Study of Ruthenium Diimine Complexes – Solutions of 20 μM of ruthenium diimine complexes in phosphate buffered saline (PBS) solution at pH 7.4 were continuously exposed to a 765W Xenon lamp in a Sunbox (Suntest CPS^+, Atlas electric devices Co.) for 30 mi. The fluorescence intensities of the indicators were acquired every 5 min using a spectrofluorometer.

Cell Culture - Cultures of J774 murine macrophages were maintained according to a protocol described by Gordon *et al.* (25). The cells were cultured in Dulbecco's modified Eagle's medium supplemented with 4mM L-Glutamine, 1.5g/l sodium bicarbonate, 4.5g/l glucose, 1.0mM sodium pyruvate, and 10% fetal bovine serum. The cells were grown at 37°C under 5% CO_2. The medium was replaced three times a week. To prepare subcultures, the cells were scraped in new medium and split into new plates.

Cell Culture on the Surface of a Chambered Coverglass - The macrophages were detached from the surface of a tissue culture plate by scraping. The cells were mixed with the growth medium by a glass pipette. The cell suspension (50µl, ~$1x10^6$ cells/ml) was then placed into a chambered coverglass. 950µl fresh medium was added to the chamber. The cells were incubated to attach and grow on to the coverglass at 37°C under 5% CO_2. Typically, an 80% confluence was achieved in 3 days.

Loading of the Indicator with Macrophages – A solution of 150µl of 120µM $[(bpy)_2Ru(bpy\text{-}pyr)]Cl_2$ in phosphate buffered saline solution at pH 7.4 was added into the cell culture on a chambered coverglass. The medium and the dye solutions were mixed using a glass pipette. The cells were incubated at room temperature for 1h to allow the permeation of the dye to take place. The excess dye was washed off with a PBS solution at pH 7.4.

Materials - $[(bpy)_2Ru(bpy\text{-}pyr)]Cl_2$ was a gift from Dr. Russell H. Schmehll of Tulane University. Tris (1,10- phenanthroline) ruthenium chloride ($Ru(phen)_3$) was purchased

from Aldrich Chemical Company. Glucose, glucose oxidase from Aspergillus niger with enzymatic activity of 10,000 units/ml, Dulbecco's modified Eagle's medium and bovine serum albumin were purchased from Sigma. J774 murine macrophages were purchased from ATCC (American Type Culture Collection). Lab-Tek II chambered coverglass was purchased from Fisher Scientific. Aqueous solutions were prepared with 18 MΩ deionized water from a purification system (Barnstead Thermolyne Nanopure). PBS solution at pH 7.4 was prepared from PBS tablets (Amresco). All reagents were used as received without further purification.

RESULTS AND DISCUSSION

Spectral properties of Ru(bpy-pyr)(bpy)$_2$ – The chemical structure of Ru(bpy-pyr)(bpy)$_2$ is shown in Figure 2a. The excitation and emission spectra of a solution of 80μM [(bpy)$_2$Ru(bpy-pyr)]Cl$_2$ in a PBS buffer at pH 7 buffer are shown in Figure 2b. A concentration dependence of the fluorescence intensity of Ru(bpy-pyr)(bpy)$_2$ at 632nm (λ=460nm) in aqueous solution is shown in figure 3. The fluorescence intensity of the dye increases with increasing dye concentration. This is explained by self-fluorescence quenching of the dye that occurs at concentrations greater than 80μM.

Oxygen Sensing Properties of Ru(bpy-pyr)(bpy)$_2$ in aqueous solutions – Figure 4 shows the fluorescence spectra of Ru(bpy-pyr)(bpy)$_2$ in nitrogen-, air-, and oxygen-saturated solutions. Due to dynamic quenching by molecular oxygen, the fluorescence intensity of Ru(bpy-pyr)(bpy)$_2$ in nitrogen saturated solutions, I(N_2), is higher than the fluorescence intensity in air saturated one, I(air), which is also higher than the fluorescence intensity in oxygen saturated solution, I(O_2). The response factor between nitrogen and oxygen, I(N_2)/I(O_2), is 13. The response is reversible. The dependence of the fluorescence intensity of Ru(bpy-pyr)(bpy)$_2$ on the concentration of dissolved molecular oxygen is described by the Stern-Volmer equation:

$$I_0/Ic = 1 + Ksv\,[O_2]$$

where I_0 is the fluorescence intensity of Ru(bpy-pyr)(bpy)$_2$ in a nitrogenated solution, Ic is the fluorescence intensity of Ru(bpy-pyr)(bpy)$_2$ in a given dissolved oxygen concentration, and Ksv is the Stern-Volmer quenching constant. Oxygen quenches the fluorescence intensity of Ru(bpy-pyr)(bpy)$_2$. In principle, higher quenching constants

result in higher accuracy at low levels of oxygen. This is due to the larger signal change per oxygen concentration interval. However, high quenching constants result in a more limited linear dynamic range. We found that Ksv for Ru(bpy-pyr)$(bpy)_2$ is 13,333 ± 3% M^{-1}. The linear dynamic range is between 0.1 and 12 ppm molecular oxygen with a correlation coefficient of 0.996. It is commonly assumed that oxygen diffuse freely through cell membranes and therefore the intracellular oxygen tension would be very close in value to the extracellular oxygen tension. Under aerated conditions the level of intracellular oxygen tension is around 8 ppm well within the range of our oxygen indicator. The standard deviation between 10 consecutive fluorescence measurements in air-saturated solutions is ca. 3%. The standard deviation increases up to 10% at high oxygen levels where the signal is low.

Photostability of Ru(bpy-pyr)$(bpy)_2$ in Aqueous Solution- The Photostability of the new indicator is determined by comparing its photobleaching rate with that of the highly photostable complex tris (1,10 phenanthroline) ruthenium chloride, $Ru(phen)_3$. The two dyes are exposed to a 765W xenon lamp light source in a Sunbox continuously for 1h. Both dyes have a 50% drop of their fluorescence intensity in 30 min continuous exposure to light (data not shown). The photobleaching rates are comparable.

Stability of Loaded Cells with Respect to Dye Leakage and Photostability – Ru(bpy-pyr)$(bpy)_2$ permeates passively into the cells when the cells are incubated with a 50 μM dye solution for 1 h at room temperature. Transmission and fluorescence images of cells loaded with the dye are shown in figure 5. The signal to background ratio in the

fluorescence image is 37. The cellular structure remains intact for at least 5 h after the permeation of the dye. Monitoring the fluorescence intensity of the cells for 1 h shows an unnoticeable leakage of the indicator.

Excitation light at 480 nm is used to excite the dye loaded cells to minimize the photobleaching rate of Ru(bpy-pyr)$(bpy)_2$ and the effect of cellular auto-fluorescence on the signal to noise ratio. Additionally, a neutral density filter of 1.0 is applied to ensure the photostability of the indicator. To monitor the photobleaching rate of dye loaded cells under these conditions; a chambered coverglass of the loaded cells is placed on the microscope stage and illuminated continuously. The fluorescence intensity of the cells decreases by 5% in 30 min of illumination. During our kinetic measurements, the cells are exposed to the excitation light for 3 sec in each measurement. Each experiment lasts less than 30 min and images are taken in 2-4 min intervals. It is fair to conclude that under our experimental conditions, the loaded cells remain photostable throughout the experiment.

Oxygen Sensing in Living Macrophages – The intracellular oxygen sensing properties of Ru(bpy-pyr)$(bpy)_2$ were assessed by exposing the dye-loaded cells to oxygen, air and nitrogen saturated PBS at 7.4. The fluorescence intensity of the cells was acquired and plotted in figure 6. The fluorescence intensity of the cells increases 4-fold when the oxygenated solution is replaced with a nitrogenated one. Replacing the oxygenated or nitrogenated solutions with an air-saturated solution restores the signal to it original level. The response is reversible. It should be noted that such harsh treatments lead to cell death

as verified by Trypan Blue staining. Under these stressful conditions, high level of reactive oxygen species (ROS) may present in cells. In spite of these conditions Ru(bpy-pyr)$(bpy)_2$ maintains its oxygen sensitivity. It should also be noted that other commonly used ruthenium diimine complexes like tris 1,10 phenanthroline ruthenium chloride [$Ru(phen)_3$] partially loose their oxygen sensing properties in the cellular environment under these conditions. It is possible that the addition of a large organic ligand prevents the degradation of the complex due to steric hindrances and/or stabilizing interactions with hydrophobic cellular components. The significance of these interactions is not clear at this time and further studies are needed to fully understand the structure/stability relationships of ruthenium diimine complexes in the cellular environment.

Response of Single Macrophages to Hypoxia induced by Glucose Oxidase – To test the sensitivity of Ru(bpy-pyr)$(bpy)_2$ under less destructive conditions, we applied the indicator to monitor the kinetic response of individual macrophages to hypoxia induced by enzymatic oxidation of glucose. Glucose oxidase catalyzes the oxidation of glucose as follows:

$$\text{Glucose} + O_2 \xrightarrow{\text{Glucose oxidase}} \text{Gluconic acid} + H_2O_2$$

The enzymatic oxidation consumes molecular oxygen. The rate of oxidation and the steady state level of oxygen in the medium depend on the glucose concentration and glucose oxidase activity. Figure 7 describes the response of cells to hypoxia caused by different concentrations of glucose/glucose oxidase. Curve (c) describes the control experiment where Ru(bpy-pyr)$(bpy)_2$ loaded cells are incubated in a PBS buffer at pH 7.4

in a glucose and glucose oxidase free solution. The curve shows that during a 10 min experiment, the fluorescence intensity of cells keeps constant. Curves (a) and (b) describe the fluorescence intensities of the cells when they are incubated with a medium containing 10 mM glucose and 1.5mM glucose, respectively, with 5 units/ml glucose oxidase. A 50% (a) and 40% (b) fluorescence increase is obtained in 2 min and 4 min, indicating a decrease in intracellular oxygen levels to 4ppm and 3.2ppm, respectively. The errors between data points obtained from 2 different batches of cells are ca. 3% in the control experiment. The variation between the fluorescence intensities of loaded cells increases to about 6% with decreasing intracellular oxygen levels. This may be attributed to an increase in the percentage of dead cells. Once the glucose/glucose oxidase solution is replaced with a PBS solution at pH 7.4, the fluorescence intensity of the cells returns to its original value in 2 min, indicating that a normal intracellular oxygen level has been restored. Trypan Blue staining indicates that 85% of the cells survive this treatment.

SUMMARY AND CONCLUSIONS

$Ru(bpy\text{-}pyr)(bpy)_2$ is utilized for the first time as an oxygen indicator for intracellular oxygen measurements. Aside from its strong visible absorption, efficient fluorescence, and relatively long-lived excited state, the new indicator exhibits high oxygen sensitivity, large Stoke shift and high photo-/chemical- stability in the cellular environment. Due to the long emission wavelength of the indicator the fluorescence signal is shifted away from cellular auto-fluorescence, which causes serious perturbation when UV sensing indicators are used. $Ru(bpy\text{-}pyr)(bpy)_2$ maintains its oxygen sensing properties in living cells for at least 5 h after loading. Using high-resolution digital fluorescence imaging microscopy we were able to quantitatively monitor the kinetic response of macrophages loaded with $Ru(bpy\text{-}pyr)(bpy)_2$ to hypoxia. We have clearly shown that a low oxygen level is produced in living cells when they are exposed to hypoxia.

It is still possible that undesired interactions between the indicator and the complex cytoplasm contribute to the observed fluorescence readings. It is also possible that heterogeneity in dye distribution affects the fluorescence intensity of the cells and contributes to the cell-to-cell variations observed in our cellular measurements. Nevertheless, the ability to measure the average response of a large number of cells to conditions of hypoxia may prove to be valuable in studies designed to understand the effect of prolonged hypoxia on cells and tissues. Minimization of the interaction between the sensing indicator and cytoplasmic constituents is imperative to further improve the accuracy of intracellular oxygen measurements. Currently, we are developing a new intracellular oxygen sensor where $Ru(bpy\text{-}pyr)(bpy)_2$ is immobilized to the surface of

phospholipid coated polystyrene particles. The phospholipid membrane is permeable to molecular oxygen but protects the fluorescence indicator from the cellular environment. These sensors will be applied in a variety of intracellular studies including intracellular oxygen measurements in macrophages.

ACKNOWLEDGEMENT

This work is supported by the National Science Foundation through CAREER grant CHE-9874498. The authors thank Tom Weise from Xavier University of Louisiana School of Pharmacy for the use of his cell culture laboratory. The authors thank Dr. Russell H. Schmehll from Tulane University Department of Chemistry for the gift of the oxygen indicator $Ru(bpy\text{-}pyr)(bpy)_2$.

REFERENCES

1. Lau, Y. Y., Abe, T., and Ewing, A.G. (1992) *Anal. Chem.* **64(15)**, 1702-1705.
2. Chen, K., Ng, C. E., Zweier, J. L., Kuppusamy, P., Glickson, J. D., and Swartz, H. M. (1994) *Magn. Reson. Med.* **31(6)**, 668-672.
3. Robiolio, M., Rumsey, W. L., and Wilson, D. F. (1989) *Am. J. Physiol.* **256 (6 pt 1)**, C1207-1213.
4. Glockner, J. F., Swartz, H. M., and Pals, M. A. (1989) *J. Cell. Physol.* **140(3)**, 505-511.
5. Titovets, E. (1987) *Anal. Biochem.* **166(1)**, 79-82.
6. Vaughan, W. M., and Weber, G. (1970) *Biochemistry* **9**, 464-473.
7. Knopp, J. A., and Longmuir, I. S. (1972) *Biochim. Biophys. Acta* **279**, 393-397.
8. Benson, D. M, Knopp, J. A., and Longmuir, I. S. (1980) *Biochim Biophys Acta* **591(1)**, 187-97.
9. Opitz, N., and Lubbers, D. W. (1984) *Adv. Exp. Med. Biol.* **180**, 261-267.
10. Rumsey, W., Vanderkooi, J. M., and Wilsonm D. F. (1988) *Science,* **241**, 1649-1651.
11. Vanderkooi, J. M., Maniara, G., Green, T. J., and Wilson, D. F. (1987) *J. Biol. Chem.* **262(12)**, 5476-5482.
12. Pawlowski, M., and Wilson, D. F. (1992) *Adv. Exp. Med. Biol.* **316**, 179-85.
13. Wilson, D. F., Rumsey, W. L., Green, T. J., and Vanderkooi, J. M. (1988) *J. Biol. Chem.* **263(6)**, 2712-2718.
14. Rumsey, W. L., Schlosser, C., Nuutinen, E. M., Robiolio, M., and Wilson, D. F., *J. Biol. Chem.* **265(26)**, 15392-15402.

15. Carraway, E. R., Demas, J. N., DeGraff, B. A., and Bacon, J. R. (1991) *Anal. Chem.* **63**, 337-342.

16. Sacksteder, L., Demas, J. N., and DeGraff, B. A. (1993) *Anal. Chem.* **65**, 3480-3483.

17. Demas, J. N., and DeGraff, B. A. (1991) *Anal. Chem.* **63**, 829A-837A.

18. Xu, W., McDonough, R.C. III, Langsdorf, B., Demas, J. N., and DeGraff, B. A. (1993) *Anal. Chem.* **66**, 4133-4141.

19. Wolfbeis, O. S., Ed. (1991) Fiber Optic Chemical Sensors and Biosensors, CRC Press: Boca Raton.

20. Rosenzweig, Z., and Kopelman, R. (1995) *Anal. Chem.* **67**, 2650-2654.

21. Zhao, Y., Richman, A., Storey, C, Radford, N. B., and Pantano, P. (1999) *Anal Chem* **71(17)**, 3887-93.

22. Velasco-Garcia, N., Valencia-Gonzalez, M. J., and Diaz-Garcia, M. E. (1997) *Analyst* **122(11)**, 1405-1409.

23. Asiedu, J. K., Ji, J., Nguyen, M., Rosenzweig, N., and Rosenzweig, Z. (2000) *Journal of Biomedical Optics*, in press.

24. Simon, J. A., Curry, S. L., Schmehl, R. H., Schatz, T. R., Piotrowiak, P., Jin, X. Q., and Thummel, R. P. (1997) *J. Am. Chem. Soc.* **119**, 11012-11022.

25. Gordon, S. (1995) *BioEssays* **17(11)**, 977-986.

FIGURE CAPTIONS:

Figure 1 - Digital fluorescence imaging microscopy system. The experimental setup consists of an inverted fluorescence microscope equipped with a 20X objective (NA = 0.5), a high performance charge-coupled device camera (Roper Scientific, 16-bit resolution, 512 × 512 chip size) and a microcomputer for image analysis.

Figure 2 - (a) Structure of $Ru(bpy\text{-}pyr)(bpy)_2$. bpy=2,2'-bipyridine, bpy-pyr=4-(1"-pyrenyl)-2,2'-bipyridine; (b) Fluorescence excitation spectrum (detected at 632nm) and emission spectra (excited at 460nm) of 80μM $Ru(bpy\text{-}pyr)(bpy)_2$ in a PBS buffer at pH 7.4.

Figure 3 - Fluorescence intensity of $Ru(bpy\text{-}pyr)(bpy)_2$ in solution as a function of its concentration. Self-quenching occurs at concentrations greater than 80μM.

Figure 4 - Response of free $Ru(bpy\text{-}pyr)(bpy)_2$ to different oxygen levels in aqueous solutions.

Figure 5 - (a) a transmission image and (b) a digital fluorescence image of $Ru(bpy\text{-}pyr)(bpy)_2$ labeled J774 macrophages in air-saturated PBS buffer at pH 7.4. The images are taken through a CCD with a 20X objective (NA = 0.5). Exposure time is 0.5 sec.

Figure 6 - Response of Ru(bpy-pyr)$(bpy)_2$ labeled J774 macrophages to different oxygen levels in the medium. Rapid diffusion of oxygen causes the fluorescence intensity changes of the dye-loaded cells. The response is reversible.

Figure 7 - The response of Ru(bpy-pyr)$(bpy)_2$ loaded macrophages to hypoxia induced by gluocose oxidase in a glucose solution. Curves (a) (b) describe the fluorescence intensity of Ru(bpy-pry)$(bpy)_2$ loaded cells when suspended in a solution containing (a) 10 mM glucose and 5 units/ml glucose oxidase; and (b) 1.5mM glucose and 5 unit/ml glucose oxidase. Curves (c) is a control experiment where the loaded cells are suspended in a glucose and glucose oxidase free solution.

Figure 1

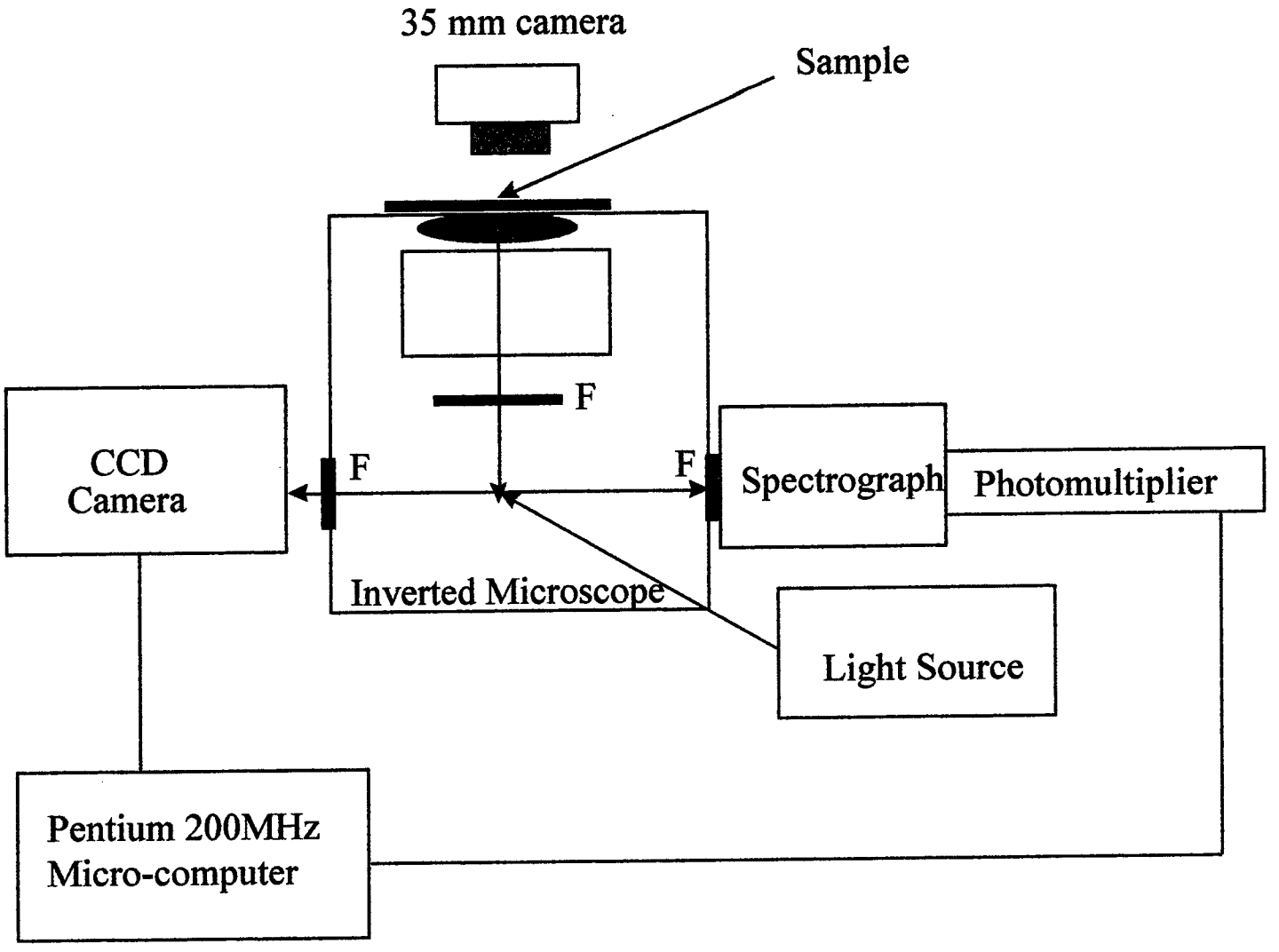
35 mm camera
Sample
F
CCD
Camera
F
F
Spectrograph
Photomultiplier
Inverted Microscope
Light Source
Pentium 200MHz
Micro-computer

Figure 2

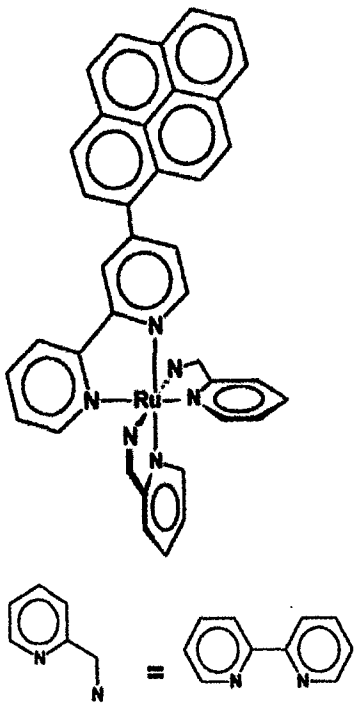
N
Ru
N
N
N
N
N
N
=
N
N

(a)

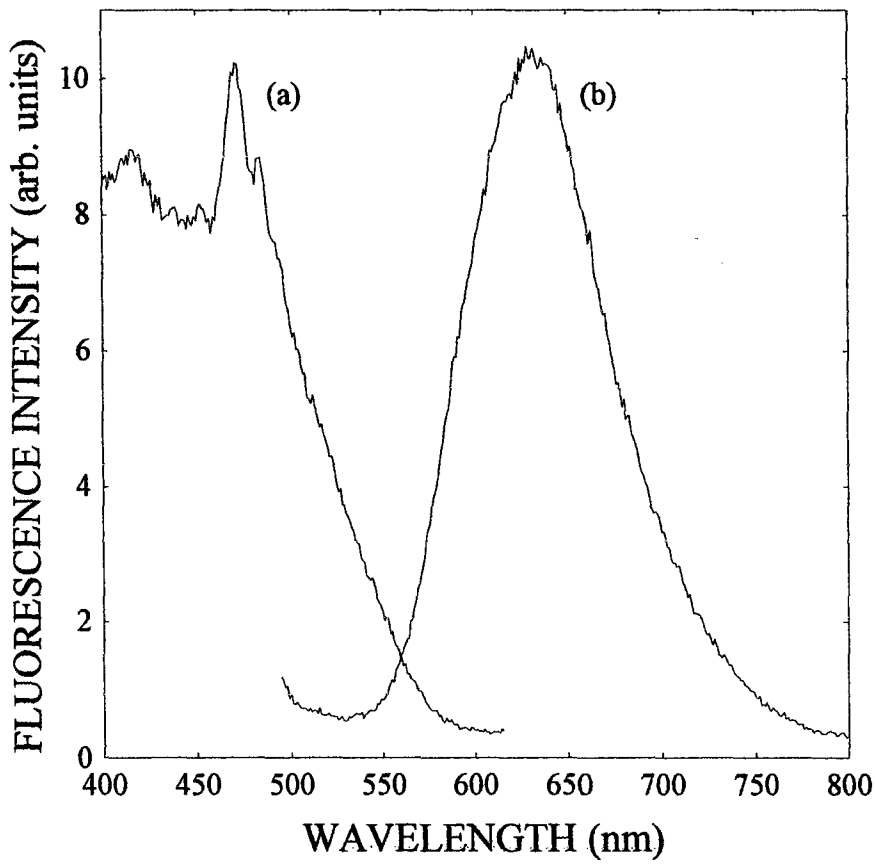
FLUORESCENCE INTENSITY (arb. units)
0
2
4
6
8
10
(a)
(b)
400
450
500
550
600
650
700
750
800
WAVELENGTH (nm)

(b)

Figure 3

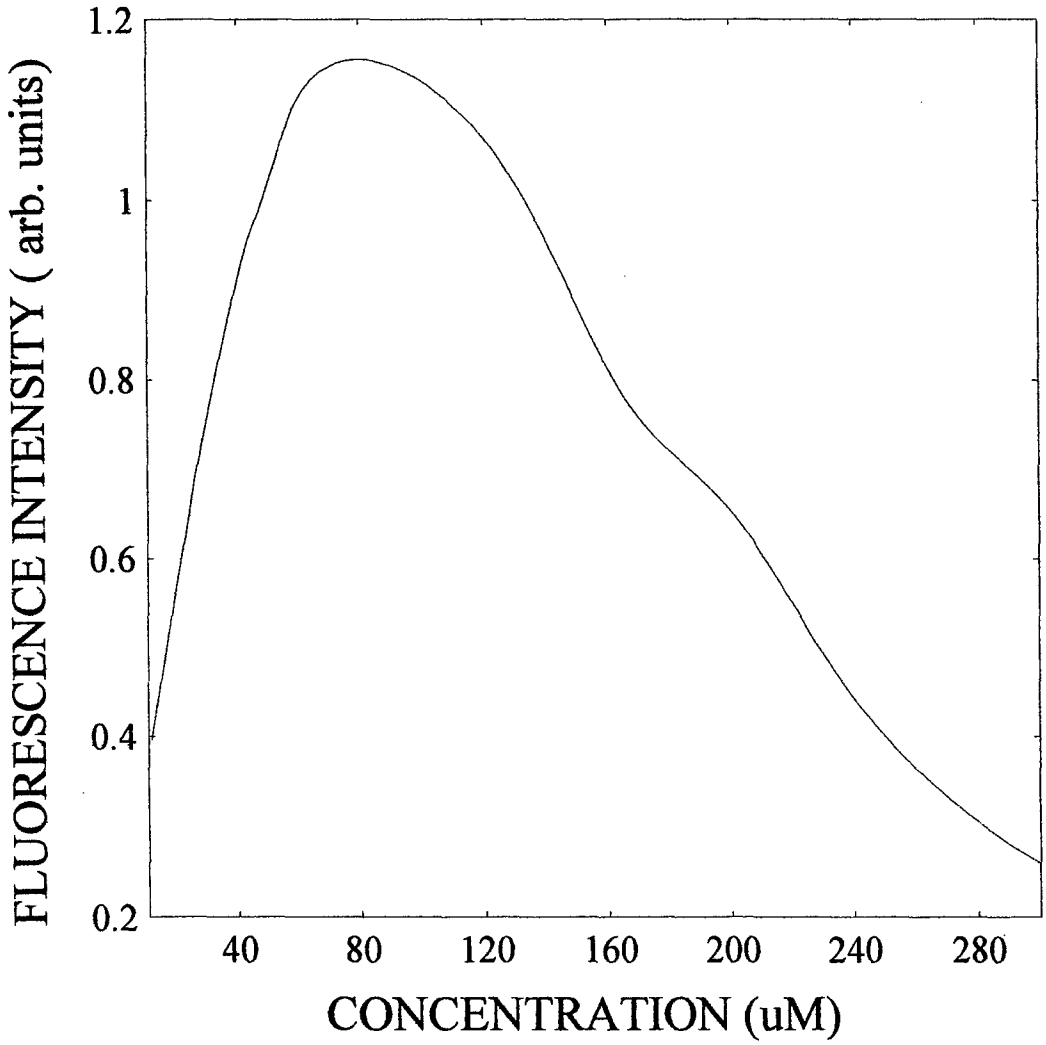
FLUORESCENCE INTENSITY (arb. units)
1.2
1
0.8
0.6
0.4
0.2
40
80
120
160
200
240
280
CONCENTRATION (uM)

Figure 4

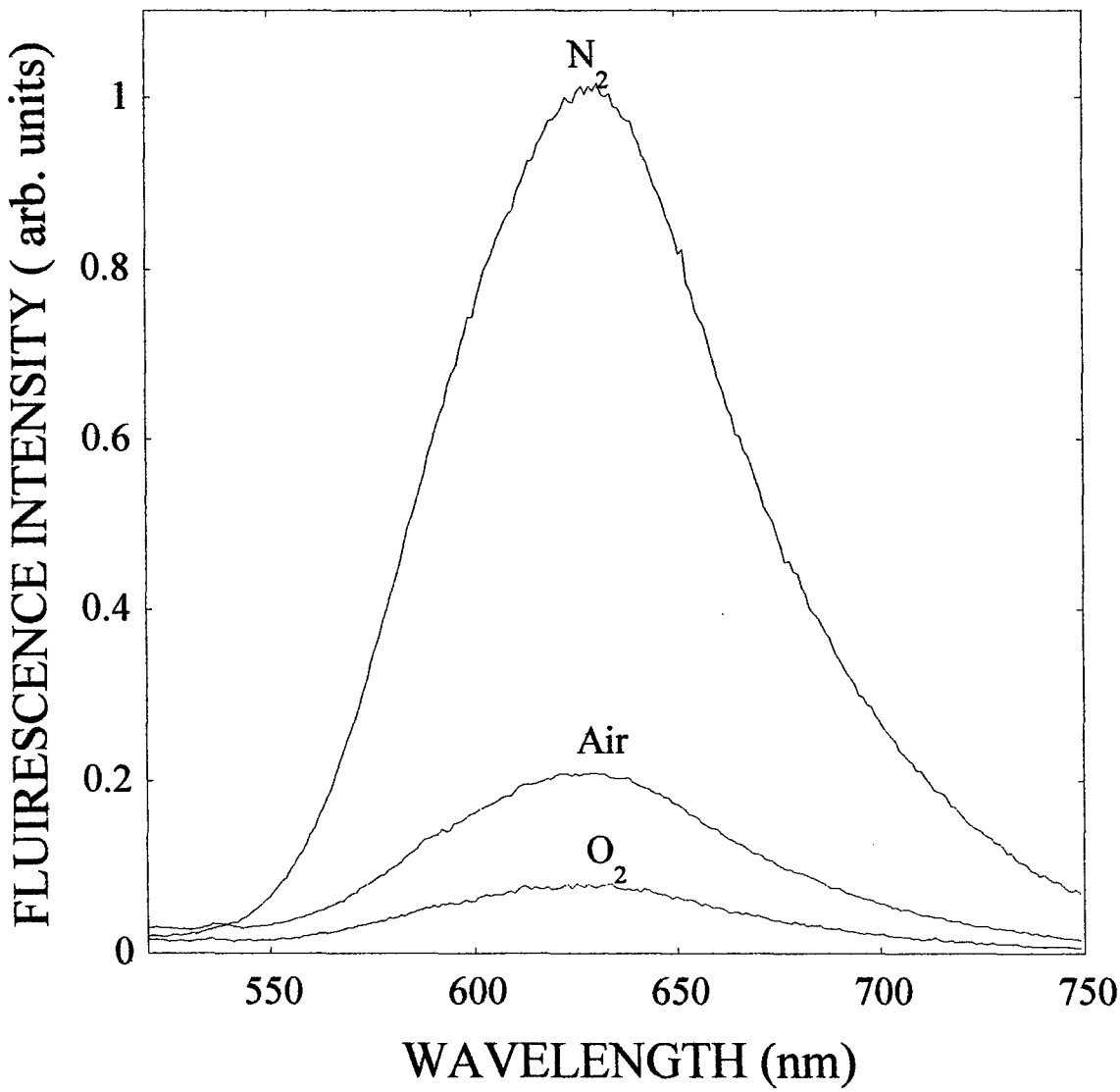
FLUIRESCENCE INTENSITY (arb. units)
1
0.8
0.6
0.4
0.2
0
N2
Air
O2
550
600
650
700
750
WAVELENGTH (nm)

Figure 5

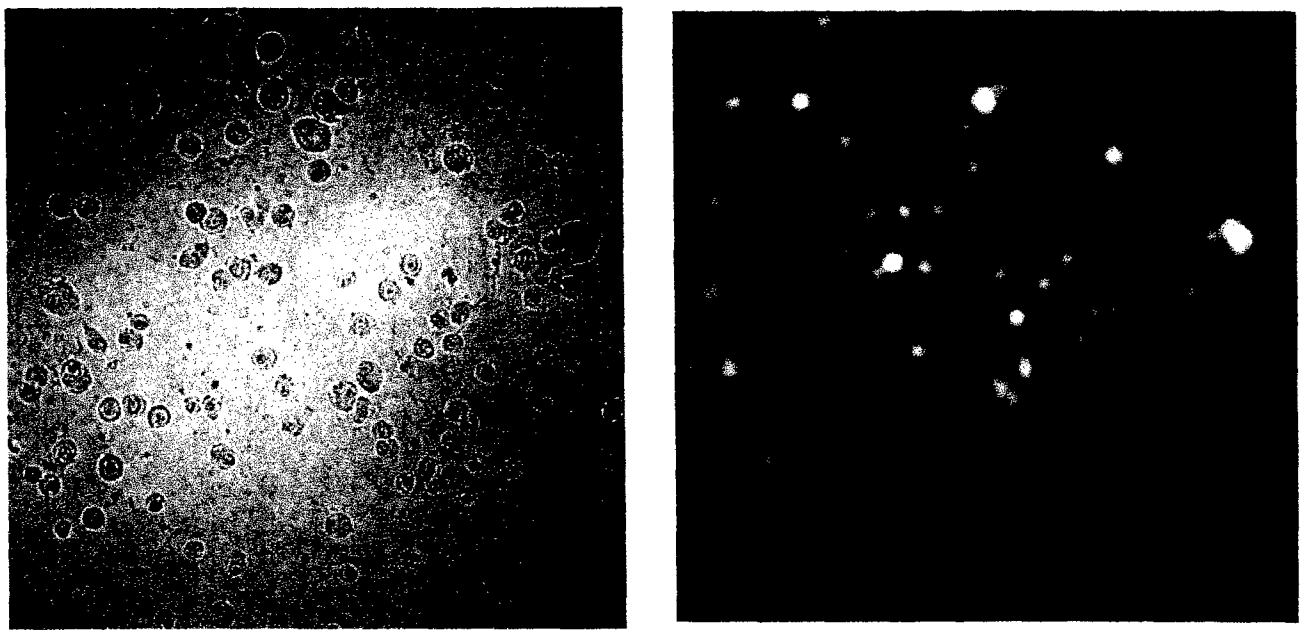

(a) (b)

Figure 6

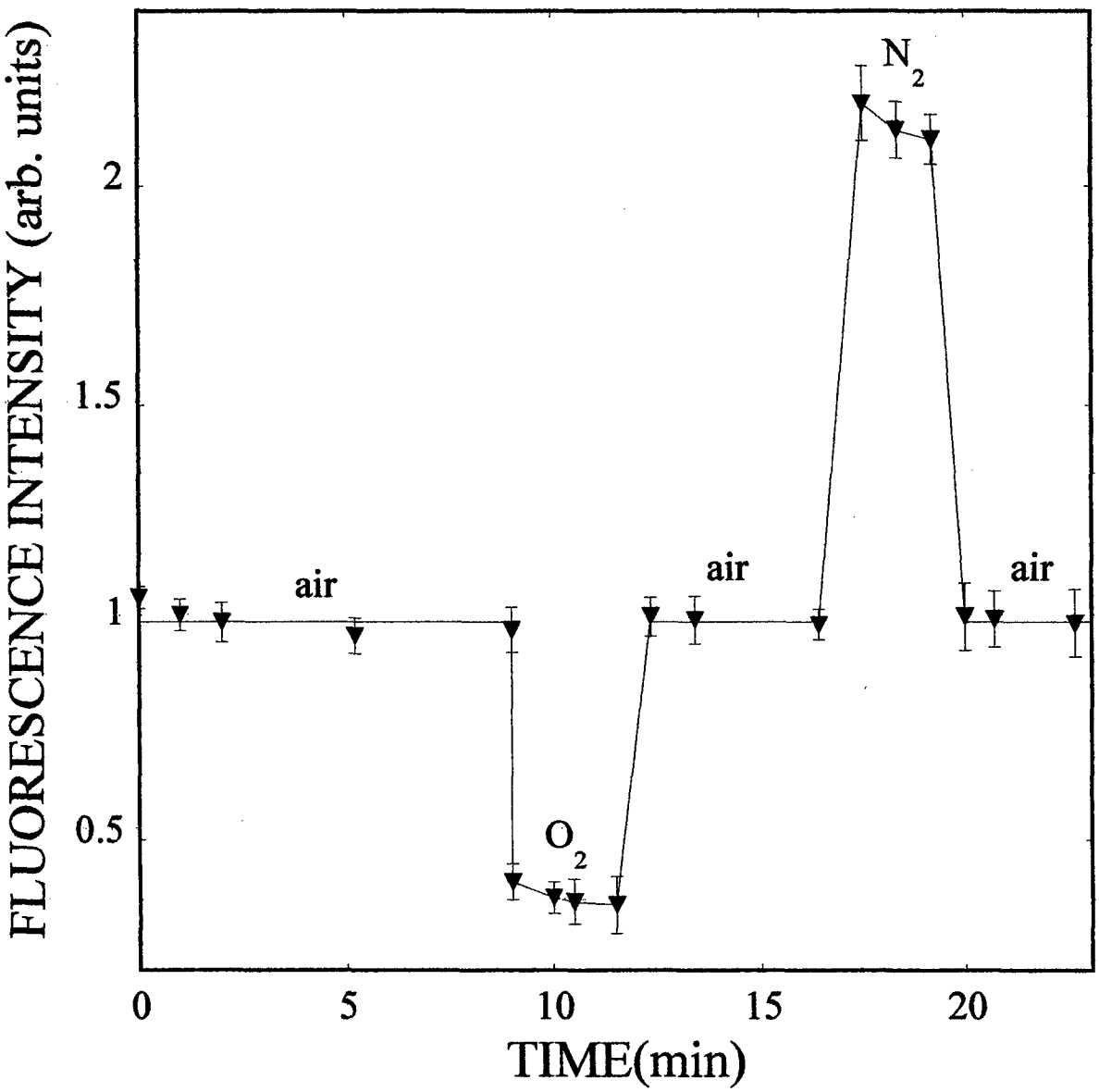
FLUORESCENCE INTENSITY (arb. units)
2
1.5
1
0.5
air
air
air
N_2
O_2
0
5
10
15
20
TIME(min)

Figure 7

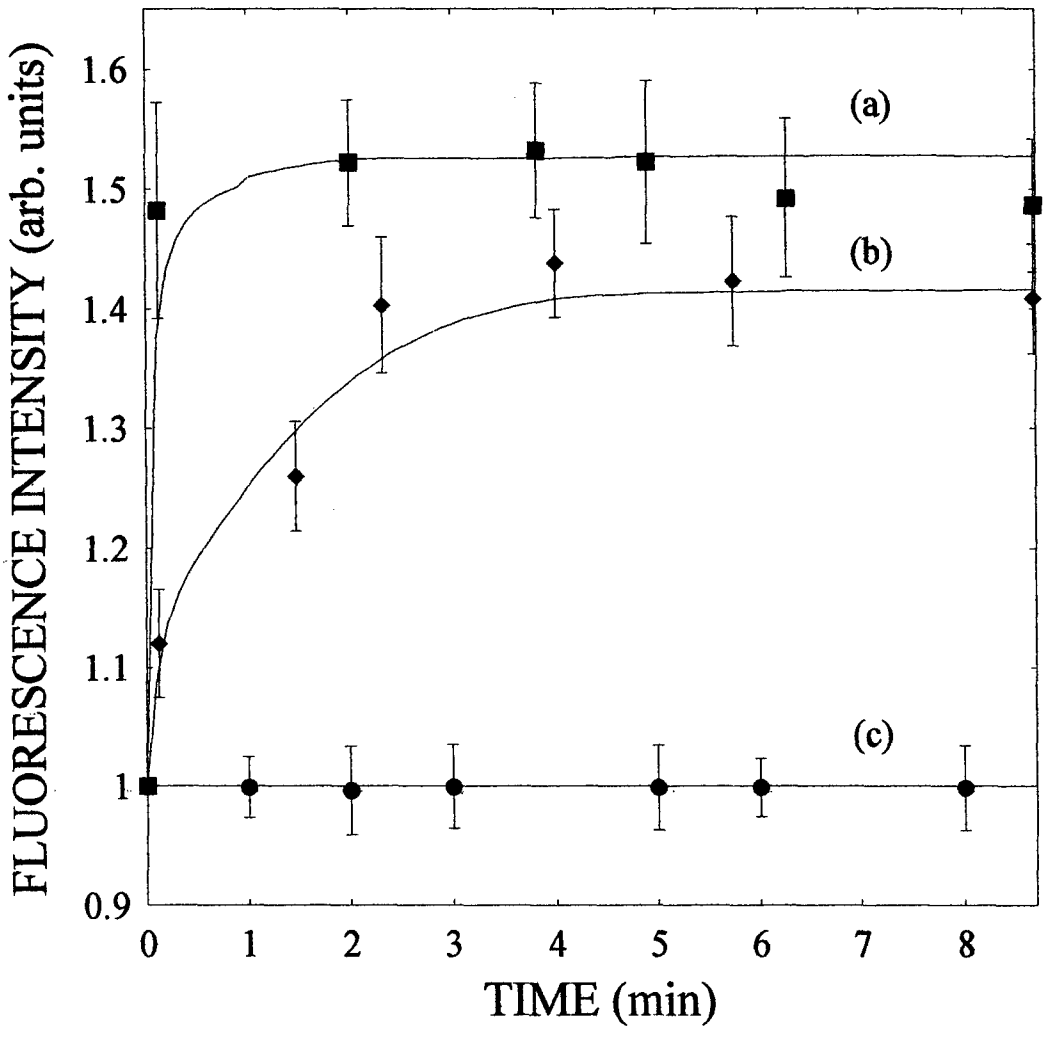
FLUORESCENCE INTENSITY (arb. units)
1.6
1.5
1.4
1.3
1.2
1.1
1
0.9
0
1
2
3
4
5
6
7
8
TIME (min)
(a)
(b)
(c)

APPENDICE 8 – Poster Presentation: "MOLECULAR OXYGEN SENSITIVE FLUORESCENT LIPOBEADS FOR SINGLE CELL ANALYSIS", JIN JI [1] , IMANI JONES [2], NITSA ROSENZWEIG [2], AND ZEEV ROSENZWEIG[1] , Pitcon 2001, New Orleans Louisiana, March 2001

Pitcon 2001, New Orleans Louisiana, March 2001

392

MOLECULAR OXYGEN SENSITIVE FLUORESCENT LIPOBEADS FOR SINGLE CELL ANALYSIS

JIN JI [1] , IMANI JONES [2], NITSA ROSENZWEIG [2], AND ZEEV ROSENZWEIG[1]
1) Department of Chemistry, University of New Orleans, New Orleans, LA 70148
2) Department of Chemistry, Xavier University of Louisiana, LA 70125

With the increasing attention in biological studies at the single cell level, there is a growing interest in the development of miniaturized fluorescence-based sensors. Particle based nanosensors enable non-invasive site-specific intracellular measurements. However, the biocompatibility and sensitivity of current particle-based sensors are limited. More biocompatible and sensitive sensors are needed.

In this presentation, we describe the development and application of oxygen sensitive fluorescent for molecular oxygen measurements in macrophages. A highly hydrophobic ruthenium metal complex [(bpy)2Ru(bpy-pyr)]Cl2 (bpy=2,2'-bipyridine, bpy-pyr=4-(l"-pyrenyl)-2,2'-bipyridine) is used as the oxygen indicator. The indicator exhibits high chemical stability and excellent response to changing oxygen concentrations. The indicator is absorbed onto the surface of the polystyrene beads, and trapped on the surface by a phospholipid membrane that coats the polystyrene particles. The lipobeads show a 4-fold increase in their fluorescence signal when the level of oxygen in the solution changes from 100% oxygen to 0% oxygen. The oxygen sensitive lipobeads are applied for oxygen measurements in single murine macrophages. The lipobeads maintain their spectral properties for at least 18h in cells when the cells are stored in PBS 7.4 buffer. The photostability, lifetime and the application of the lipobeads in monitoring the effect of drugs on the intracellular oxygen balance measurements in J774 macrophages will be discussed.

APPENDICE 9 – Poster Presentation: "Application of FRET microscopy for real time monitoring of drug delivery into single cells", Dumitrascu, Gabriela; Lane, Crystal; Jones, Imani; Rosenzweig, Nitsa; Rosenzweig, Zeev. 223rd ACS National Meeting, Orlando, FL, United States, April 7-11, 2002

223rd ACS National Meeting, Orlando, FL, United States, April 7-11, 2002

Application of FRET microscopy for real time monitoring of drug delivery into single cells. Dumitrascu, Gabriela; Lane, Crystal; Jones, Imani; Rosenzweig, Nitsa; Rosenzweig, Zeev. Department of Chemistry, University of New Orleans, New Orleans, LA, USA. Abstracts of Papers, 223rd ACS National Meeting, Orlando, FL, United States, April 7-11, 2002 (2002), ANYL-033. Publisher: American Chemical Society, Washington, D. C CODEN: 69CKQP Conference; Meeting Abstract written in English. AN 2002:186070 CAPLUS

Fluorescence resonance energy transfer (FRET) is characterized by the transfer of photon energy from a fluorophore (donor) to another molecule (acceptor). The usefulness of this technique derives from the fact that the efficiency of fluorescence energy transfer process varies as the inverse of sixth power of distance separating the donor and the acceptor molecules. Due to this fact the interactions between cellular components and drugs can be monitored on the scale of 10—80 Å.

By coupling optical microscopy with FRET is possible to obtain quantitative, temporal and spatial information about binding and interactions of drugs with living cells. However steady state FRET microscopy measurement can suffer for several source of distortion, which need to be corrected. The methods used to address these problems will be illustrated in this paper.

The concept of the method was proved by the measurement of interaction of free dyes loaded in cells. Both quenching and sensitized fluorescence of acceptor were observed in the microscope. FRET microscopy was used in the J 774 murine macrophage culture. The intracellular organelles were labeled with Sulfo Rhodamine B. FRET was observed in cells doubly labeled with Fluorescein diacetate and Rhodamine B.

We conclude that FRET microscopy can be used to monitor the delivery and intracellular drug action

APPENDICE 10 – Poster Presentation: "Fluorescence transfer energy- new analytical tool for the drug delivery follow up", Gabriela Dumitrascu, Imani Jones, Nitsa Rosenzweig, and Zeev Rosenzweig Pittcon Conference, New Orleans, LA, March 17-22, 2002

Pittcon Conference, New Orleans, LA, March 17-22, 2002

Fluorescence transfer energy- new analytical tool for the drug delivery follow up

Gabriela Dumitrascu, Imani Jones, Nitsa Rosenzweig, and Zeev Rosenzweig

Department of Chemistry, University of New Orleans, New Orleans, LA 70148

Fluorescence resonance energy transfer (FRET) is characterized by the transfer of photon energy from a fluorophore (donor) to another molecule (acceptor). The usefulness of this technique derives from the fact that the efficiency of fluorescence energy transfer process varies as the inverse of sixth power of distance separating the donor and the acceptor molecules. Due to this fact the interactions between cellular components and drugs can be monitored on the scale of 1—10 Å.

This presentation describes the application of FRET microscopy to quantitatively monitor the kinetic of drug delivery from liposomes into the living cells. Murine macrophages were loaded Sulfo Rhodamine B, which serves as acceptor in the FRET microscopy measurements. The cells were incubated with Fluorescein diacetate solution and with a solution of liposomes containing Fluorescein diacetate. FRET signals were observed in cells doubly labeled with Sulfo Rhodamine B and Fluorescein diacetate. The rate of delivery of Fluorescein diacetate was studied as a function of pH and temperature. The kinetic data and its applications on the effectiveness of liposomal drug delivery will be discussed.

APPENDICE 11 – Poster Presentation: "Correlation Between Oxygen Free Radicals and Cytochrome P-450 Activity in Breast Cancer", Keiana Thomas, Tasha Smith, Maryam foroozesh, Nitsa Rosenzweig CUR April 2002.

Correlation Between Oxygen Free Radicals and Cytochrome P-450 Activity in Breast Cancer

Keiana Thomas, Tasha Smith, Maryam foroozesh, Nitsa Rosenzweig

CUR april 2002.

Cytochrome P-450 enzymes use molecular oxygen in their metabolic pathways for oxidizing a large number of endogenous and exogenous compounds into more polar and excretive metabolites. These enzymes play an important role in the detoxification processes but are also involved in the bioactivation of procarcinogens into ultimate carcinogens. Cytochrome P-450 enzymes produce oxygen free radicals that oxidize DNA.

In this study, we measured the levels of oxygen free radical produced in MCF-7 breast cancer cells exposed to the 7-ethoxyresorufin substrate (1.0mM) in the presence and absence of the cytochrome P-450 inhibitor, 2-adamantyl propargyl ether (2-APE).

Our hypothesis is that the oxygen free radical production is a P-450 dependent process.

To test the hypothesis, we used the amino-reactive OxyBurst reagent 2'7'-dichlorodihydroflurescein diacetate (H_2DCFDA) to detect the oxygen free radical concentration (fluorescence) in the cells. Measurement of the oxygen free radical production was done by using microscopic procedures, the Win32 computer program, and measurements of the total fluorescence with a plate reader.

Future studies: Our results show that the OFR levels in the breast cancer cell line MCF-7 is cytochrome P-450-dependent. These findings provide a clue to an innovative drug design.

APPENDICE 12 – Unpublished Results (Future poster for The Era of Hope Conference):

Figure I: Measurement of OFR in Breast Cancer Cells and in Normal Breast Cells

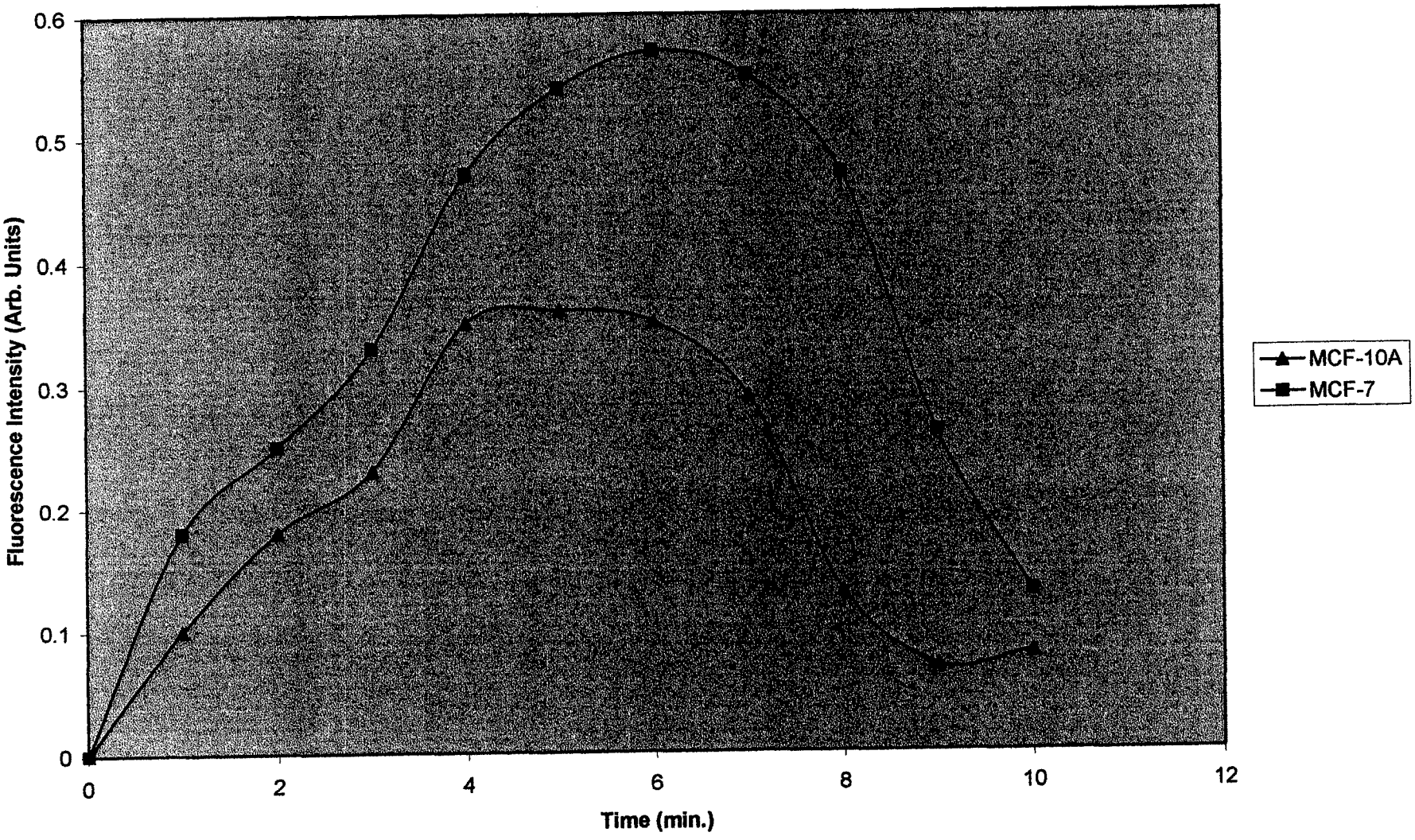

Figure IIA: Effect of H2O2 on Apoptosis

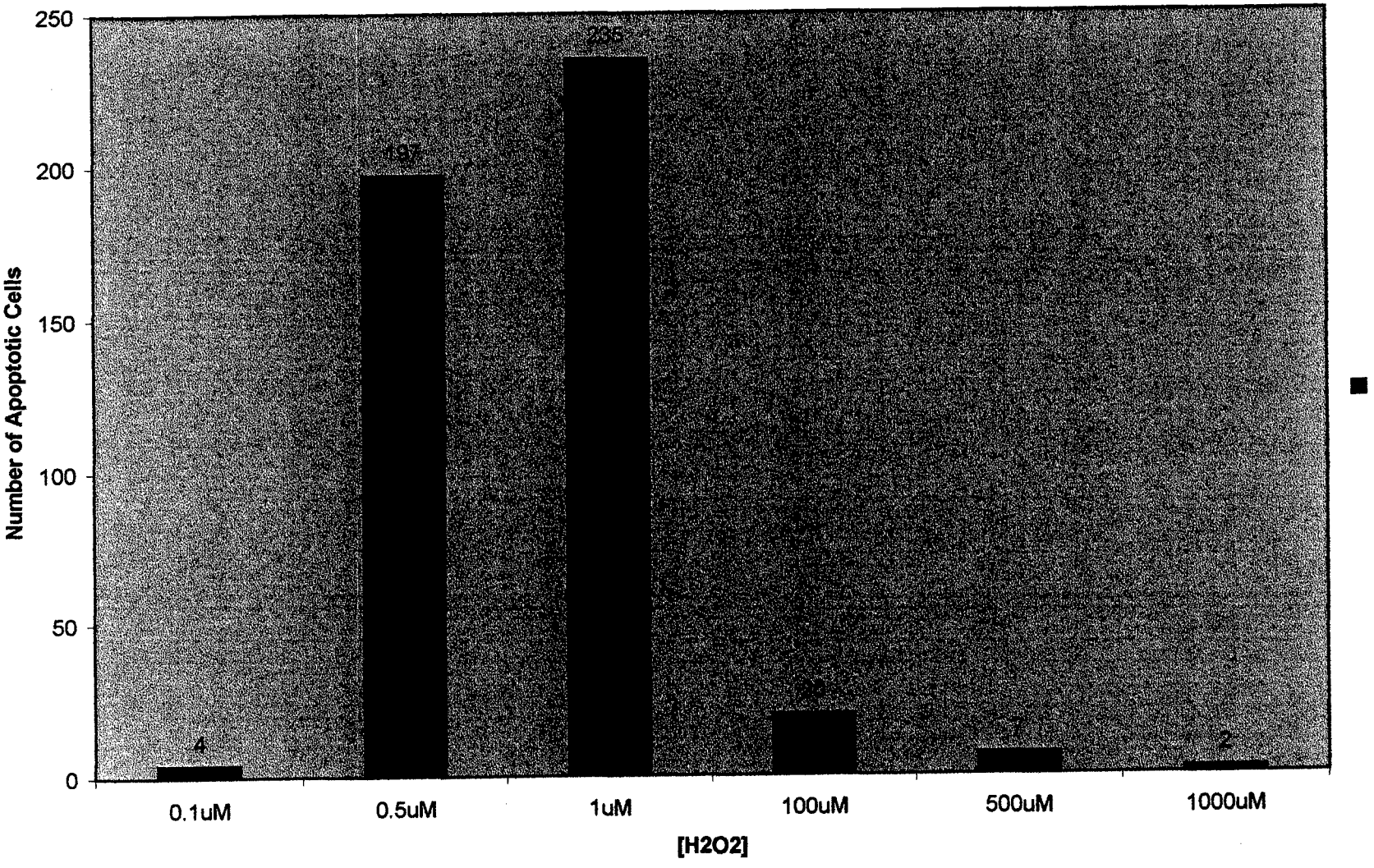

Figure IIB: Effect of H2O2 on Cell Death

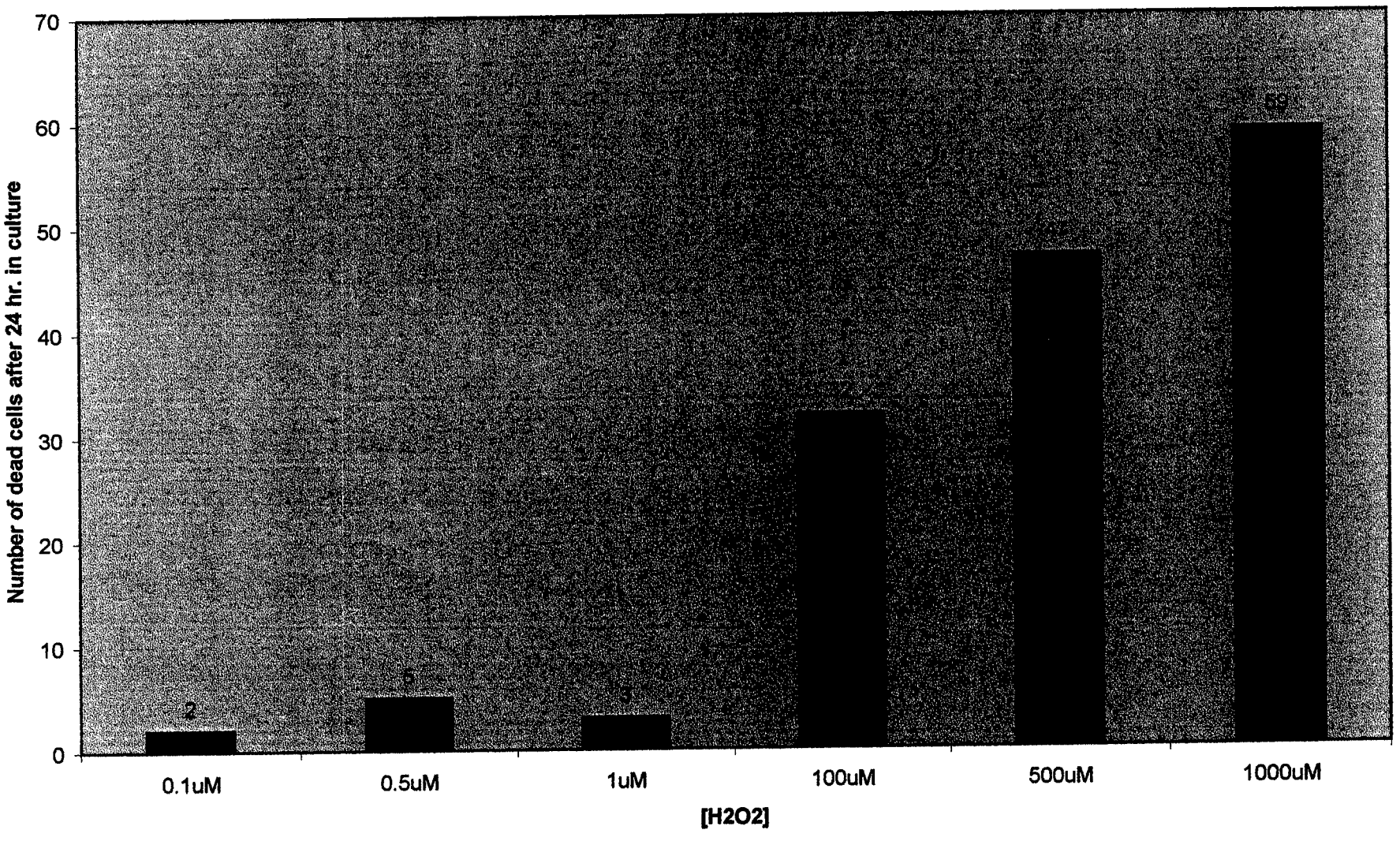

Figure IIIA: Effect of H2O2 on Cell Growth

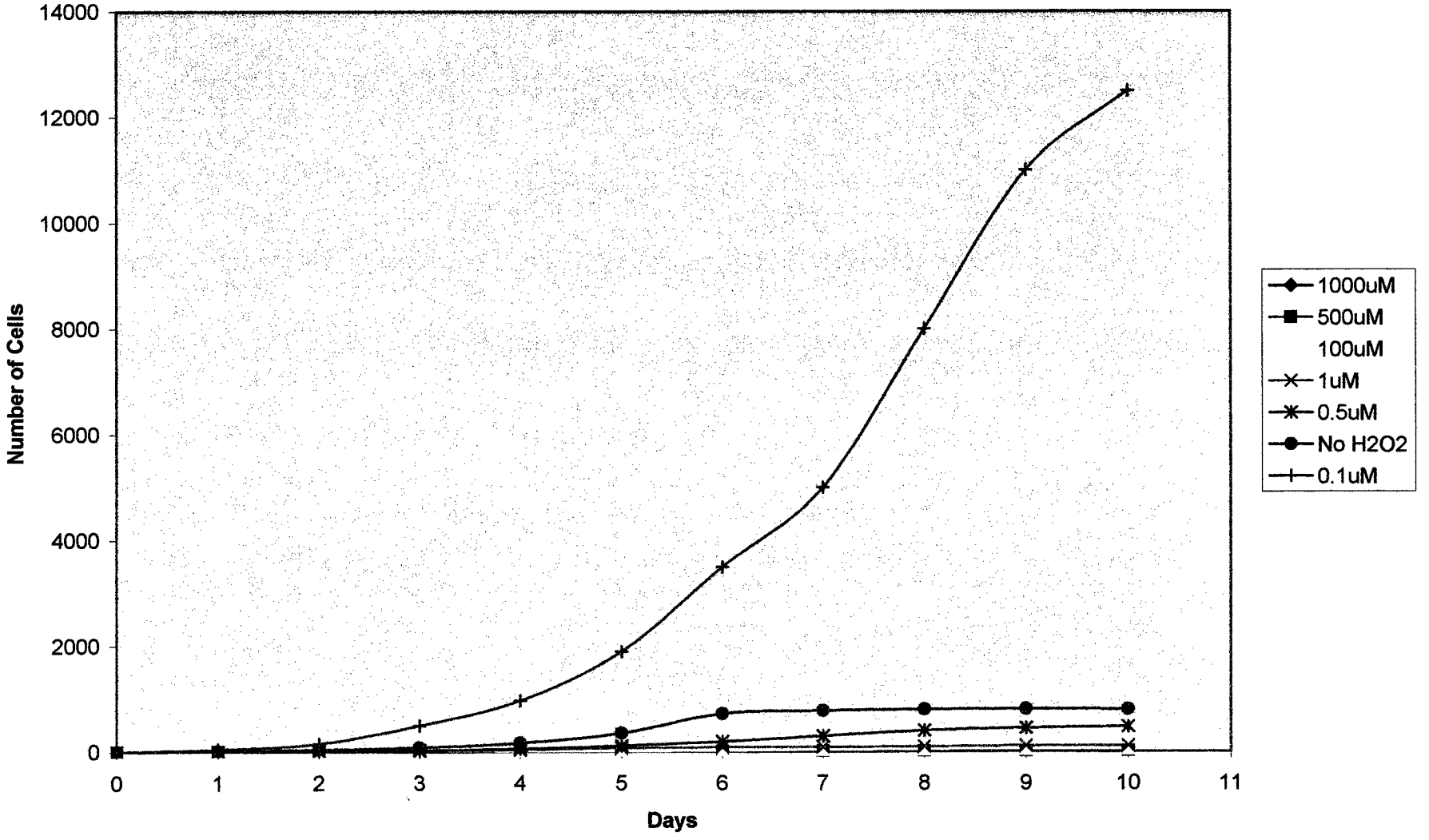

Figure IIIB: Effect of H2O2 on Cell Growth (Without 0.1uM)